Rockefeller University
Digital Commons @ RU

Student Theses and Dissertations

2021

Transcriptional Regulation of the Metabolic Response to Therapy in Leukemia

Robert Thomas Williams

Follow this and additional works at: https://digitalcommons.rockefeller.edu/student_theses_and_dissertations

 Part of the Life Sciences Commons

TRANSCRIPTIONAL REGULATION OF THE METABOLIC RESPONSE TO THERAPY IN LEUKEMIA

A Thesis Presented to the Faculty of
The Rockefeller University
in Partial Fulfillment of the Requirements for
the degree of Doctor of Philosophy

by
Robert Thomas Williams
June 2021

© Copyright by Robert Thomas Williams 2021

TRANSCRIPTIONAL REGULATION OF THE METABOLIC RESPONSE TO THERAPY IN LEUKEMIA

Robert Thomas Williams, Ph.D.
The Rockefeller University 2021

Cancer cells are under constant stress due to their uncontrolled growth, oncogenic signaling, and the metabolic insufficiencies of their microenvironments. Under various stresses, cells activate the integrated stress response (ISR), a transcriptional program to restore cellular homeostasis. Activating transcription factor 4 (ATF4) acts as the master transcriptional regulator of the ISR by promoting the transcription of genes that mitigate stress or promote cell death if the stress remains unresolved. Despite being the common mediator of various stress response and metabolic pathways, ATF4 generates tailored transcriptional outputs to distinct cellular stresses by cooperating with other transcriptional machinery. The precise mechanisms by which ATF4 activates an appropriate transcriptional program in response to metabolic stresses, however, remain unclear. In this work, we used forward genetic screens, metabolic profiling, and biochemical approaches to identify transcriptional regulators required for the cellular response to various metabolic stress conditions.

This work revealed that ATF4 is universally required under amino acid starvation, but identified the transcription factor, Zinc Finger and BTB domain-containing protein 1 (ZBTB1), as a critical regulator of the response to asparagine deprivation in acute lymphoblastic leukemia (ALL). We found that under asparagine depleted conditions ZBTB1 enables cellular proliferation by promoting the synthesis of asparagine from aspartate. Mechanistically, ZBTB1 binds directly to a sequence within the promoter of asparagine synthetase (ASNS), the enzyme responsible for the synthesis of asparagine from aspartate. Loss of ZBTB1 results in a dramatic reduction in the transcription of ASNS, and, subsequently, a reduced capacity for cells to synthesize asparagine from aspartate. ZBTB1 knockout T-ALLs are not only sensitive to asparagine deprivation *in vitro* but are also sensitive to treatment with L-asparaginase, a chemotherapy that reduces serum asparagine, in *in vivo* xenograft models of ALL.

Additionally, this work clarifies the metabolic stress induced by CPI-613, a lipoic acid analog designed to inhibit the function of Pyruvate Dehydrogenase (PDH), the enzyme responsible for the decarboxylation of pyruvate to acetyl-CoA. In line with the proposed mechanism of CPI-613, genetic screens suggested a synthetic lethal relationship between electron transport chain or TCA cycle enzymes and CPI-613. Unexpectedly, however, glycerolipid synthesis genes were found to be essential for the cellular response to CPI-613-induced stress. Further work revealed a substantial incorporation of CPI-613 into glycerolipid species, a finding that correlates with sensitivity to the drug.

Altogether, our work defines novel metabolic and transcriptional mechanisms of the response of acute leukemias to metabolic stresses. In acute lymphoblastic leukemia, we have identified a critical transcriptional regulator of the cellular response to asparagine deprivation. The role of ZBTB1 in the transcriptional regulation of ASNS in parallel with ATF4 has direct relevance to the therapeutic response of ALLs to L-

asparaginase. We have also determined a novel mechanism of action of CPI-613, a first-in-class PDH inhibitor currently in phase III clinical trials for acute myeloid leukemia (AML). This work revealed the incorporation of CPI-613 into glycerolipid species which may be relevant to toxicity of the drug. Altogether this work provides a framework for investigating the metabolic and transcriptional mechanisms by which leukemias respond to cellular stresses such as those induced by metabolically targeted therapies.

To the late Lisa Smith, Dave Frazier, and Veronica Lennon

ACKNOWLEDGMENTS

This work was only possible with the help of a large number of people. First, thanks are due to my thesis mentor, Kıvanç Birsoy, without whom none of this work would have been possible. Kıvanç's breadth and depth of knowledge in the field of metabolism is astounding, and it has truly been an honor to work with such an accomplished and talented scientist. As a mentor, Kıvanç pushed me to work harder, think deeper and question my scientific results in ways I had not before. Kıvanç goes out of his way to support his mentees and has provided me advice for my future career countless times.

The Birsoy lab is a group of exceptionally talented scientists, all of whom are eager to offer their help and advice. I owe a great debt of gratitude to Roy Guarecuco with whom I worked side-by-side studying L-asparaginase. Max Stahl, with whom I studied CPI-613, was both a great scientific partner and clinical mentor. Throughout my PhD, I benefitted from the advice, feedback and teachings of an exceptional postdoc Javier Garcia-Bermudez. I relearned many, if not all, of our laboratory techniques, figure-making and any other miscellaneous lab skill with the altruistic help of Xiphias Ge Zhu. Konnor La assisted with all computational efforts and was an accountability partner throughout my PhD for grant and paper deadlines. Lou Baudrier is, perhaps, the best lab manager you could ask for - she works tirelessly to help with anything and everything the lab needs. My Gateways summer student, and now Tri-I MD/PhD student, Swarna Jeewajee was essential to the development of ATF4 knockout cells. Benjamin Prizer quickly became an expert at the tail vein injection technique, critical for the *in vivo* leukemia experiments. Rebecca Timson, Mariluz Soula, Erol Bayraktar, Ying Wang, Ross Weber, Frederick Yen, Yuyang Liu, Gokhan Unlu, Maria Liberti, Tim Kenny, Hsi-wen Yeh and all other members of the lab past and present I may have omitted eased the trials and tribulations of the PhD experience through technical help and companionship. Eiko Nishiuchi helped with all administrative tasks and helped tremendously as I applied for an F30 graduate fellowship. Every single member of the Birsoy lab, new or old, helped me in one way or another and put up with my constant questions and advice seeking. I offer a sincere thanks to everyone in the lab for all of the good times, coffee breaks, extended lab lunches and company for late nights in the lab.

Outside of the lab, I benefitted tremendously from the expertise of collaborators both at Rockefeller University and elsewhere. My classmate Maria Passarelli was crucial to setting up our *in vivo* ALL xenograft experiments and was a constant source of support throughout my PhD. Leah Gates, Doug Barrows and Bryce Carey of the Allis lab were essential for applying ChIP-sequencing in this project. Thomas Carroll was both an essential computational collaborator and an exceptional teacher and mentor through his

Bioinformatics class. Jason Cantor provided human physiological media to validate our ZBTB1 findings in a more relevant tissue culture model. Zachary Stine, Matt McBride, Josh Rabinowitz, and Navdeep Chandel are invaluable ongoing collaborators investigating CPI-613's mechanism of action.

I am very thankful to the support and mentorship of my academic thesis committee composed of Sohail Tavazoie, Omar Abdel-Wahab, and Bob Roeder. It's been a privilege to learn from such accomplished accomplished scientists and physicians and to receive their advice and constructive feedback. I am grateful for their guidance throughout the various stages of my PhD. As an outside mentor, Chi Dang has provided important lessons in science, medicine and the career of a physician scientist. My PhD training was greatly simplified by the help and assistance of the Dean's Office at the Rockefeller University. Finally, I am extremely thankful for the opportunity to have enrolled in the Tri-I MD-PhD program, and particularly for those individuals who have supported me throughout my training including Ruth Gotian, Hanna Silvast, Olaf Anderson, Jochen Buck, and Catharine Boothroyd.

Finally, I am thankful to my friends and family for their support and love throughout my PhD. The MD/PhD program wouldn't have been manageable without the support of my close friends and classmates including Roy, Maria, Andrew, Ally, Debby, Hanan and Danny among many others. My mother, Lysa Williams, immigrated to this country to provide a better life for her and her future children. She instilled in me the importance of education and has lovingly supported my long and winding scholarly career. My father, Cecil Williams, has always been a model of hard work and dedication. My brother Nick lived with me for a year of my PhD helping me to balance hard work with fun. Nick is a constant source of inspiration and pride for me as he now serves as an officer in the United States Army.

TABLE OF CONTENTS

LIST OF FIGURES

LIST OF TABLES

CHAPTER 1. Introduction

1.1 The integrated stress response restores cellular homeostasis under various stress conditions

Mammalian cells respond to nutrient deprivation, protein folding stress, viral infection and redox imbalances through a conserved signaling and transcriptional pathway known as the integrated stress response[1]. These stresses are detected by one of four different kinases: PERK, GCN2, PKR and HRI. Upon activation, these kinases phosphorylate a serine residue on the eukaryotic translation initiation factor, eIF2. The eIF2 complex is composed of three subunits (α, β, and γ), guanosine 5'-triphosphate. (GTP), and a methionine tRNA molecule. This complex, called the ternary complex, facilitates the initiation of translation by coupling the hydrolysis of the GTP to the binding of the methionine tRNA to the ribosome. Phosphorylation of EIF2 by PERK, GCN2, PKR or HRI prevents recycling of GDP to GTP within the ternary complex by the guanine nucleotide exchange factor, EIF2B, preventing the initiation of translation.

Phosphorylation of serine-51 of the α subunit of eIF2 results in a global suppression of protein translation through both the inability of EIF2 to initiate translation and through the direct inhibition of eIF2B by phosphorylated eIF2 (eIF2-P). Interestingly, a subset of mRNAs remains efficiently translated after eIF2 phosphorylation. The mechanism by which these select mRNAs are translated during the integrated stress response was originally described in yeast for the gene, GCN4, which remains translated during the integrated stress response[2]. Both GCN4 and its mammalian counterpart, activating transcription factor 4 (ATF4), contain upstream open reading frames (uORFs) that normally inhibit translation at their coding reading frame[2–4]. Under the integrated stress response, ribosomes scan past the uORFs, due to a lower abundance of ternary complexes, and translation initiates at their coding ORFs.

Upon translation under the ISR, ATF4 directs a transcriptional program to restore cellular homeostasis and survival[3,5–7]. Among its many transcriptional targets, ATF4 upregulates metabolic enzymes, amino acid transporters and other cytoprotective genes. ATF4 dimerizes with a number of different transcription factors to direct differential gene regulation depending on the heterodimerization partner[8]. Dimerization with C/EBP homologous protein (CHOP), for example, prevents ATF4-mediated activation of Asparagine Synthetase (ASNS) and promotes cell death under prolonged or significant ER stress[9]. Likewise, dimerization of ATF4 with ATF3 promotes transcription of Phorbol-12-Myristate-13-Acetate-Induced Protein 1 (PMAIP1) and activates the intrinsic apoptosis pathway[10]. Further diversity in transcriptional output is thought to be controlled by the degree of ATF4 expression, which is controlled transcriptionally, translationally and post-translationally. Altogether these mechanisms yield a degree of complexity to address the range of stresses that initially activate the ISR.

In addition to activating genes to address the initiating stress, ATF4 activates the transcription of genes responsible for the termination of the ISR. Growth Arrest And DNA-Damage-Inducible 34 (GADD34), a regulatory subunit of the protein phosphatase 1 (PP1) complex, is upregulated to dephosphorylate eIF2 as a negative feedback mechanism[11]. Furthermore, ATF4-induced activation of Tribbles Pseudokinase 3 (TRIB3) inhibits the transcriptional upregulation of CCAAT/Enhancer-Binding Protein Homologous Protein (CHOP) and ASNS in a negative feedback manner[12]. Ultimately, if the ISR is maintained due to an inability of the ATF4 transcriptional program to alleviate stress and restore homeostasis, apoptosis is triggered.

Interestingly, whereas in yeast the integrated stress response is activated by a single eIF2α kinase, GCN2p, mammalian cells have at least four eIF2α kinases. Each of these kinases are activated by distinct stress signals but our current understanding is that these signals converge upon a single gene, ATF4, to coordinate the transcriptional stress response. The diversity of stress inputs converging on a single transcriptional output is surprising as multiple transcriptional regulators could be used to address each unique cellular stress. Future work may reveal additional transcriptional regulators of the integrated stress response that cooperate with ATF4 to manage the far-ranging cellular stresses from unfolded protein accumulation to hypoxia that induce the stress pathway.

1.1.1 The amino acid stress response enables cell adaptation to nutrient deprivation

In cancer, the tumor microenvironment induces several cellular stresses that are addressed by the integrated stress response including hypoxia, nutrient deprivation and/or oxidative stress. Cancer cells may also face intrinsic stresses due to the activation and expression of oncogenes or inactivation of tumor suppressor genes, both of which may activate the integrated stress response. Both N-Myc and C-Myc, for example, have been shown to activate the unfolded protein response (UPR) and ATF4 through PERK activation[13]. Indeed, it has recently been shown that Myc co-opts ATF4 activity through activation of GCN2 in order to maintain an enhanced rate of translation in lymphoma[14]. Interestingly, ablation of ATF4 significantly delayed the development of these models of lymphomas, suggesting a critical role of ATF4 in Myc-driven tumorigenesis.

Under nutrient deprivation, there is an increase in the level of deacetylated transfer RNAs (tRNAs) due to the lack of amino acids present for tRNA synthetase enzymes to catalyze tRNA aminoacylation reactions. Eukaryotic translation Initiation Factor 2 Alpha Kinase 4 (EIF2AK4), also known as GCN2, is directly activated by the accumulation of deacetylated histidine tRNAs to which it may bind[15,16]. GCN2 phosphorylates the α subunit of eIF2, which leads to the translational upregulation of ATF4. Among its diverse transcriptional targets, ATF4 activates a number of amino acid synthesis and transport proteins. Under nutrient deprivation, ATF4 binds to amino acid response elements (AAREs) or nutrient-sensing response elements (NSREs) within the promoters of target genes to promote transcription[17]. In addition to activating the expression of amino acid

synthesis and uptake genes, ATF4 promotes the expression of genes involved in autophagy to increase the removal of unfolded proteins and damaged organelles[18]. In promoting autophagy, ATF4 further restores amino acid abundance to alleviate nutrient stress.

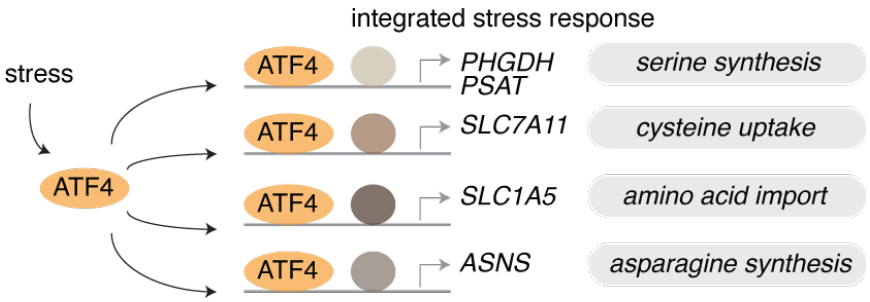

Figure 1.1. Metabolic genes regulated by ATF4, the effector of the integrated stress response
Schematic depicting the various metabolic genes known to be directly regulated by ATF4 with adjacent unknown factors that may specifically assist in the regulation of these genes.

While much has been learned about the role of ATF4 in the response to nutrient deprivation, there remains much to be defined. The mechanisms by which ATF4 restores homeostasis under conditions of specific amino acid deprivation, for example, remain unclear. When cells are deprived of serine, for example, the optimal strategy for a cell would be to upregulate serine transporters and serine synthesis enzymes, phosphoserine aminotransferase 1 (PSAT1) and D-3-phosphoglycerate dehydrogenase (PHGDH). Instead, it seems ATF4 coordinates the upregulation of an entire network of amino acid transporters and enzymes in a non-specific manner under select amino acid deprivation. Whether this finding is true in all amino acid deprivation conditions or whether transcription becomes focused in later stages of nutrient deprivation to efficiently resolve nutrient stress remains unclear.

Furthermore, the transcriptional mediators of the integrated stress response must extend beyond ATF4 as less than half of the genes upregulated in cells upon ER or nutrient stress are direct regulatory targets of ATF4[19]. Further investigations into the mediators of the integrated stress response will identify the mechanisms by which cells respond to various cellular stresses. In the context of cancer, such work may reveal transcription factors required for cancers to overcome hypoxia, nutrient limitation and oxidative stress within the tumor microenvironment, or reveal factors required to support oncogenic transcriptional programs, such as that of Myc.

1.2 Cancer cells reprogram their metabolism to support proliferation and survival in nutrient deplete microenvironments

It has become clear that in the course of cancer development, cancer cells reprogram their metabolism to suit the needs of unrestrained proliferation. Otto Warburg first described the observation that cancer cells reprogram their metabolism toward glycolysis, even in the presence of oxygen, a process termed “aerobic glycolysis”[20]. More recent work defines this energetically unfavorable switch to glycolysis a product of an increased reliance on glycolytic intermediates for various biosynthetic pathways to support cellular growth[21]. Deregulation of cellular energetics is an emerging hallmark of cancer mediated by the oncogenic factors responsible for other core cancer hallmarks[22,23]. Furthermore, a number of oncogenes present across a variety of cancers have been implicated in the regulation of metabolic pathways[24].

Acute leukemias have significantly altered metabolism secondary to oncogenic transformation. ALLs, for example, show increased Myc expression due to translocation events that place the gene downstream of the T-cell receptor or immunoglobulin gene promoters[25]. Myc is also regulated downstream of NOTCH1, which is activated in 60% of T-ALLs[26,27]. Increased Myc expression leads to the upregulation of glycolysis, glutaminolysis and mitochondrial biogenesis, among other metabolic processes. Furthermore, mutations in the RAS-MAPK pathway, as well as, loss of function mutations in PTEN, the negative regulator of the PI3K-AKT pathway are commonly seen in ALL resulting in enhanced glycolysis and mitochondrial metabolism[28,29]. Likewise, AMLs have increased mitochondrial mass and activity resulting in an increased rate of oxygen consumption as compared to their normal hematopoietic stem cell counterparts[30]. Additionally, in line with Otto Warburg’s findings, AMLs exhibit increased rates of glycolysis at diagnosis with high levels of glycolysis predicting improved outcomes[31].

The significantly altered metabolism of cancer, and specifically acute leukemias, has led to the design of therapies targeting metabolic liabilities subsequent to oncogenic transformation. Induction chemotherapy for acute lymphoblastic leukemia, for example, uses L-asparaginase, a bacterial enzyme that depletes serum asparagine, to target the asparagine auxotrophy observed in the disease. Furthermore, L-asparaginase has seen efficacy in acute myeloid leukemia, though this relies upon the off-target depletion of glutamine by this enzyme[32]. Likewise, mutations in isocitrate dehydrogenase 1 and 2 occur in 20% of AMLs resulting in the generation of an oncogenic metabolite, 2-hydroxyglutarate (2-HG)[33,34]. 2-HG has been shown to directly impact alpha-ketoglutarate-dependent dioxygenase activity resulting in alterations in DNA and histone methylation, and, ultimately, altering differentiation[35–37]. Mutant IDH inhibitors have been developed and approved for the treatment of IDH-mutant AML[38,39]. Given the recent identification of a number of nutrient dependencies in cancer, these may be the first of many examples of the therapeutic targeting of metabolism in leukemia, and cancer more broadly[40].

Additional metabolic pathways have been proposed as potential therapeutic targets in acute leukemia and cancer. In AML, dihydro-orotate dehydrogenase (DHODH), an enzyme required for de-novo pyrimidine synthesis, was identified as a target whose inhibition led to AML cell differentiation[41]. Recent work to target mitochondrial activity through targeting mitochondrial translation or protease activity has seen positive results in AML[30,42]. Furthermore, a clinical grade electron transport chain inhibitor, IACS010759, is currently in phase I clinical trial for AML[43]. Finally, most AML patients have been shown to have absent arginosuccinate synthetase-1 (ASS1) expression. This enzyme is responsible for the production of argininosuccinate from citrulline and aspartate. This observation suggested a dependency on extracellular arginine in AMLs, which is currently being tested through the use of a pegylated arginine deiminase in a similar manner to L-asparaginase[44,45].

Interestingly, it has even been shown that deletion of the pyruvate kinase isoform (PKM2) or lactate dehydrogenase A (LDHA) significantly extends the latency of acute myeloid leukemia development in BCR-ABL and MLL-AF9 mouse models of the disease[46]. Importantly, loss of these metabolic enzymes did not alter normal hematopoiesis as quickly as leukemic cell growth suggesting that there may be a therapeutic window wherein leukemic cells have a dependency on these enzymes. Altogether, these results suggest that targeting the altered metabolism of cancer may be a viable therapeutic strategy, and, as such, a thorough understanding of the cellular response to such metabolic therapies will inform sensitivity and resistance to these therapies.

1.3 L-Asparaginase targets the amino acid stress response in the treatment of acute lymphoblastic leukemia

The asparagine dependency of certain blood cancers was fortuitously discovered by John Kidd and his colleagues in 1953. While testing animal sera as a source of complement for the treatment of lymphomas, Kidd and colleagues found that serum of guinea pigs, but not that of other animals, caused a strong regression of engrafted mouse lymphomas[47]. Eight years later, JD Broome identified the component of guinea pig serum responsible for tumor regression as asparaginase, an enzyme that effectively depletes serum asparagine[48]. Although earlier studies established the requirement for L-asparagine supplementation for the growth of these lymphomas, the discovery of L-asparaginase was the first conclusive demonstration of a tumor metabolic requirement[49]. Initial attempts to exploit this dependency in patients involved the use of guinea pig serum until the isolation of an *E. coli* L-asparaginase, which accelerated the clinical use of the strategy[50,51]. As a monotherapy, L-asparaginase has been shown to cause tumor regression in 20-60% of ALL patients and is a critical component of induction chemotherapy for ALL[52–54].

Unlike leukemias, most human cell types can synthesize asparagine from aspartate through an ATP dependent reaction catalyzed by asparagine synthetase (ASNS)[55].

Consistent with this, normal cells can survive asparagine depletion by upregulating ASNS transcription and de novo asparagine synthesis. ASNS transcription is mediated by the integrated stress response (ISR). Under asparagine deprivation, the ISR is activated and ATF4 is expressed to coordinate the upregulation of several nutrient transporters and enzymes, such as ASNS, providing essential nutrients required for survival under nutrient deprivation. The role of asparagine in leukemia cells is likely limited to its proteogenic use in translation as ribosome profiling studies have shown that asparagine limitation halts translation at asparagine residues[56–58]. Indeed, reduction of serum asparagine with L-asparaginase potently restricts global protein synthesis and induces apoptosis in ALL cells[58–60]. Recent work, however, has also highlighted a function of asparagine as an amino acid exchange factor potentially coordinating both protein and nucleotide synthesis[61].

Building upon the success of L-asparaginase for the treatment of blood cancers, there is growing interest in its use for the treatment of solid tumors. Early clinical trials of L-asparaginase across neoplastic diseases found a partial response in melanoma and lymphoma patients[53]. Additionally, hepatocellular carcinomas, gastric and pancreatic cancers with low expression of ASNS exhibit sensitivity to L-asparaginase[62–64]. Finally, asparagine availability strongly regulates metastatic potential as L-asparaginase treatment reduces the epithelial-to-mesenchymal transition, invasiveness and metastatic progression[65]. It should be noted that administration of L-asparaginase may also result in significant depletion of serum glutamine levels at higher doses[66,67]. However, in cells expressing low levels of ASNS, the asparaginase activity, and not the glutaminase activity of L-asparaginase, is sufficient to induce cell death[68]. To overcome this challenge, L-asparaginases have been engineered with negligible off-target glutaminase activity, which may reduce these toxic side-effects associated with therapy[69].

As a clinical therapy for ALL, L-asparaginase represents the most successful exploitation of a metabolic sensitivity of a cancer type for therapy. The mechanisms by which ALLs develop resistance to L-asparaginase, however, are debated (Figure 1.2). Given the role of the integrated stress response in governing the restoration of cellular homeostasis under nutrient deprivation, it is likely that ATF4 is critical to the development of resistance to L-asparaginase, but the precise mechanisms of resistance remain unexplored. Furthermore, it has not been determined whether additional factors are required for ATF4-mediated upregulation of genes required specifically under asparagine deprivation. Studying both resistance to the therapy, and determinants of sensitivity to L-asparaginase have implications for the clinical success of the drug both within ALL and in other cancer types in the future.

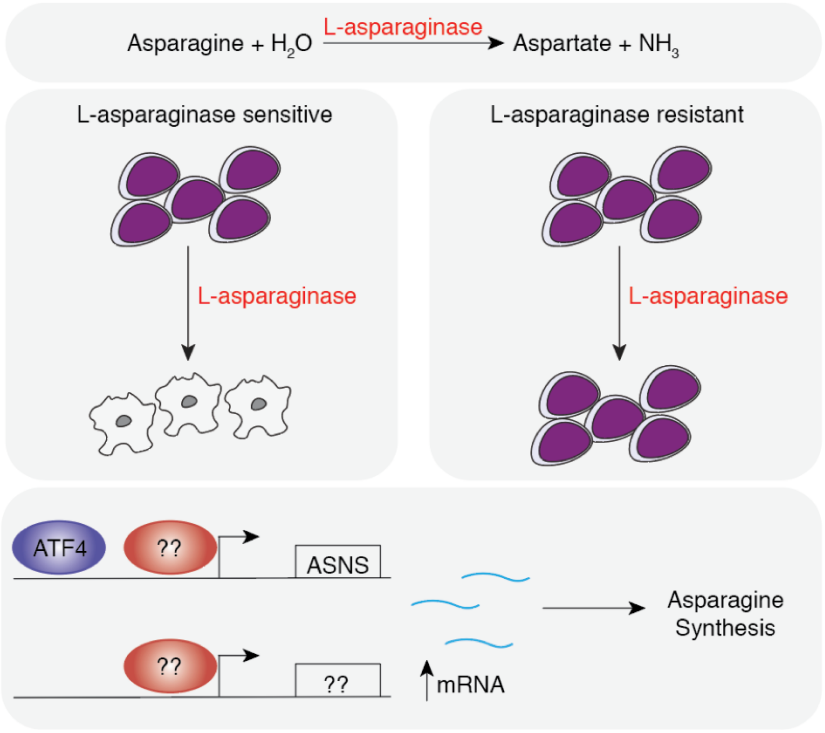

Figure 1.2 L-asparaginase degrades asparagine inducing cell death in ASNS-deficient ALLs

1.4 Toxic lipid incorporation as a potential therapeutic approach in acute myeloid leukemia

Cancer cells rely upon fatty acid synthesis to generate membrane phospholipids required for continued cellular growth and division. Fatty acids (FAs) are synthesized from cytoplasmic acetyl-CoA, which can be produced from glutamine, glucose or acetate[70,71]. This process provides “non-essential” fatty acids, those that can be synthesized by mammalian cells, whereas lipid uptake is required to provide very long-chain and poly-unsaturated fatty acids, or “essential” fatty acids, which come from the diet.

Normal, non-neoplastic tissues rely almost entirely upon circulating dietary fat for their free fatty acid requirements, and show absent or limited fatty acid synthase (FASN) activity[72]. FA synthesis is generally restricted to adipose tissue, the liver and the breast, however, increased fatty acid synthesis through the activities of FASN, acetyl-CoA carboxylase (ACACA) and stearoyl-CoA desaturase 1 (SCD1) has been observed across nearly all types of cancers[73,74]. Indeed, analogous to Warburg’s discovery of aerobic glycolysis, Grace Medes identified a significant contribution of heavy labeled glucose to lipogenesis within tumor tissue[75]. Importantly, this phenomenon occurs irrespective of the availability of circulating lipids that could be taken up by these lipogenic cells.

While the precise benefits of enhanced lipid synthesis within tumors remain unclear, it has been demonstrated that excessive fatty acid synthesis within cancer cells increases the proportion of saturated or monounsaturated fatty acids protecting cells from oxidative damage and ferroptosis associated with an abundance of poly-unsaturated fatty acids[76]. Indeed, the enrichment of saturated lipid species has also been shown to protect cells from chemotherapeutics, such as daunorubicin or BRAF inhibition in melanoma[77]. While these lipogenic tumors rely upon increased rates of fatty acid synthesis, they also rely upon increased uptake of fatty acids through the cell surface receptor CD36[78,79].

Leukemic cells primarily grow within the bone marrow, a lipid rich microenvironment. Adipocytes represent a large proportion of the cells within human bone marrow and their number increases with age[80]. In co-culture experiments, AML blasts induce lipolysis within adipocytes to increase free fatty acid availability[81]. Fatty acids are imported into AML cells by the cell surface transporter CD36, and subsequent fatty acid oxidation (FAO) by AML cells can generate over twice as much ATP as the oxidation of an equimolar amount of glucose[82]. Free fatty acids can serve both as a source of acetyl-CoA for anaplerosis of the TCA cycle and as lipid biomass for future cellular divisions. The abundance of adipocytes within the bone marrow and evidence that leukemic cells can influence their activity for their benefit has been confirmed in mouse models of leukemia where higher rates of relapse after chemotherapy are seen in obese mice. Indeed, mice fed a high-fat diet show enhanced outgrowth of acute myeloid leukemias[83,84]. Altogether, this evidence suggests that AMLs, and potentially leukemias in general, are lipogenic tumors that not only upregulate fatty acid synthesis, but also rely upon uptake of exogenous fatty acids.

Targeting the lipogenic phenotype in AML has been successful *in vitro*, however, there has been difficulty in translating these findings *in vivo*. Inhibition of fatty acid synthase (FASN) and steroyl CoA desaturase 1 (SCD1) can promote apoptosis in AML among other cancers[85,86]. Furthermore, FAO inhibitors, such as etomoxir, ranolazine, perhexiline, or ST1326, similarly induce apoptosis or inhibit proliferation in AML[87–89]. A novel FAO inhibitor derived from the avocado fruit, avocatin B, for example, directly inhibits the proliferation of AML cells grown *in vitro.* Co-culture of AML cells with adipocytes facilitates resistance to inhibition of beta oxidation through a metabolic switch to glycolysis. Interestingly, numerous reports suggest that a combination of FAO inhibition and chemotherapy, even in adipocyte co-culture experiments, can overcome therapy resistance and the metabolic switch to glycolysis. Whether sensitivity of these drugs relate to beta oxidation for metabolic purposes, or to the balance of saturated and unsaturated lipids within membranes remains to be determined. Altogether, however, these results suggest that targeting various aspects of lipid metabolism within rapidly growing and dividing AML cells may be worthwhile therapeutically[90,91]. Indeed, disruption of cholesterol biosynthesis through the inhibition of HMG CoA reductase with simvastatin has been shown to impact the proliferation of AML cells, *in vivo*[92].

Whether for the purposes of beta oxidation or lipid biomass accumulation, extracellular lipid uptake may represent a potential therapeutic intervention point for acute myeloid leukemia and other cancers. Rapidly proliferating mammalian cells need a continuous supply of polyunsaturated fatty acids thus requiring constant lipid uptake[93]. As such, manipulation of this lipogenic phenotype through the delivery of xenobiotic lipid species with toxic payloads that are activated by beta oxidation or upon lipid incorporation may represent a tactic with a viable therapeutic window.

Previous studies have identified xenobiotic species that incorporate into lipids in a manner dependent on the presence of a carboxylic acid (Figure 1.3)[94,95]. Ibuprofen and the entire profen drug family, for example, have been shown to incorporate into lipid triacylglycerols[96,97]. Xenobiotic carboxylic acids are modified by acyl-CoA synthetase enzymes (ACSLs) which replace the carboxylic acid with a CoA ester in order to activate the xenobiotic for manipulation by acyl transferase enzymes. The fibrates, a class of drugs used for the treatment of hypertriglyceridemia and hypercholesterolemia, incorporate into lipid species in the same fashion. Physiologically, the fibrates activate peroxisome proliferator-activated receptor alpha (PPAR-A) leading to increased fatty acid uptake, conversion to fatty acyl-CoA, and enhanced peroxisomal and mitochondrial beta-oxidation within the liver[98–100]. Furthermore, fibrates increase the removal of low-density lipoproteins (LDLs) and decrease triglyceride-rich lipoproteins within the plasma.

While the fibrates are effective at lowering circulating lipid levels in a generally non-toxic manner, it may be possible to design xenobiotic carboxylic acids that produce cellular toxicity within target tissues. The precise mechanism by which existing xenobiotic carboxylic acids cause toxicity, however, is unclear. Through their lipid incorporation, xenobiotic carboxylic acids may inhibit mitochondrial beta oxidation and lipid metabolism through the sequestration of coenzyme A and carnitine, or through the direct inhibition of enzymes[101–103]. Indeed, protonated species may pass from the intermembrane space to the mitochondrial matrix to, in effect, reverse the mitochondrial membrane potential and inhibit both oxidative phosphorylation and beta oxidation. Second, xenobiotic carboxylic acids may be metabolized to acyl-CoA and subsequently transacylate glutathione to generate acyl-glutathione adducts, thereby reducing free glutathione available for the reduction of oxidative species leading to oxidative stress and subsequent cell death[104]. Finally, carboxylic acids can be used to transacylate proteins, though the implications of such protein-carboxylic acid conjugates remain poorly understood[105,106].

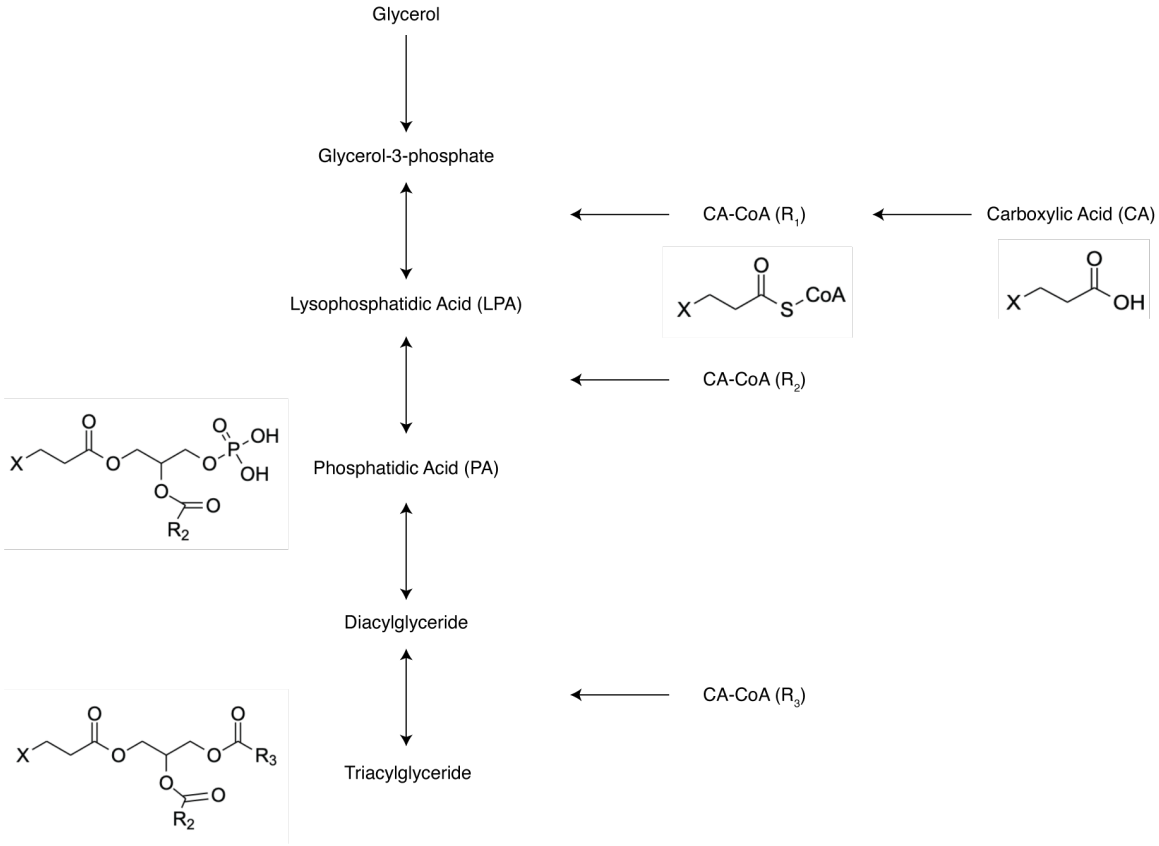

Figure 1.3 Incorporation of xenobiotic carboxylic acids
Schematic depicting the pathway and enzymes involved in the synthesis of glycerolipids with a generalized carboxylic acid depicted to demonstrate the incorporation of xenobiotic carboxylic acids.

Regardless of their precise mechanism of action, xenobiotic carboxylic acids have been shown to disturb mitochondrial membrane potential and cause mitochondrial damage. Such mitochondrial damage underlies the hepatotoxicity observed with non-steroidal anti-inflammatory drugs (NSAIDs) which are similarly conjugated to lipids and cause mitochondrial uncoupling resulting in mitochondrial dysfunction and cellular death[107–109]. Given the increased reliance of leukemias upon mitochondrial oxidative phosphorylation and beta oxidation, a rationally designed toxic carboxylic acid species capable of lipid incorporation and direct mitochondrial inhibition should be explored as a novel therapeutic approach in leukemia.

1.5 Overview and Significance of findings

We have investigated the transcriptional machinery required for the proliferation of cells under various metabolic stresses. Our work has pinpointed a number of known transcriptional regulators important for cell growth in certain nutrient deprivation and metabolic stress conditions. Additionally, this work provides a framework for identifying novel transcriptional regulators of cellular stress response pathways. As a proof-of-principle, here, we identified a transcription factor, Zinc Finger and BTB Domain Containing 1 (ZBTB1), that is required for the growth of T-ALLs under asparagine deprivation. We have shown that ZBTB1 directly binds to the promoter of ASNS to regulate its transcription. Upon loss of ZBTB1, cells have diminished transcription of ASNS, and, as a result, cannot synthesize sufficient asparagine for proliferation in the absence of the amino acid. We found that ZBTB1 knockout sensitized therapy resistant T-ALLs to treatment with L-asparaginase, a bacterial enzyme that depletes serum asparagine, *in vitro* and *in vivo*. This work further defines the transcriptional regulation of ASNS, a gene critical for resistance to L-asparaginase. Furthermore, this work investigates the mechanism of action of a compound, CPI-613, currently in clinical trials for the treatment of acute myeloid leukemia and pancreatic cancer. While CPI-613 was designed as a lipoic acid analog capable of inhibiting TCA cycle enzyme complexes, our work reveals that CPI-613 is incorporated into lipid species and that its toxicity may instead relate to its presence within triacylglycerol species. This work defines the precise mechanism of an investigational new drug and suggests a novel therapeutic strategy to target the reliance upon exogenous lipid uptake for cancer growth and resistance to chemotherapy.

CHAPTER 2. Transcriptional determinants of cellular proliferation under various metabolic stress conditions

2.1 CRISPR-based genetic screens identify transcription machinery essential for proliferation under metabolic stress

In order to investigate the transcriptional regulators required for the cellular response to various metabolic insults, I designed and generated a CRISPR-Cas9 library composed of 20,051 single guide RNAs (sgRNAs) targeting 2,509 genes involved in transcription. I hypothesized that I could use this library to identify transcriptional regulators that are required for cellular proliferation under particular metabolic and nutrient stresses (Figure 2.1). Guides targeting ATF4, for example, should sensitize cells to most, if not all, of the cellular stresses that activate the integrated stress response given ATF4's central role in directing the transcriptional program under the ISR. In order to identify transcriptional regulators required for proliferation under metabolic stresses, I performed negative selection, loss-of-function genetic screens under lipotoxic conditions, chemical inhibition of the electron transport chain, and amino acid deprivation.

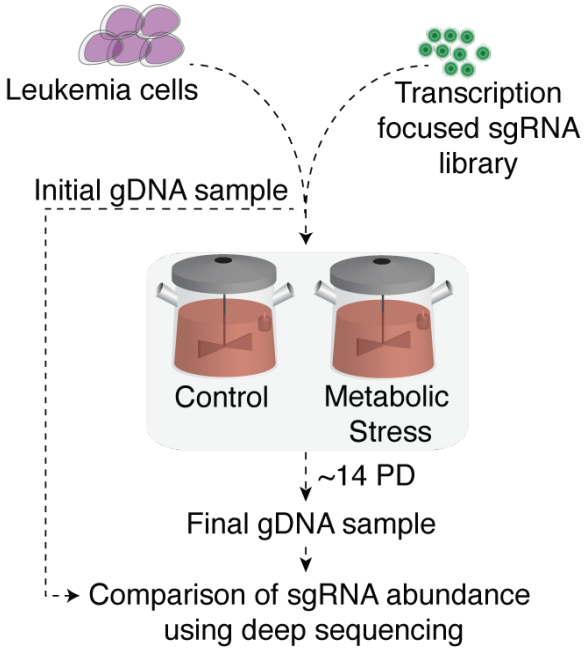

Figure 2.1 CRISPR-based screen for transcriptional regulators of metabolic stress response
Schematic depicting pooled transcription focused CRISPR screens.

2.1.1 Sterol regulatory element-binding protein 1 is required for proliferation in excess saturated fatty acid conditions

Previous work in our laboratory used a saturated fatty acid, palmitate, in order to identify regulators of glycerolipid synthesis[110]. High concentrations of palmitate induce lipotoxicity through the imbalance of saturated and unsaturated fatty acids which inhibits cellular proliferation through a number of mechanisms including mitochondrial dysfunction and increased reactive oxygen species production which ultimately contribute to apoptosis[111,112]. Increased rigidity of the endoplasmic reticulum's membrane also occurs subsequent to saturated fatty acid overload leading to the activation of PERK and stimulation of the integrated stress response[113,114]. Palmitate toxicity permits negative selection genetic screening to identify genes involved in both the resistance and sensitivity of cells to saturated fatty acid overload. I used palmitate to identify transcriptional regulators of the response of cells to toxic doses of this saturated fatty acid. I hypothesized that this genetic screen would identify important regulators of fatty acid metabolism and, perhaps, regulators of the ISR induced by ER stress.

This screen revealed that Sterol Regulatory Element Binding Transcription Factor 1 (SREBF1) was required for the survival of cells under palmitate treatment (Figure 2.2). The sterol regulatory element-binding proteins (SREBPs) are a family of helix-loop-helix leucine zipper transcription factors. The SREBF1 gene encodes two isoform, SREBP1a and SREBP1c, whereas the SREBF2 gene encodes SREBP2. Upon migration from the ER to the golgi, SREBPs are proteolytically activated by SREBP cleavage activating protein (SCAP) and translocate to the nucleus. SREBPs bind to sterol regulatory elements (SREs) within the promoter of genes to regulate transcription[115,116]. It has previously been shown that a critical role of SREBP is to coordinate fatty acid synthesis with desaturation in order to maintain a balance of saturated and unsaturated fatty acids within the cell. Knockdown of SREBP results in a loss of desaturation while saturated fatty acid synthesis is maintained. Simply providing monounsaturated fatty acids could rescue the effects of SREBP knockdown within cells[117].

This genetic screen did not identify ATF4 or other members of the integrated stress response as required for the proliferation of cells under ER stress driven by saturated fatty acid overload suggesting this may not be a predominant mechanism of toxicity within this cell line. The identification of SREBF1, however, served as proof-of-principle that this genetic screening approach could identify transcriptional regulators pertinent to a specific cellular stress.

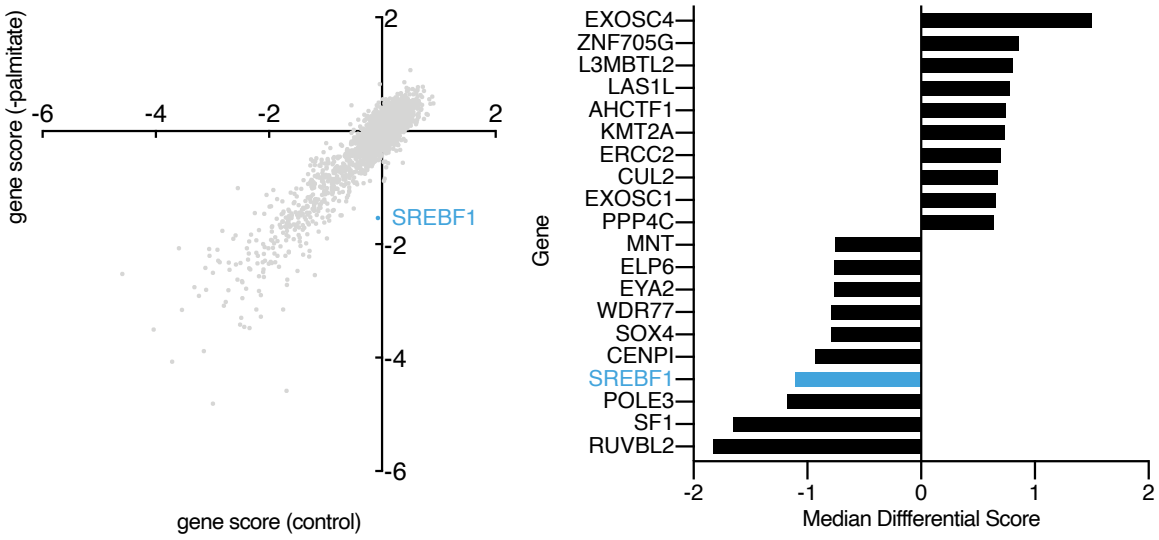

Figure 2.2. CRISPR-based screen for transcriptional regulators of glycerolipid synthesis
(Left) Gene scores for untreated versus palmitate (12.5uM) treated Jurkat cells. Most genes scored similarly under untreated or treated conditions.
(Right) Median differential score for top 10 genes in either the positive or negative direction.

2.1.2 KANSL1 is required for the cellular response to electron transport chain inhibition

The mechanisms by which cells detect, sense and respond to mitochondrial- stress remain poorly understood. It has been established that mitochondrial dysfunction activates the integrated stress response, and ATF4 activates a transcriptional program to restore homeostasis[118]. Until recently, however, it was unclear which of the four eIF2α kinases was responsible for the initiation of the integrated stress response under mitochondrial stress. Two groups independently identified heme-regulated inhibitor (HRI) as the eIF2α kinase that senses mitochondrial stress through interactions with DELE1[119,120]. Upon mitochondrial stress, the protease, Overlapping Activity With M-AAA Protease (OMA1), is activated and cleaves DAP3 Binding Cell Death Enhancer 1 (DELE1), a protein associated with the inner mitochondrial membrane. Upon cleavage, DELE1 moves to the cytosol to activate HRI and stimulate the integrated stress response. To explore the induction of mitochondrial stress and determine whether any particular transcriptional regulator was required for cellular proliferation under electron transport chain inhibition, we performed a transcription-focused genetic screen under chemical inhibition of complex I and III using piericidin and antimycin, respectively (Figure 2.3).

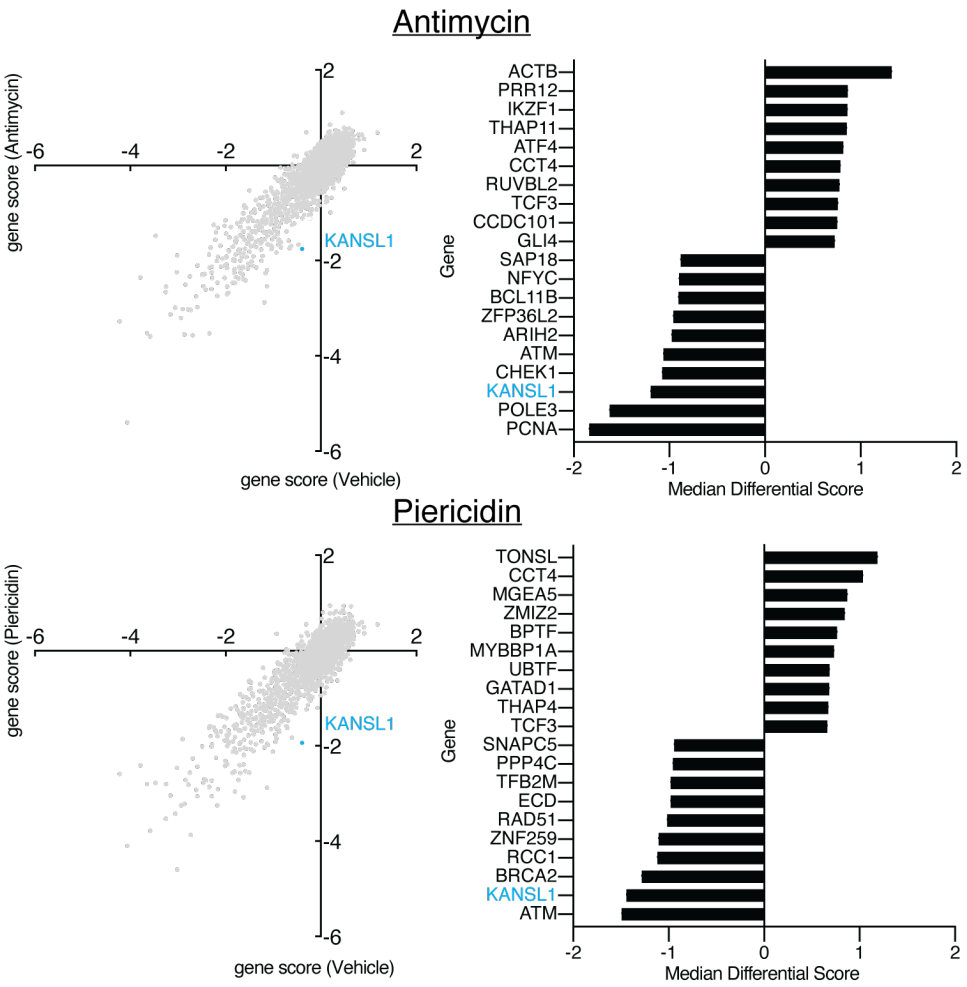

Figure 2.3 CRISPR-based screen for transcriptional regulators of the cellular response to electron transport chain inhibition
(Left) Gene scores for untreated versus antimycin (top) or piericidin (bottom) treated Jurkat cells. Most genes scored similarly under untreated or treated conditions. (Right) Median differential score for top 10 genes in either the positive or negative direction.

Interestingly, ATF4 was not essential under piericidin or antimycin treatment, suggesting that the mitochondrial stress faced under ETC inhibition is distinct from that of other mitochondrial stresses, such as mitochondrial translation inhibition or loss of mitochondrial membrane potential. Future screens to under such stresses may yield transcriptional regulators under the integrated stress response as induced by mitochondrial stress.

Interestingly, KAT8 regulatory NSL complex subunit 1 (KANSL1) was required for proliferation under both piericidin and antimycin treatment. This gene is a member of a nuclear histone acetyltransferase complex known as the MOF (males absent on the first) complex. KANSL1 and the MOF complex were recently described to enrich in the

mitochondria to regulate mitochondrial gene expression. MOF knockout was shown to result in respiratory defects consistent with our findings that KANSL1 and the MOF complex may be essential under ETC inhibition[121].

2.1.3 An outer mitochondrial membrane ubiquitin ligase is essential for proliferation in the absence of conditionally essential amino acids

Essential amino acids, as opposed to non-essential amino acids, are those which cannot be synthesized by mammalian cells. As such, essential amino acids must come from exogenous sources. Conditionally essential amino acids are those which can be synthesized, but under certain stress conditions synthesis of these amino acids alone is insufficient for survival. Arginine, for example, may be synthesized from glutamine, however, in catabolic states arginine may be limiting and thus uptake from exogeneous sources is necessary[122]. Similarly, tyrosine can be synthesized from phenylalanine by the enzyme phenylalanine hydroxylase, which is absent in the inherited disorder known as phenylketonuria (PKU). In PKU, phenylalanine accumulates within the blood and tyrosine becomes an essential amino acid. Jurkat cells lack the ability to grow in the absence of tyrosine and arginine due to their lack of expression of these synthesis enzymes, however, the amount of each amino acid present within media is sufficient for cell growth. As such, I performed a transcription-focused CRISPR-based genetic screen in Jurkat cells grown in media lacking one of these amino acids (Figure 2.4).

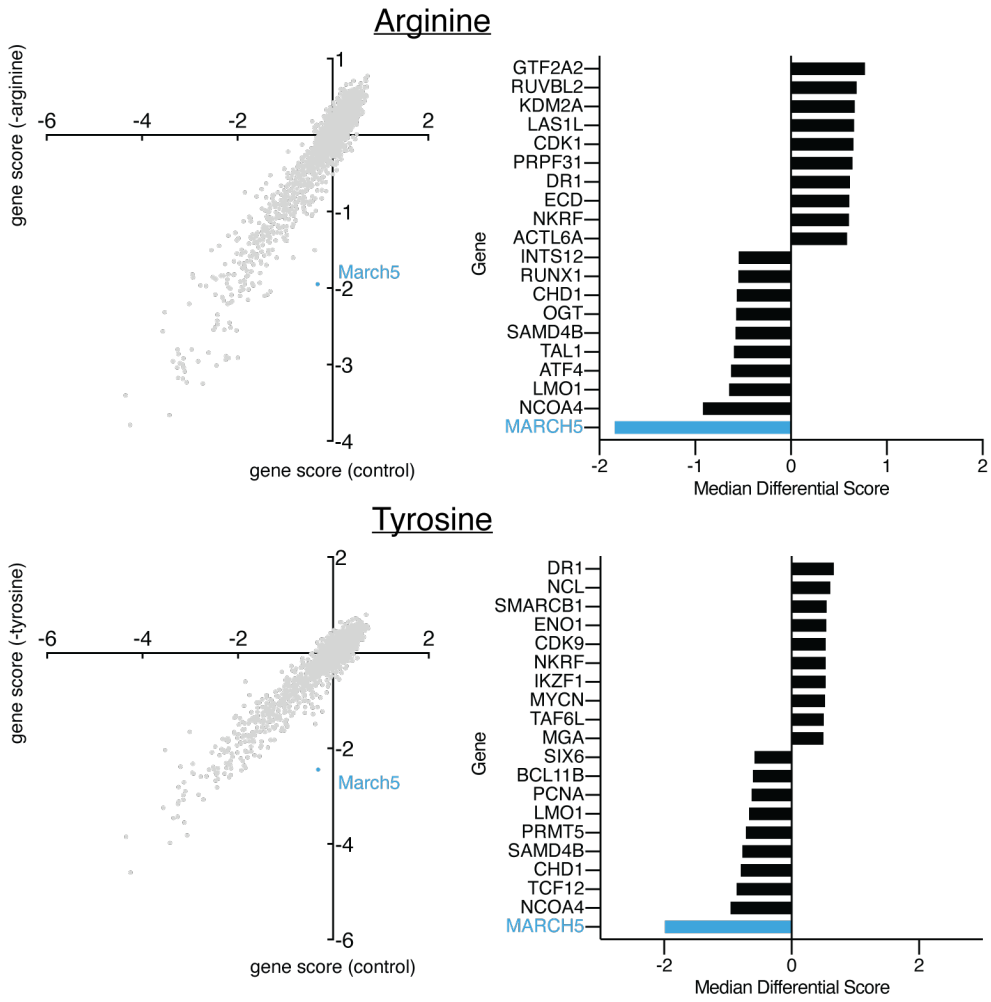

Figure 2.4 CRISPR-based screen for transcriptional regulators of the cellular response to non-essential amino acid deprivation
(Left) Gene scores for Jurkat cells grown in complete versus -arginine (top) or -tyrosine (bottom) media. Most genes scored similarly under both conditions.
(Right) Median differential score for top 10 genes in either the positive or negative direction.

Interestingly, cells expressing sgRNAs targeting the MARCH5 gene were incapable of proliferating when deprived of arginine or tyrosine. Membrane Associated Ring-CH-Type Finger 5 (MARCH5) is a ubiquitin ligase protein that resides on the outer mitochondrial membrane. This gene has been described to play a role in the regulation of mitochondrial fission and fusion, as well as, mitophagy and apoptosis[123]. Similar to the process of autophagy, mitophagy is a mechanism by which cells respond to starvation or nutrient deprivation by recycling mitochondria to provide amino acids and other nutrients[124]. I hypothesize that loss of MARCH5 sensitizes cells to the deprivation of both arginine and tyrosine due to the inability of MARCH5 knockout cells to induce mitophagy. Future work is needed to delineate the precise mechanisms by which MARCH5 induces sensitivity to these conditionally essential amino acids. Importantly,

arginase, an enzyme designed to reduce arginine within the serum, is currently under clinical investigation for the treatment of AML, thus insights into the cellular response to arginine deprivation may be pertinent to sensitivity to this therapy[125,126].

2.2 A CRISPR-based genetic screen identifies transcription machinery essential for proliferation under non-essential amino acid deprivation

When depleted of individual amino acids such as serine or asparagine, human cells upregulate the expression of several nutrient transporters and biosynthetic enzymes in an ATF4-dependent manner to conserve amino acid pools (Figure 2.5). Among the major targets of ATF4 are asparagine synthetase (ASNS) and serine synthesis enzymes, phosphoglycerate dehydrogenase (PHGDH) and phosphoserine aminotransferase (PSAT), which enable human cells to proliferate under asparagine or serine deprivation, respectively[127,128]. Dependencies on these distinct biosynthetic enzymes provide an opportunity to identify transcriptional machinery regulating specific branches of ATF4-induced metabolic gene expression. We therefore performed negative selection genetic screens to identify genes whose loss would inhibit the fitness of human cells upon serine or asparagine depletion (Figure 2.7). Additionally, for our screens, we used a T-cell acute lymphoblastic leukemia cell line, Jurkat, because of its ability to grow in the absence of serine and asparagine (Figure 2.6). Comparing essentialities under different amino acid deprivation conditions should reveal transcriptional processes unique to distinct ATF4 targets and identify novel transcriptional programs.

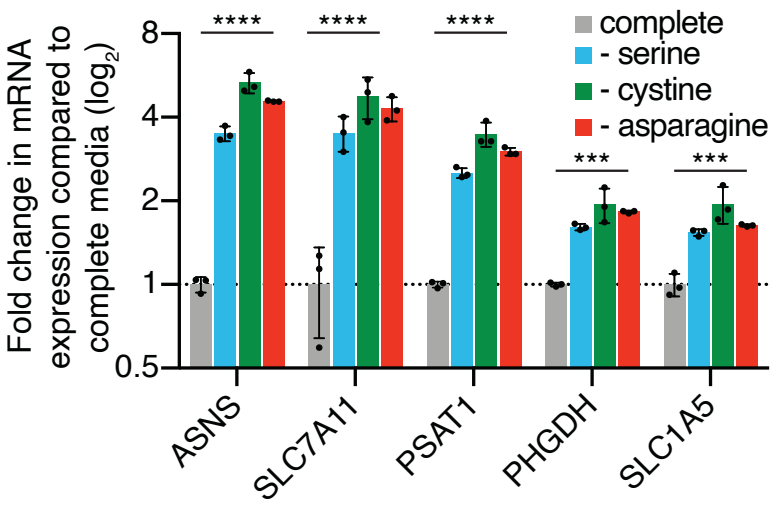

Figure 2.5. ATF4 upregulates the transcription of nutrient import and synthesis genes
Relative mRNA levels of indicated genes in parental Jurkat cells grown in complete (gray), serine-free (blue), cystine-free (green) or asparagine-free (red) media for eight hours (mean ± SD, n=3). Statistics: two-tailed unpaired t-test. **P<0.05, ***P<0.01, ****P<0.001.

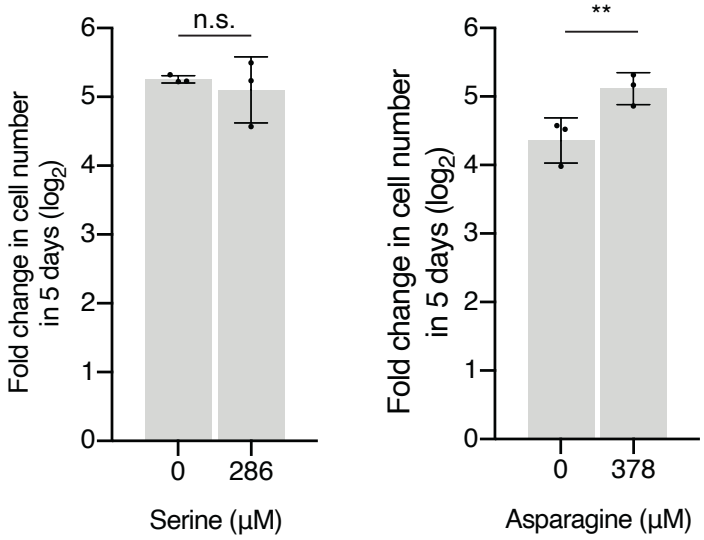

Figure 2.6. Jurkat T-ALL cells can grow in the absence of serine or asparagine
Fold change in cell number (log_2) of parental Jurkat cells after growth in media with indicated serine (left) or asparagine (right) concentrations for 5 days (mean ± SD, n=3). Statistics: two-tailed unpaired t-test. **P<0.05, ***P<0.01, ****P<0.001.

2.2.1 ATF4 is universally required for cellular proliferation under amino acid deprivation

Among the genes universally essential in the absence of asparagine or serine was ATF4, confirming its general role in the adaptive response to amino acid deprivation (Figure 2.7). Our screens also identified factors that have been previously reported to be selectively essential under particular amino acid deprivations. For example, the histone H3 methyltransferase G9A (also known as EHMT2) was selectively required for cellular proliferation under serine, but not asparagine deprivation (Figure 2.7). EHMT2 has previously been shown to catalyze the mono and dimethylation of H3K9 and to regulate serine-glycine biosynthesis[129]. Similarly, another gene required under serine deprivation, SF3B1, regulates PHGDH splicing and serine synthesis[130,131] (Figure 2.7). Relatedly, serine/arginine-rich splicing factor 1 (SRSF1), which contains over 20 serine residues predominantly within its C-terminus, was essential for cellular proliferation under serine deprivation. These data suggested that non-essential amino acid dependencies can be utilized to discover transcriptional machinery regulating essential biosynthetic pathways.

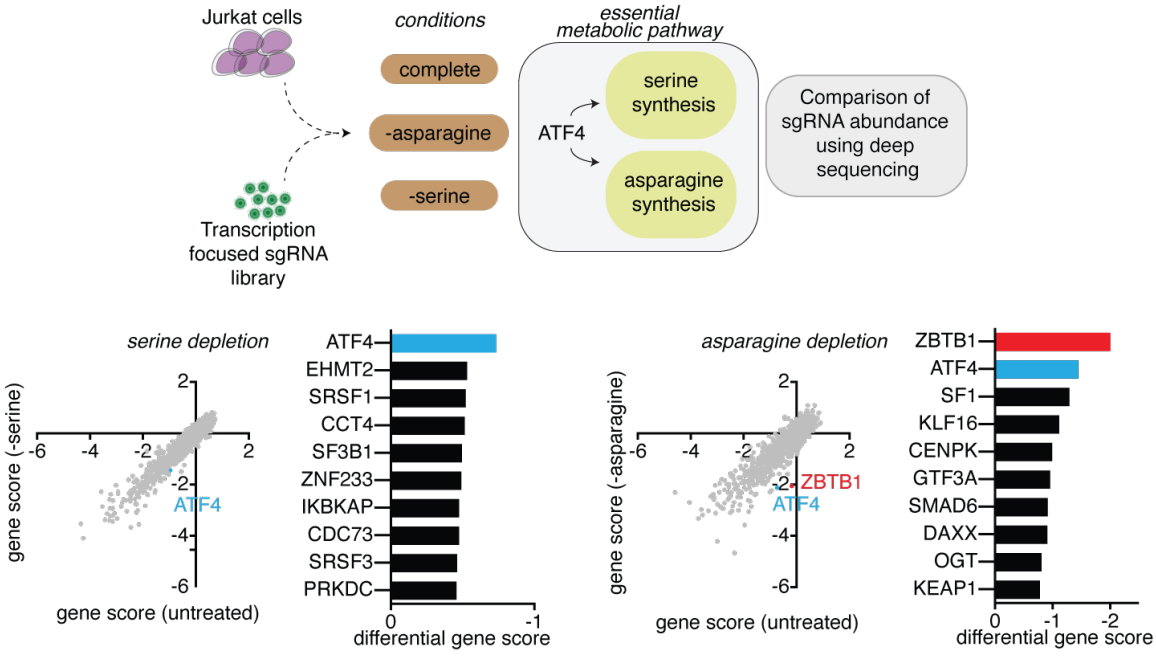

Figure 2.7. CRISPR-based screen under asparagine or serine deprivation
(Top) Schematic depicting pooled CRISPR screens under asparagine or serine deprivation using a transcription-focused sgRNA library.
(Bottom left) Gene scores for complete (x-axis) versus serine deprivation (y-axis) and top 10 transcriptional genes differentially required under serine deprivation.
(Bottom right) Gene scores for complete (x-axis) versus asparagine deprivation (y-axis) and top 10 transcriptional genes differentially required under asparagine deprivation.

2.2.2 ZBTB1 is required for cellular proliferation in asparagine depleted conditions

Remarkably, under asparagine deprivation, Zinc Finger and BTB Domain Containing 1 (ZBTB1) was the highest scoring gene with 7 out of 8 sgRNAs being differentially depleted under asparagine, but not serine deprivation (Figure 2.8). ZBTB1 is a transcription factor with a described role in T-cell differentiation that has not previously been associated with the response to asparagine deprivation or with a role in cellular metabolism[132–134]. To validate the results of our screen, we used the CRISPR-Cas9 system to generate two clonal knockouts of ZBTB1, in which ZBTB1 protein was undetectable (Figure 2.9). While loss of ZBTB1 did not impact proliferation under standard culture conditions, ZBTB1 knockout cells were highly sensitive to asparagine deprivation and to treatment with L-asparaginase, a drug that depletes serum asparagine levels. Notably, overexpression of an sgRNA resistant ZBTB1 cDNA completely rescued both phenotypes, confirming the results of our genetic screens.

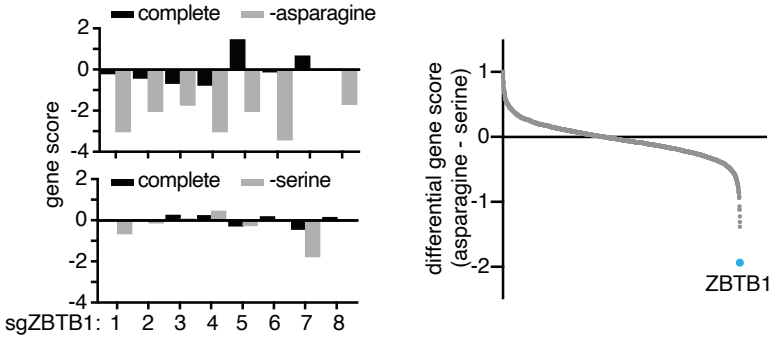

Figure 2.8. Guide RNAs targeting ZBTB1 are depleted under asparagine deprivation conditions
(Left) Changes in the abundance of individual ZBTB1 sgRNAs in complete media (black) or in the absence (gray) of asparagine (top) or serine (bottom).
(Right) Differential scores of genes required specifically under asparagine deprivation relative to serine deprivation. ZBTB1 is highlighted in blue.

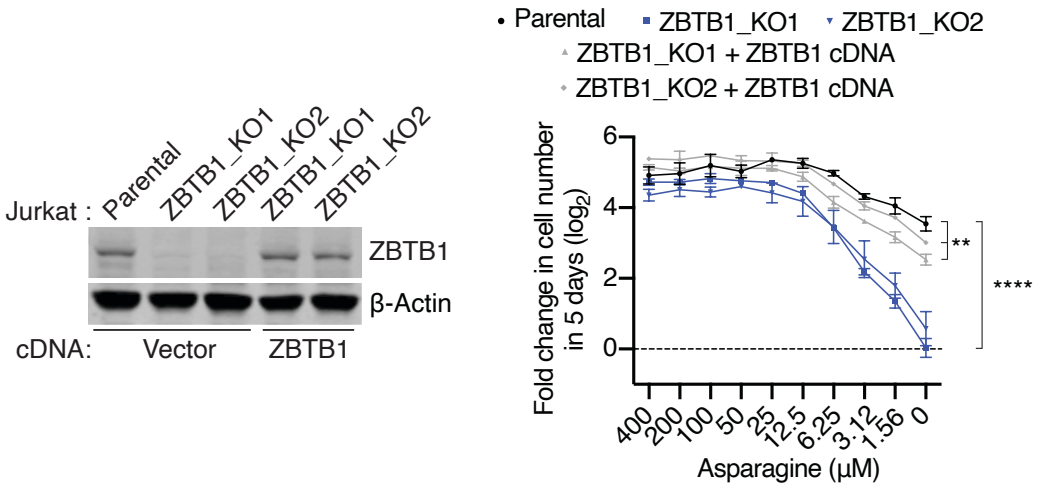

Figure 2.9. ZBTB1 enables proliferation under asparagine deprivation
(Left) Immunoblot analysis of parental, ZBTB1 knockout, and rescued ZBTB1 knockout Jurkat cells (top). β-actin was used as a loading control.
(Right) Fold change in cell number (log_2) of parental (black), ZBTB1 knockout (blue), and rescued ZBTB1 knockout (gray) Jurkat cells after growth in media with indicated asparagine concentrations for 5 days (mean ± SD, n=3).

We next asked whether ZBTB1 was involved in the cellular response to deprivation of other amino acids in addition to asparagine in a role similar to ATF4. To test this possibility, we generated clonal knockouts of ATF4 (Figure 2.10). Interestingly unlike ATF4 knock out cells, which cannot grow in the absence of asparagine, serine, glutamine or cysteine, ZBTB1 knock out cells were only sensitive to asparagine depletion (Figure 2.11).

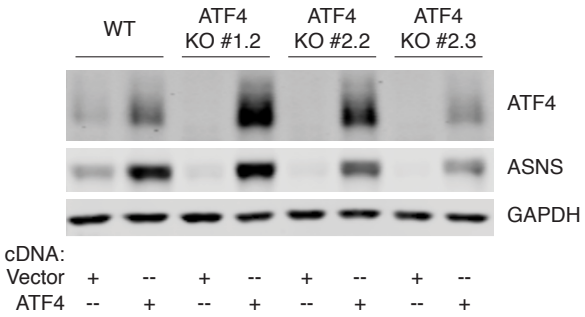

Figure 2.10. Generation and validation of ATF4 knockout cells
Immunoblot analysis of parental, ATF4 knockout, and ATF4 knockout expressing ATF4 cDNA Jurkat cells, as indicated. GAPDH was used as a loading control.

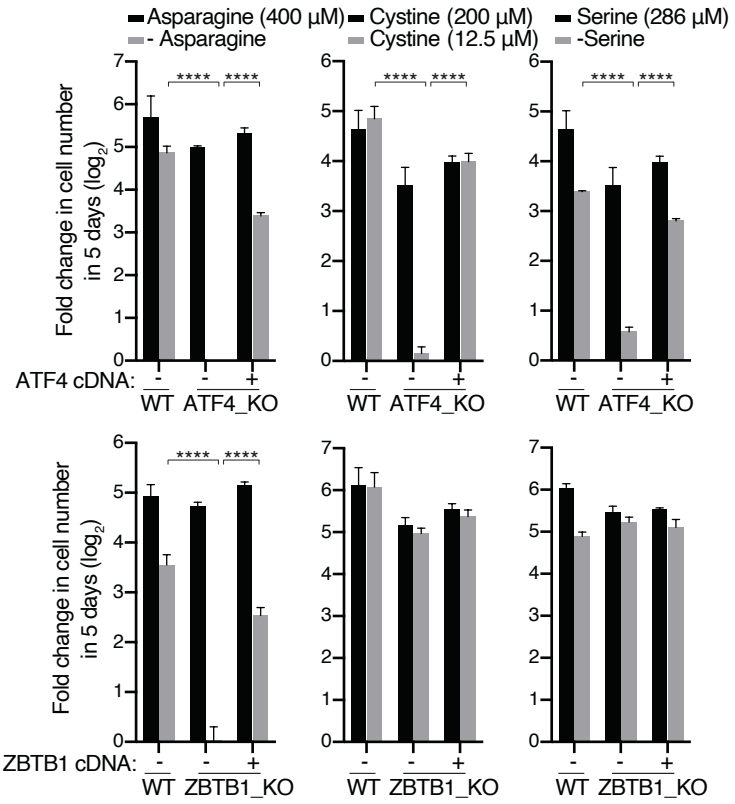

Figure 2.11. ZBTB1 cells are sensitive to asparagine, but not serine or cystine deprivation

(Top) Fold change in cell number (log_2) of parental, ATF4 knockout, and rescued ATF4 knockout Jurkat cells after growth in complete media (black) or media with indicated asparagine, serine or cysteine concentrations (gray) for 5 days (mean ± SD, n=3). (Bottom) Fold change in cell number (log_2) of parental, ZBTB1 knockout, and rescued ZBTB1 knockout Jurkat cells after growth in complete media (black) or media with indicated asparagine, serine or cysteine concentrations (gray) for 5 days (mean ± SD, n=3). Statistics: two-tailed unpaired t-test. **P<0.05, ***P<0.01, ****P<0.001.

Furthermore, overexpression of ATF4 did not rescue the sensitivity of ZBTB1 knockout cells (Figure 2.12), suggesting that ATF4 requires ZBTB1 to enable cell proliferation under asparagine deprivation. In line with this finding, cell lines that do not express ASNS under treatment with L-asparaginase remain capable of activating ATF4 (Figure 2.13).

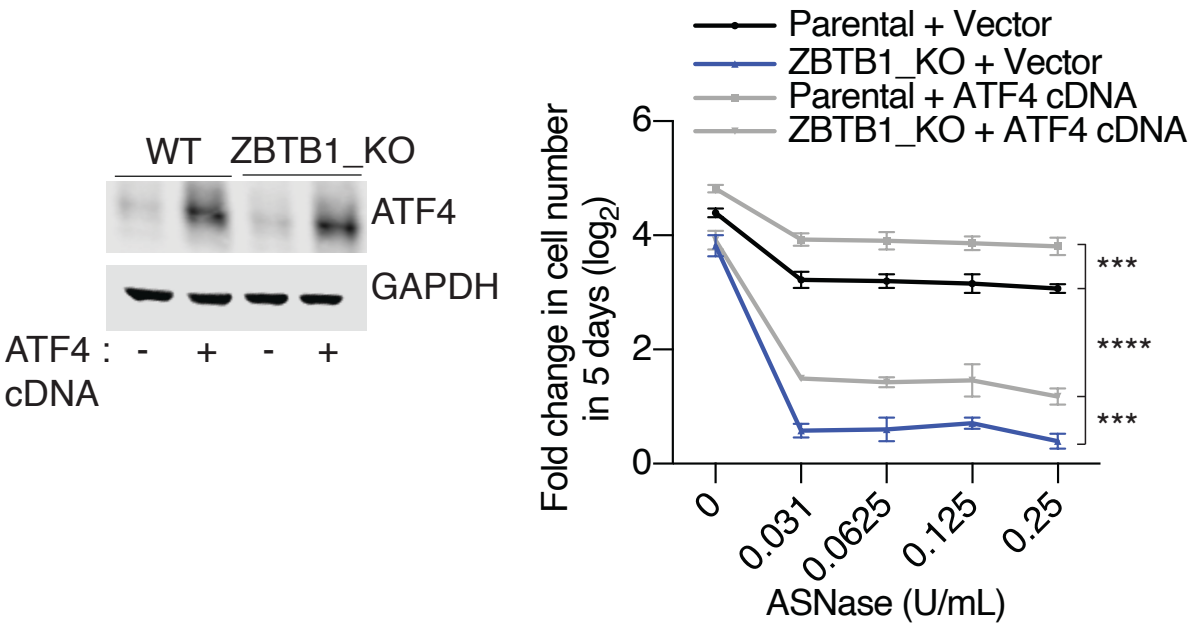

Figure 2.12. ATF4 is insufficient to rescue the proliferation of ZBTB1 knockout cells under asparagine deprivation

(Left) Immunoblot analysis of parental and ZBTB1 knockout Jurkat cells expressing a control vector or ATF4 cDNA (left). GAPDH was used as a loading control.

(Right) Fold change in cell number (log_2) of parental and ZBTB1 knockout Jurkat cells expressing a control vector or ATF4 cDNA after treatment with indicated asparaginase concentrations for 5 days (mean ± SD, n=3).

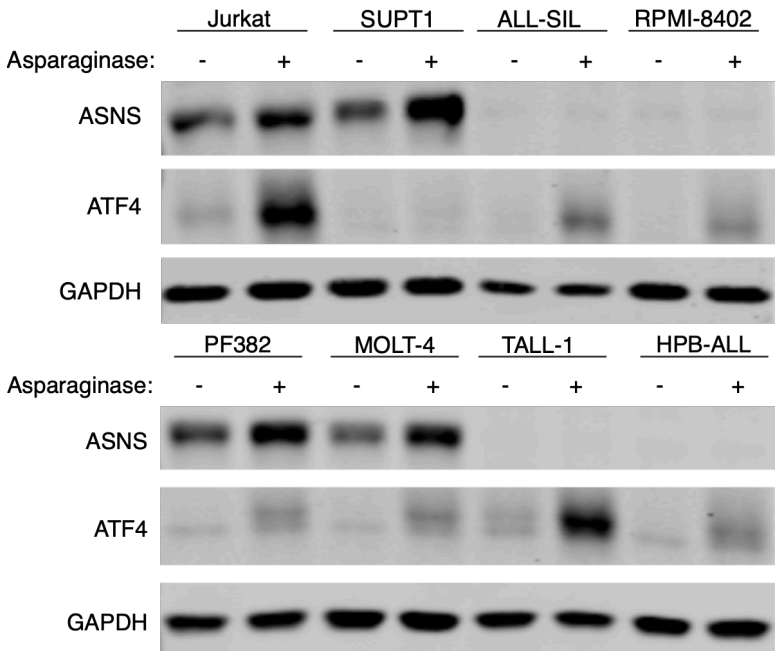

Figure 2.13. ATF4 expression is not sufficient to induce expression of ASNS under L-asparaginase treatment
Immunoblot analysis of indicated cell lines treated with vehicle or L-asparaginase as indicated. Cell lines on the left of each blot (Jurkat, SUPT1, PF382, and MOLT-4) are resistant to treatment with L-asparaginase, whereas those on the right (ALL-SIL, RPMI-8402, TALL-1 and HPB-ALL) are sensitive to L-asparaginase. GAPDH was used as a loading control.

Altogether this suggests that ATF4 expression is not sufficient, though it is necessary, to induce the expression of ASNS arguing for the role of other transcriptional mediators, such as ZBTB1, in the regulation of ASNS. Altogether these results indicate that ZBTB1 is specifically involved in the adaptive response to deprivation of asparagine, but not of other amino acids.

CHAPTER 3. ZBTB1 enables de novo asparagine synthesis and is essential for proliferation under asparagine deprivation

3.1 ZBTB1 is required for asparagine synthesis from glutamine under asparagine deprivation

To understand how loss of ZBTB1 impacts the cellular metabolism of Jurkat cells, we profiled polar metabolites within ZBTB1 knockout Jurkat cells using liquid-chromatography-mass spectrometry (LC-MS) in the presence or absence of asparagine. While asparagine depletion caused few changes, we were able to detect significant differences in 20 metabolites between knockout and rescued cells under asparagine depletion (Figure 3.1, left). Of note, [U-13C]-L-glutamine uptake was similar in ZBTB1 knockout cells and their rescued counterparts (Figure 3.3). Among the most significantly altered metabolites were TCA cycle intermediates (malate and fumarate) and nucleotides (ATP, GTP and CTP). Across all detected amino acids, asparagine was the only one that decreased substantially in ZBTB1 knockout cells, exhibiting three-fold lower levels as compared to wild type or ZBTB1 cDNA expressing cells (Figure 3.1, right). This finding suggests that loss of ZBTB1 may decrease asparagine availability either by reducing de novo synthesis of asparagine or decreasing its uptake from other sources.

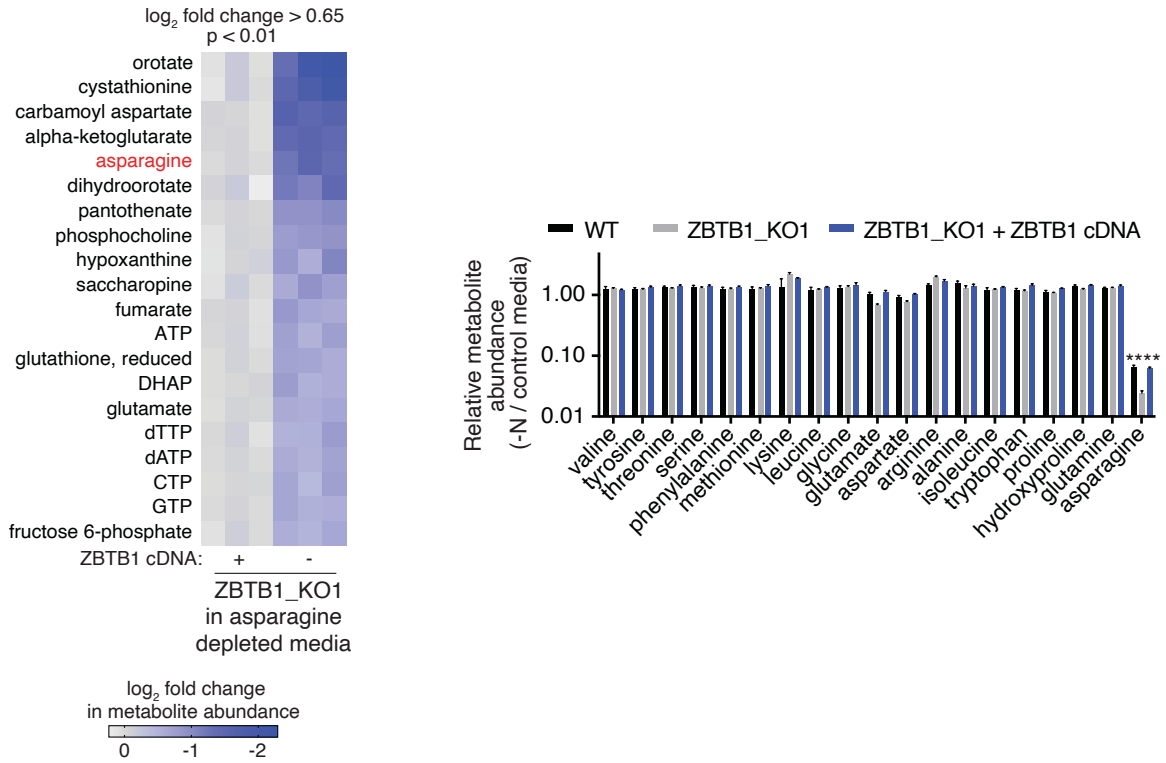

Figure 3.1. ZBTB1 knockout cells have reduced asparagine levels under asparagine deprivation

(Left) Metabolites significantly altered between ZBTB1 knockout (right) and rescued ZBTB1 knockout (left) Jurkat cells grown in asparagine-free medium, ranked by p-value. (Right) Differential intracellular amino acid abundances of parental (black), ZBTB1 knockout (gray), and rescued ZBTB1 knockout (blue) Jurkat cells grown in asparagine-free medium relative to complete medium (mean ± SD, n=3).

To determine whether these cells exhibit reduced asparagine synthesis, we measured the production of asparagine from uniformly heavy carbon labeled glutamine ([U-13C]-L-glutamine) in wild type and ZBTB1 knockout Jurkat cells (Figure 3.2, left). In the presence of asparagine, Jurkat cells synthesize most of their TCA cycle metabolites, nucleotide intermediates and aspartate from glutamine, but they do not synthesize appreciable levels of asparagine (Figure 3.2, right). In contrast, upon asparagine depletion, oxidative metabolism of the uniformly labeled glutamine to asparagine is the predominant route of asparagine synthesis (Figure 3.2, left). Interestingly, loss of ZBTB1 substantially inhibited the reductive (m+3) and oxidative (m+4) labeling of asparagine from glutamine with minimal impact on glutamine-derived aspartate, suggesting a block in asparagine synthesis in these cells (Figure 3.2).

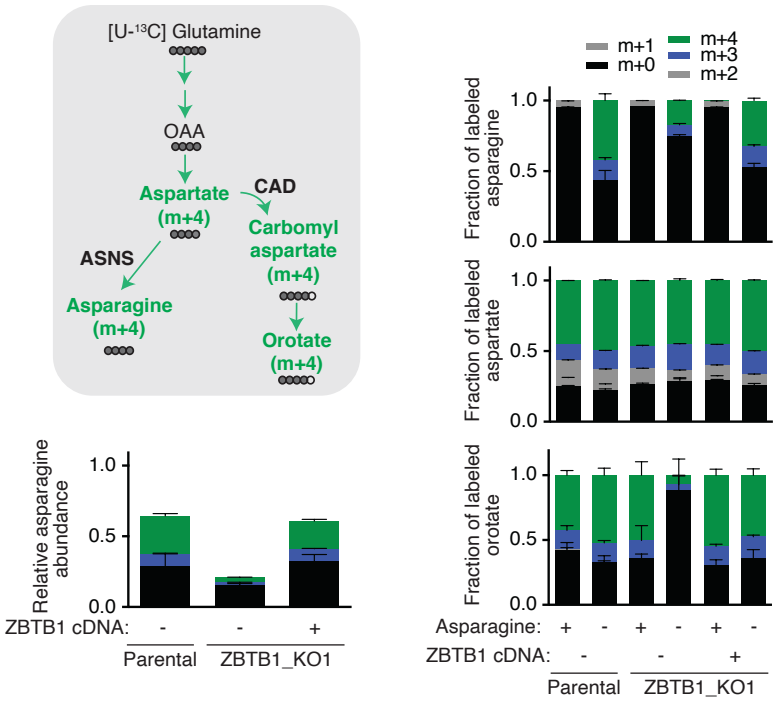

Figure 3.2. Isotope tracing reveals reduced synthesis of asparagine from glutamine with loss of ZBTB1

(Top left) Schematic depicting the metabolic routes of asparagine and orotate synthesis from glutamine. Filled circles represent 13C atoms derived from [U-^{13}C]-Glutamine.
(Bottom left) Abundance of asparagine derived from labeled glutamine in parental, ZBTB1 knockout and rescued ZBTB1 knockout Jurkat cells cultured for 8 hours in media containing [U-13C]-glutamine (2000 uM) in the absence of asparagine. Colors indicate mass isotopomers (mean ± SD, n=3).
(Right) Fraction of labeled asparagine (top), aspartate (middle), and orotate (bottom) derived from labeled glutamine in parental, ZBTB1 knockout and rescued ZBTB1 knockout Jurkat cells cultured for 8 hours with [U-13C]-glutamine (2000 uM) in the presence or absence of asparagine. Colors indicate mass isotopomers (mean ± SD, n=3).

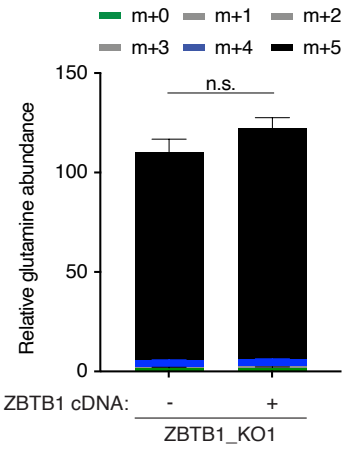

Figure 3.3. Heavy glutamine isotope uptake was equivalent in ZBTB1 knockout or addback cells

Abundance of labeled glutamine in ZBTB1 knockout or ZBTB1 knockout cells expressing ZBTB1 cDNA Jurkat cells cultured for 8 hours in media containing [U-13C]-glutamine (2000 uM) in the absence of asparagine. Colors indicate mass isotopomers, as indicated (mean ± SD, n=3).

Interestingly, the relative abundance of de novo pyrimidine synthesis intermediates (carbamoyl aspartate, dihydroorotate, orotic acid) was markedly reduced in ZBTB1 knockout cells. Indeed, heavy glutamine isotope labeling of orotate substantially decreased in ZBTB1 knockout cells grown in the absence of asparagine. This finding is consistent with recent evidence that pyrimidine synthesis is inhibited in amino acid deprived cells through inhibition of Carbamoyl-Phosphate Synthetase 2, Aspartate Transcarbamylase, And Dihydroorotase (CAD), the rate-limiting step of pyrimidine synthesis[61,135]. Lack of mTORC1 signaling reduces phosphorylation of CAD by the downstream target of mTORC1, ribosomal protein S6 kinase 1 (S6K1). Importantly, this lack of pyrimidine synthesis is not the primary mechanism of ZBTB1 cell death under asparagine deprivation as supplementation with uridine does not rescue the proliferation of ZBTB1 knockout cells under asparagine deprivation (Figure 3.5).

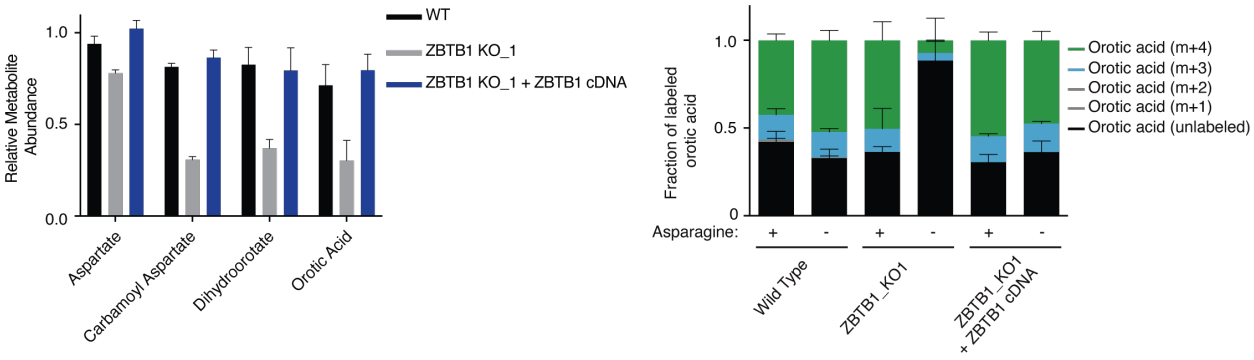

Figure 3.4 De novo pyrimidine synthesis is inhibited within ZBTB1 knockout cells under asparagine deprivation
(Left) Relative abundance of indicated metabolite in wild-type, ZBTB1 knockout or ZBTB1 knockout cells expressing ZBTB1 cDNA
(Right) Abundance of orotic acid derived from labeled glutamine in wild-type, ZBTB1 knockout and rescued ZBTB1 knockout Jurkat cells cultured for 8 hours in media containing [U-13C]-glutamine (2000 uM) in the absence of asparagine. Colors indicate mass isotopomers (mean ± SD, n=3).

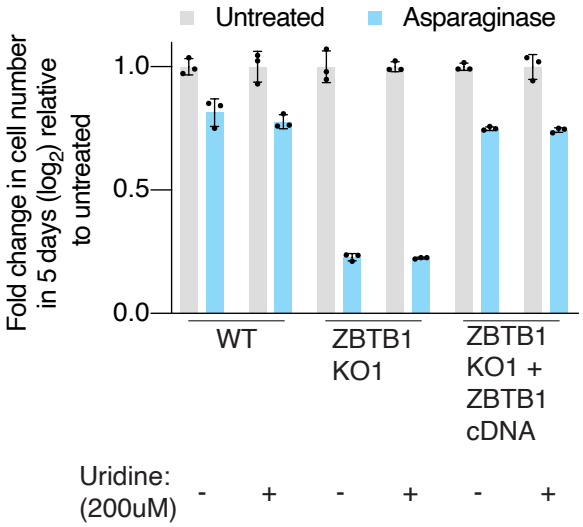

Figure 3.5 Pyrimidine supplementation does not rescue ZBTB1 knockout cell proliferation under asparagine deprivation
Fold change in cell number relative to untreated (log_2) of parental, ZBTB1 knockout or rescued ZBTB1 knockout Jurkat cells after treatment with indicated asparaginase concentrations for 5 days in the presence or absence of 200uM of uridine as indicated (mean ± SD, n=3).

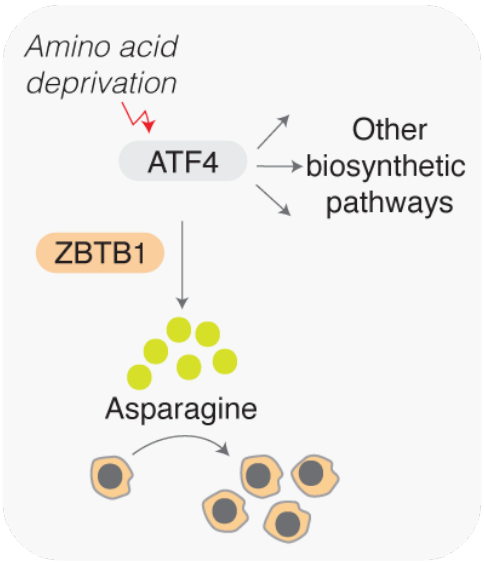

Figure 3.6. ZBTB1 is an essential transcription factor for leukemic cells to synthesize asparagine from aspartate when asparagine is limited
Schematic depicting the requirement of ZBTB1 for ATF4-mediated synthesis of asparagine and cancer cell proliferation under asparagine deprivation

Altogether, metabolite profiling of parental and ZBTB1 knockout cells in the presence or absence of asparagine suggests that ZBTB1 is an essential transcription factor for leukemic cells to synthesize asparagine from aspartate when asparagine is limited (Figure 3.6).

CHAPTER 4. ZBTB1 associates with the ASNS promoter and regulates ASNS transcription

4.1 ZBTB1 knockout reduces transcription of ASNS

ZBTB1 is a member of the mammalian ZBTB gene family and involved in the transcriptional regulation of T lymphocyte development[132–134]. Interestingly, ZBTB1 is predominantly expressed within hematopoietic tissues (Figure 4.1). Transcriptional targets of ZBTB1, however, have not been described. Given that ZBTB1 is required for asparagine synthesis, we reasoned that ZBTB1 might be involved in promoting the transcription of genes relevant to asparagine metabolism. To address this, we performed RNA-sequencing analysis and identified genes whose expression was altered in the absence of ZBTB1. Consistent with our observation that ZBTB1 is essential for Jurkat cells during asparagine deprivation, we found ASNS as one of the most downregulated genes in ZBTB1 knockout cells compared to wild type cells (Figure 4.2). Under asparagine deprivation, Jurkat cells upregulate ATF4 followed by ASNS in order to synthesize asparagine (Figure 4.3). Loss of ZBTB1, however, reduces both the baseline and induced transcription of ASNS under asparagine deprivation, but not that of other ATF4 target genes, as measured by RT-qPCR (Figure 4.2). In agreement with the mRNA expression data, we observed a marked reduction in ASNS protein levels in ZBTB1 knockout cells at baseline and following L-asparaginase treatment (Figure 4.3).

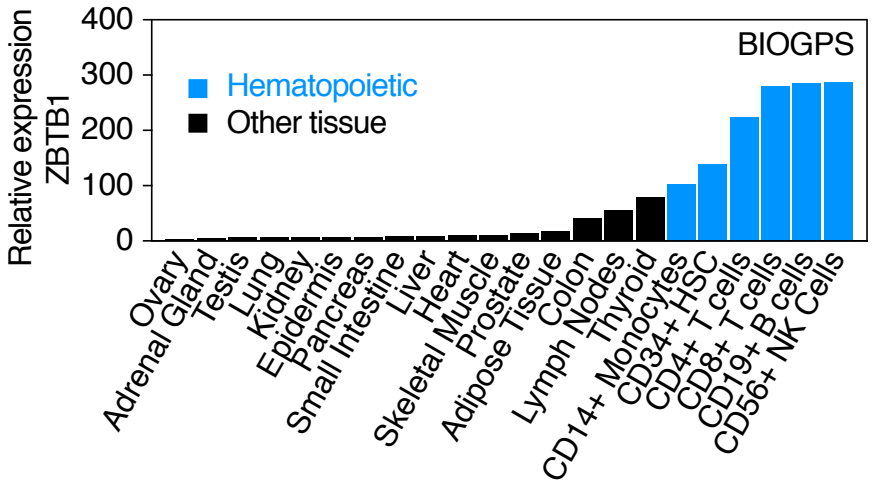

Figure 4.1. ZBTB1 is expressed primarily within hematopoietic cells
Relative mRNA expression of ZBTB1 within indicated cell or tissue types from the BIOGPS database.

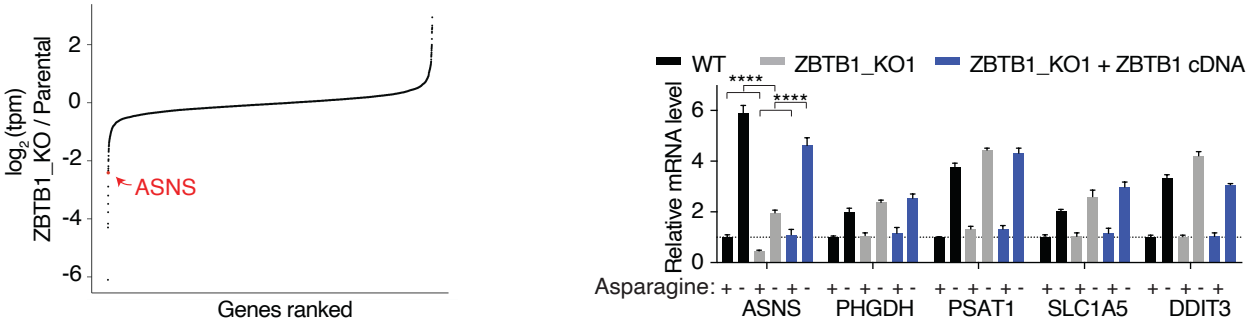

Figure 4.2. ZBTB1 regulates ASNS transcription
(Left) Log_2 fold change in transcripts per million (TPM) in ZBTB1 knockout versus parental Jurkat cells grown in standard medium. ASNS is highlighted in red.
(Right) Relative mRNA levels of indicated genes in parental (black), ZBTB1 knockout (gray) and rescued ZBTB1 knockout (blue) cells grown in complete or asparagine-lacking media (mean ± SD, n=3).

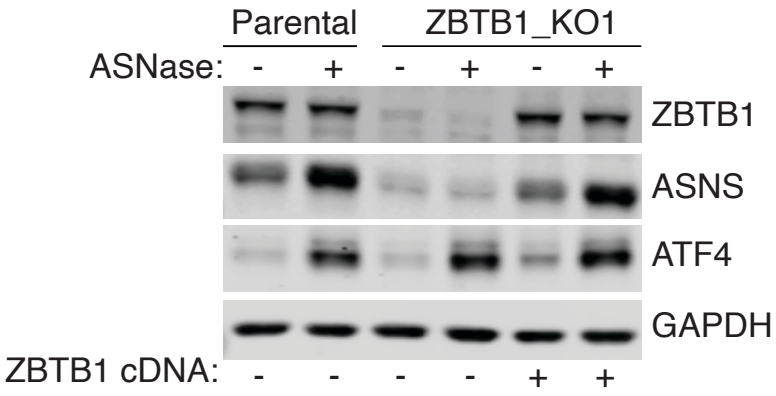

Figure 4.3. Loss of ZBTB1 reduces ASNS protein levels
Immunoblot analysis of parental, ZBTB1 knockout, and rescued ZBTB1 knockout Jurkat cells grown in the presence or absence of L-asparaginase (0.03 U/mL) for 8 hours. GAPDH was used as a loading control.

4.2 ChIP-sequencing reveals enrichment of ZBTB1 within the promoter of ASNS

To investigate the genomic localization of ZBTB1, we next performed comprehensive genome-wide mapping of ZBTB1 and ATF4 through chromatin immunoprecipitation with massively parallel DNA sequencing (ChIP-seq) in ZBTB1 knockout Jurkat cells expressing an N-terminal Flag-tagged ZBTB1 cDNA or a control Flag-GFP. The Flag-tagged ZBTB1 localized to the nucleus and rescued the proliferation of ZBTB1 knockout cells upon asparagine deprivation, indicating that the tagged protein recapitulates the function of the endogenous protein (Figure 4.4).

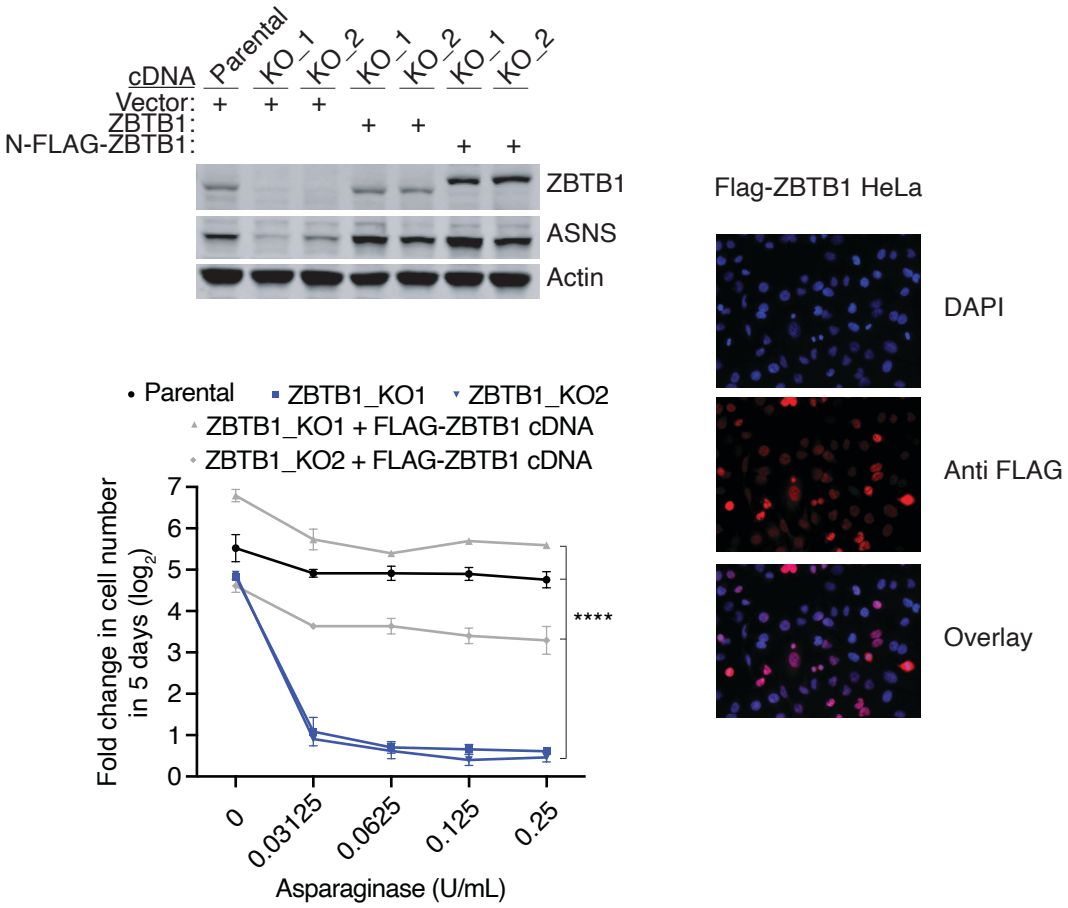

Figure 4.4. Flag-tagged ZBTB1 localizes to the nucleus and rescues ZBTB1 KO cell sensitivity asparagine deprivation

(Left top) Immunoblot analysis of parental, ZBTB1 knockout, and ZBTB1 knockout expressing ZBTB1 or N-FLAG ZBTB1 cDNA Jurkat cells, as indicated. Actin was used as a loading control. (Left bottom) Fold change in cell number (log_2) of indicated Jurkat cells after growth in media with indicated L-asparaginase concentrations for 5 days (mean ± SD, n=3).

(Right) Immunofluorescent microscopy images of HeLa cells expressing Flag-ZBTB1 cDNA after growth in 50 uM or 2mM glutamine, as indicated. Cells were stained with DAPI (top), an anti-FLAG antibody and anti-mouse secondary antibody (middle), and the two images were overlaid (bottom).

ZBTB1 peaks exhibited a distinctly promoter and intronic distribution similar to that of ATF4 (Figure 4.5). Consistent with previous ChIP-seq studies, ATF4 enriched in the promoters of many metabolic genes involved in the response to nutrient stress including PHGDH, PSAT and SLC1A5 (Figure 4.6)[136]. In agreement with the mRNA expression data, ZBTB1 enriched in the promoter of ASNS, but not in the promoters of other key ATF4 target genes that regulate asparagine metabolism (Figure 4.5 and 4.6). Notably, ZBTB1 knockout cells exhibit increased ATF4 enrichment at the ASNS

promoter, underlying the increased amino acid deprivation stress observed in these cells due to loss of asparagine synthesis (Figure 4.5).

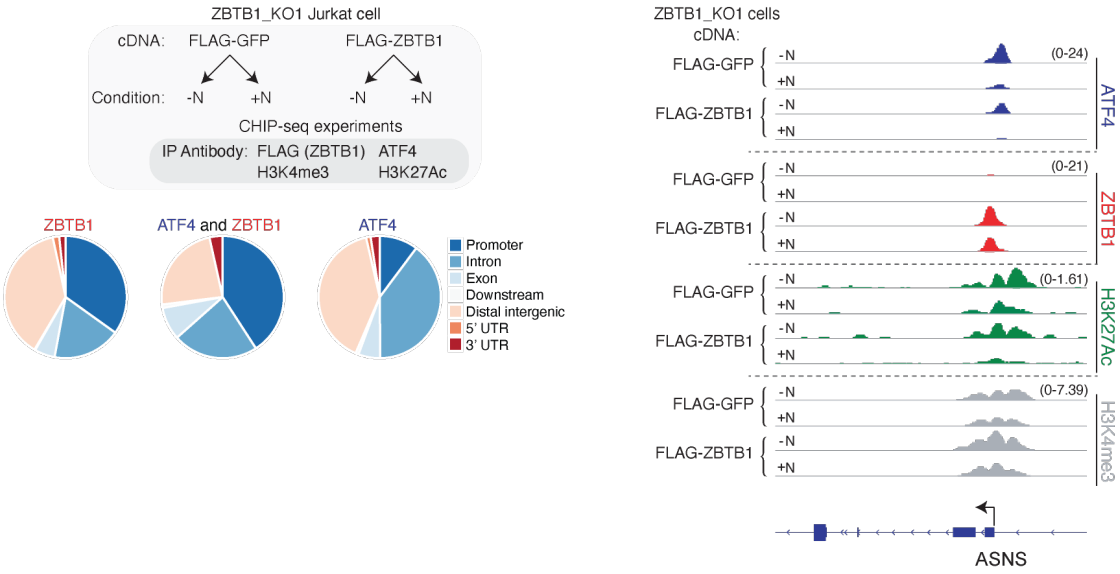

Figure 4.5. ZBTB1 associates with the ASNS promoter
(Left top) Schematic depicting ChIP-sequencing performed in FLAG-GFP versus FLAG-ZBTB1 expressing ZBTB1 knockout cells grown in complete (+N) or asparagine-lacking media (-N). Antibodies used for immunoprecipitation are indicated.
(Left bottom) The proportion of ZBTB1, ATF4 and ZBTB1-ATF4 associated peaks overlapping with specified chromatin features.
(Right) ChIP-Seq tracks near the ASNS promoter for indicated antibodies (right) in the indicated genotype (top two tracks Flag-GFP or bottom two tracks FLAG-ZBTB1) in the presence (+N) or absence (-N) of asparagine.

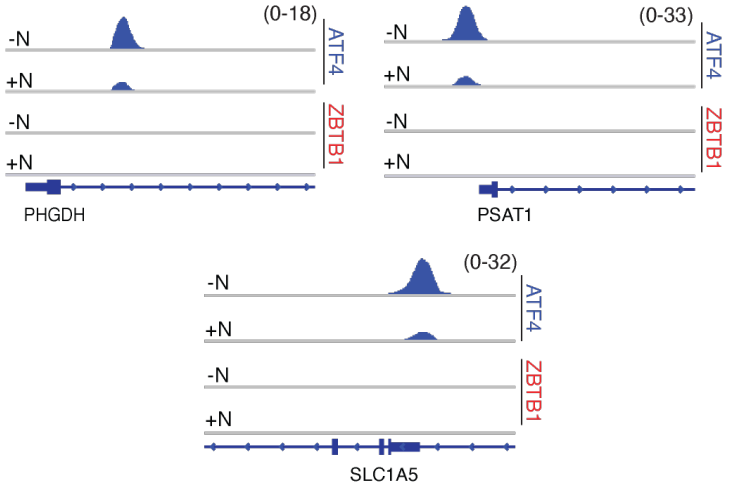

Figure 4.6. ZBTB1 does not enrich within the promoter of other ATF4-regulated metabolic genes

ChIP-Seq tracks near the indicated gene promoter for indicated antibodies (right) in FLAG-ZBTB1 expressing ZBTB1 KO Jurkat cells in the presence (+N) or absence (-N) of asparagine.

Visualization of ZBTB1 peaks in the presence or absence of asparagine revealed a high degree of similarity, and 593 high confidence peaks were defined as peaks present in both conditions (Figure 4.7). Interestingly, a portion of these ZBTB1 peaks overlap with ATF4 peaks (115 out of 593), suggesting that ZBTB1-associated gene promoters may also be regulated by ATF4 (Figure 4.7). Among these peaks overlapping between ATF4 and ZBTB1, the ASNS peak is one of the most significantly enriched for both transcription factors relative to their respective controls (Figure 4.7). Similarly, gene ontology analysis of genes having both ZBTB1 and ATF4 peaks revealed a strong enrichment for asparagine synthesis gene sets (Figure 4.7). Altogether, these findings indicate that ZBTB1 associates with the ASNS promoter and is required for ATF4 to promote ASNS transcription.

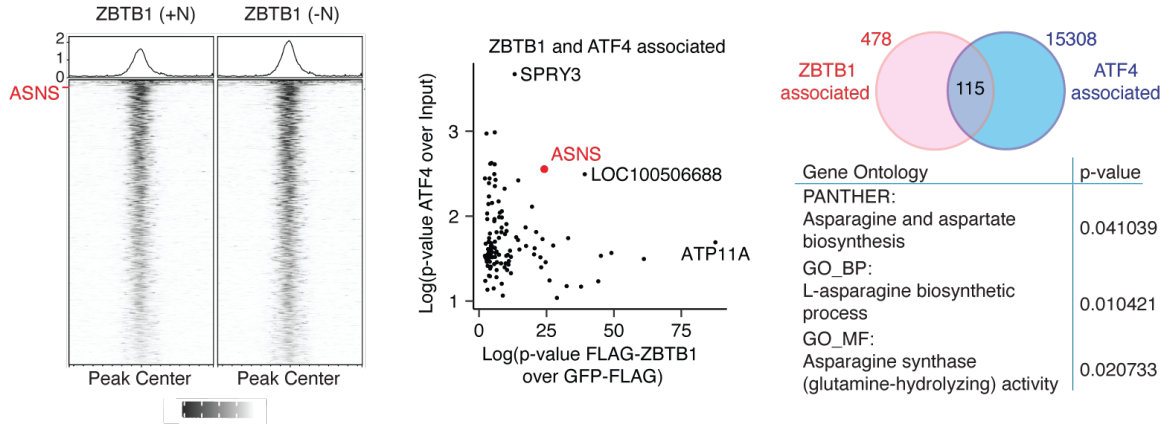

Figure 4.7. A number of genes are regulated by both ATF4 and ZBTB1
(Left) FLAG-ZBTB1 ChIP-Seq signal from normalized bigwig files quantified over all ZBTB1 peaks identified in either the presence (+N) or absence (-N) of asparagine. The row corresponding to the peak in the ASNS promoter is labeled with red text (left).
(Middle) Scatter plot of p-values of the peaks overlapping between ATF4 and ZBTB1. ASNS is highlighted in red.
(Right) Venn diagram depicting the number of ZBTB1, ATF4 and overlapping ZBTB1-ATF4 peaks genome-wide (top). Significantly enriched gene ontologies for peaks that overlap in ZBTB1 and ATF4 (bottom).

Table 4.1. Top 40 genes enriched for Flag-ZBTB1 as compared to Flag-GFP ranked by p-value

Gene	p-adj
TGFA	9.57E-150
ANO2	1.31E-108
ATP11A	4.27E-84
BRD9	5.35E-58
BAHCC1	4.72E-56
LOC441666	2.95E-52
RUNX1	3.37E-46
ADAP1	1.81E-43
PLXND1	2.04E-42
PIK3CB	1.72E-41
SNAPC3	5.48E-40
ADARB2	8.00E-39
LOC100506688	1.33E-36
BBS2	9.18E-36
VPS37C	2.76E-35
TFDP2	1.36E-30
WTAP	2.81E-30
MIR5093	4.44E-30
FAM20C	1.93E-29
MIR4436A	2.88E-28
TDRD12	3.63E-27
MYCBP2	4.35E-27
FAM156A	1.37E-26
GUCA2A	6.01E-26
CWH43	1.57E-25
STRBP	3.01E-25
CKAP4	3.49E-25
WNT10A	1.03E-24
GP5	6.34E-24
SKI	2.41E-23
NCF1C	4.87E-23
KIF17	1.51E-22
ASNS	3.40E-22
MANSC1	8.86E-22
ZNF341	1.44E-21
TNRC18	1.86E-21
ECEL1	2.12E-21
NCOA3	5.56E-21

Previous studies have characterized the role of the N terminal BTB (broad complex, tramtrack, and bric-a-brac) and ubiquitin-binding zinc-finger 4 (UBZ4) domains in the autosumoylation and targeting of ZBTB1 to sites of DNA damage[137,138]. Mutation of known sumoylation sites or deletion of the UBZ4 domain, however, did not affect the ability of ZBTB1 to rescue the proliferation of ZBTB1 knockout Jurkat cells under asparagine deprivation (Figure 4.8), suggesting that these sites are not essential for regulating ASNS expression.

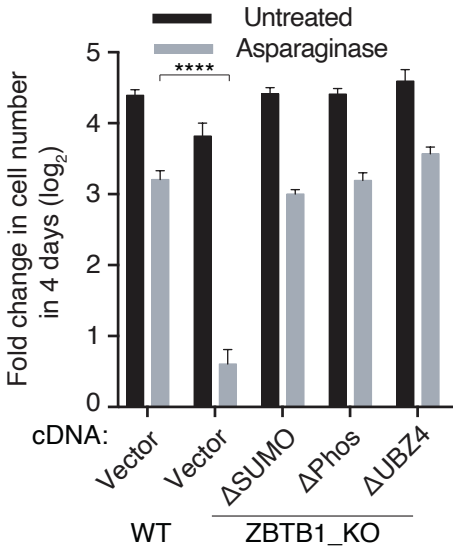

Figure 4.8. Known functional domains of ZBTB1 are not essential for ZBTB1's role under asparagine deprivation
Fold change in cell number (log_2) of parental or ZBTB1 knockout Jurkat cells expressing indicated cDNAs after treated with asparaginase (0.25 U/mL, gray) or left untreated (black) for 4 days (mean ± SD, n=3).

Given that BTB domains typically facilitate protein-protein interactions, we hypothesize that ZBTB1 might interact with ATF4 or other transcription factors to promote transcription[139]. In order to test this hypothesis, we overexpressed Flag-tagged ZBTB1 protein Jurkat cells and performed an anti-FLAG immunoprecipitation on nuclear extracts from cells treated with asparaginase or vehicle. Immunoblotting confirmed enrichment of both the Flag-tagged ZBTB1 protein, as well as wild-type ZBTB1 protein suggesting that the protein may homodimerize. ATF4 did not co-precipitate with ZBTB1 suggesting that these proteins do not directly interact (Figure 4.9).

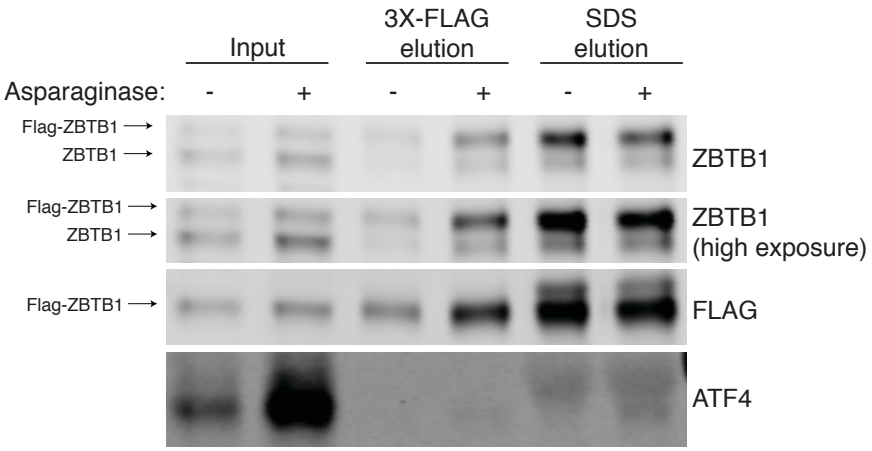

Figure 4.9 IP of Flag-ZBTB1 reveals dimerization of ZBTB1
Nuclear extracts from Flag-tagged ZBTB1 overexpressing Jurkat cells were subject to IP using an anti-Flag antibody and analyzed by western blotting. Lanes represent total input protein, 3X-FLAG elution and total elution with denaturing SDS from cells treated with L-asparaginase or vehicle. Antibodies for western blotting are indicated on the right.

In order to determine whether other proteins might interact with ZBTB1, we performed mass spectrometry on these same immunoprecipitations. Of note, peptides matching to ZBTB1 were enriched in these samples (Table 4.2). IP-MS did not reveal any other protein significantly enriched within these samples that might suggest a direct interaction with ZBTB1. Importantly, these experiments were not performed on cells in which proteins had been cross-linked prior to immunoprecipitation, so it remains possible that lower affinity interactions may exist that do not withstand sample processing.

Table 4.2 IP-MS of Flag-ZBTB1 shows no clear ZBTB1 interaction partners
Nuclear extracts from Flag-tagged ZBTB1 overexpressing Jurkat cells were subject to immunoprecipitation-mass spectrometry using an anti-Flag antibody. Immunoprecipitated proteins are listed with percentage of protein covered and total peptide-spectral matches (PSMs).

Gene	Coverage	PSMs
ZBTB1	41.65	49
DROSHA	2.55	5
UTP15	9.85	5
SCAF4	5.41	5
TWF2	18.50	4
SLC25A10	13.94	4
GTF3C2	4.94	4
KEAP1	6.25	4
ICAM5	8.86	3
CBLN1	5.00	3
MTRR	4.49	3
PPP6R1	3.29	3
PSMC2	4.85	3

Finally, to determine whether ZBTB1 is phosphorylated to activate its positive transcriptional regulation of ASNS, we analyzed our mass spectrometry data to identify serine residues that were phosphorylated or lysine sumoylation events that occurred specifically under L-asparaginase treatment. Given the low coverage of ZBTB1 by mass spectrometry, we only identified two serine residues (S304 and S411) that were phosphorylated in a differential manner and did not observe condition-dependent sumoylation of ZBTB1. The lack of context-specific sumoylation agreed with mutational studies in which the deletion of sumoylated lysine residues did not alter the ability of ZBTB1 cDNA to rescue the proliferation of ZBTB1 knockout cells in asparagine deplete conditions (Figure 4.8). In order to determine whether the phosphorylation of S304 and S411 under asparagine depletion was essential for ZBTB1's ability to rescue proliferation under asparagine depletion, we specifically mutated each serine residue to an alanine preventing phosphorylation of the residue. Both the S304A and S411A ZBTB1 mutant cDNAs were capable of rescuing ZBTB1 knockout cell proliferation under asparaginase treatment suggesting that phosphorylation of these residues is not required for ZBTB1's positive regulation of ASNS (Figure 4.9). ZBTB1 knockout cells expressing either ZBTB1 S304A or S411A were capable of proliferating under L-asparaginase treatment and showed increased expression of ASNS relative to cells expressing vector control (Figure 4.9).

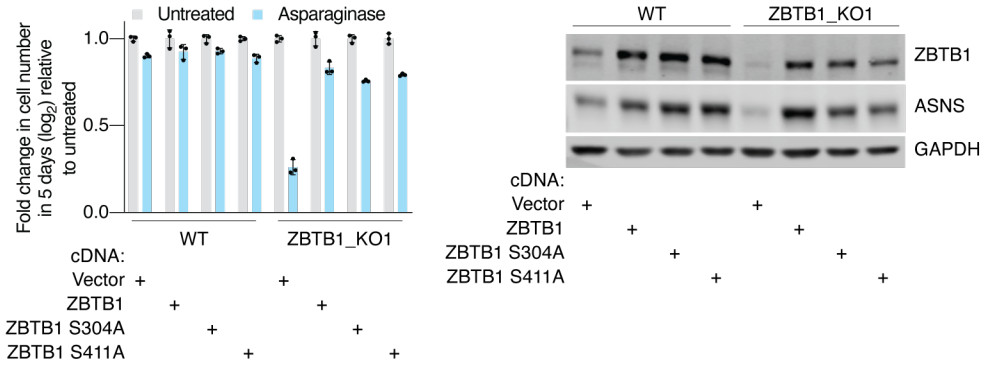

Figure 4.10 Phosphorylation of ZBTB1 serine residues 304 and 411 is not essential for ZBTB1's positive regulation of ASNS
(Left) Fold change in cell number relative to untreated control (log_2) of wild-type or ZBTB1 knockout Jurkat cells expressing indicated cDNAs after treatment with asparaginase (0.25 U/mL, blue) or left untreated (gray) for 4 days (mean ± SD, n=3). (Right) Immunoblot analysis of wild-type or ZBTB1 knockout Jurkat cells expressing indicated ZBTB1 cDNA. GAPDH was used as a loading control.

4.3 ZBTB1 directly binds to a sequence within the ASNS promoter to enhance transcription

We next asked whether ZBTB1 directly binds to DNA at a specific DNA motif[137]. Motif enrichment for ATF4 identified the previously described "TGATGHAA" binding motif, the canonical nutrient sensing response element (NSRE) within the ASNS promoter[17]. Similar analysis of ZBTB1 peaks genome-wide revealed a seven-nucleotide motif associated with ZBTB1 peaks, "ARCCRCA", which is also the RUNX1/2/3 binding motif (Figure 4.11)[140]. The ASNS promoter contains four instances of this motif near the ZBTB1 peak, including one motif directly under the region of highest read density, downstream of the canonical NSRE, where ATF4 binds (Figure 4.11). In order to determine whether ZBTB1 directly binds to this motif within the ASNS promoter, we performed an electrophoretic mobility shift assay and validated that a purified zing finger fragment of ZBTB1 binds to this segment of the ASNS promoter (Figure 4.11 and 4.12). Importantly, a fluorescent probe in which the four ZBTB1 motifs were mutated did not show an electrophoretic mobility shift, suggesting specific binding of ZBTB1 protein to the identified motif within this region of the ASNS promoter (Figure 4.11).

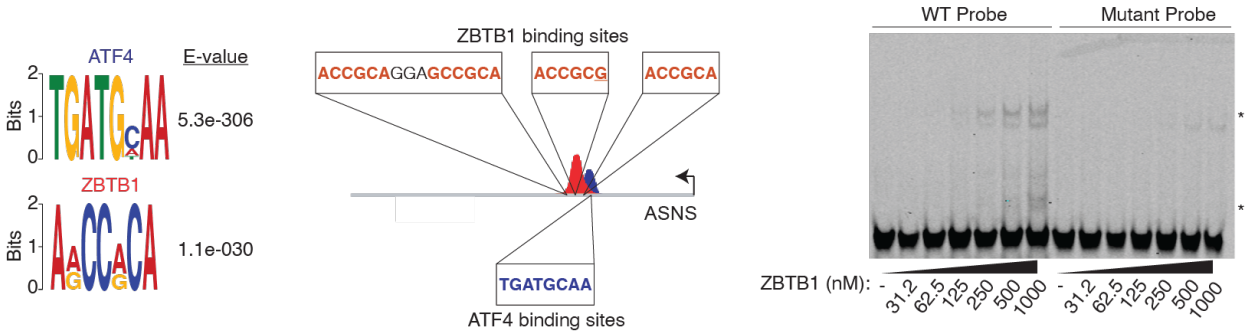

Figure 4.11. ZBTB1 directly binds to a motif present in the ASNS promoter
(Left) Motifs enriched near ATF4 and ZBTB1 peaks.
(Middle) Schematic depicting ATF4 and ZBTB1 motifs present within the promoter of ASNS.
(Right) Electrophoretic mobility shift gel of parental (WT) and mutant ASNS promoter probes with the indicated concentration of recombinant ZBTB1 protein. Stars indicate probe shifts.

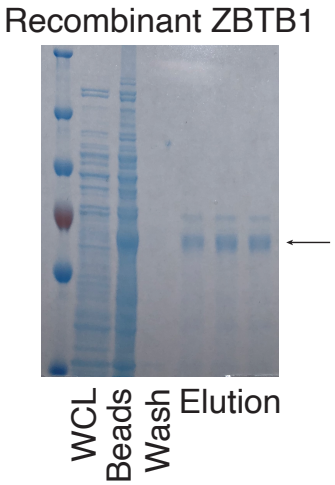

Figure 4.12. Recombinant ZBTB1 expressed in bacteria
SDS-PAGE of recombinant zinc-finger domain of ZBTB1 expressed in bacteria. Whole cell lysate (WCL), anti-His beads, wash, and elution samples are indicated. Expected purified protein is indicated (arrow).

Of note, though RUNX1 and ZBTB1 share binding motifs, RUNX1 transcript levels are unaffected by ZBTB1 loss and overexpression of RUNX1 does not rescue the proliferation of ZBTB1 knockout cells under asparagine deprivation (Figure 4.13). These transcription factors are thus unlikely to have overlapping functions in regulating ASNS transcription.

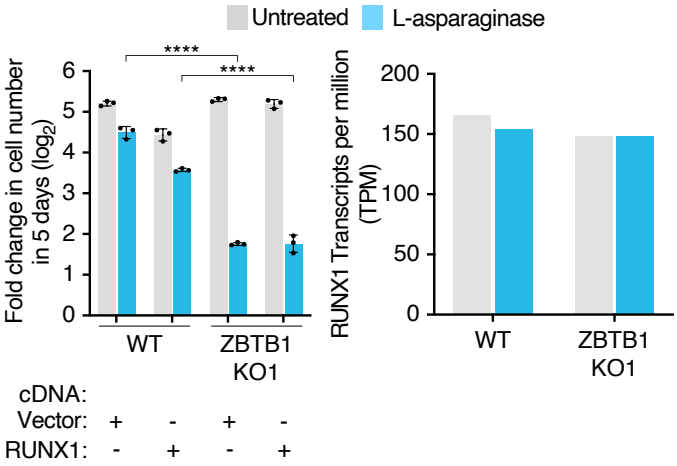

Figure 4.13. RUNX1 expression does not rescue ZBTB1 knockout sensitivity to asparagine deprivation

Fold change in cell number (log_2) of parental or ZBTB1 knockout Jurkat cells expressing vector or RUNX1 cDNA after treatment with L-asparaginase (0.03U/mL) or left untreated for 5 days (mean ± SD, n=3, left). RUNX1 transcripts per million (TPM) in parental or ZBTB1 knockout Jurkat cells.

In line with the role of ZBTB1 in ASNS regulation, overexpression of ASNS is sufficient to rescue the sensitivity of ZBTB1 knockout cells to asparagine deprivation, similar to that of asparaginase sensitive cell lines (Figure 4.14 and 4.15)[141]. Interestingly, forced overexpression of ATF4 is not sufficient to induce ASNS expression or impact GCN2 signaling in ZBTB1 knockout cells, suggesting that ATF4 likely requires ZBTB1 for maximal ASNS expression (Figure 4.16). Together, these data indicate that the direct transcriptional regulation of ASNS by ZBTB1 enables cells to proliferate upon asparagine deprivation.

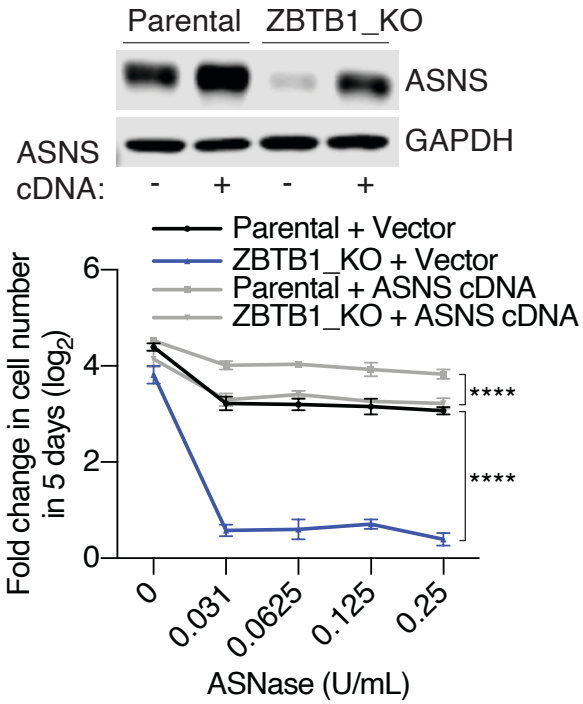

Figure 4.14. ASNS expression is sufficient to rescue the sensitivity of ZBTB1 knockout cells to asparagine deprivation

(Top) Immunoblot analysis of parental and ZBTB1 knockout Jurkat cells overexpressing a vector or ASNS cDNA. GAPDH was used as a loading control. (Bottom) Fold change in cell number (log_2) of parental (black) and ZBTB1 knockout (blue) Jurkat cells expressing a control vector or ASNS cDNA (gray) after treatment with indicated asparaginase concentrations for 5 days (mean ± SD, n=3).

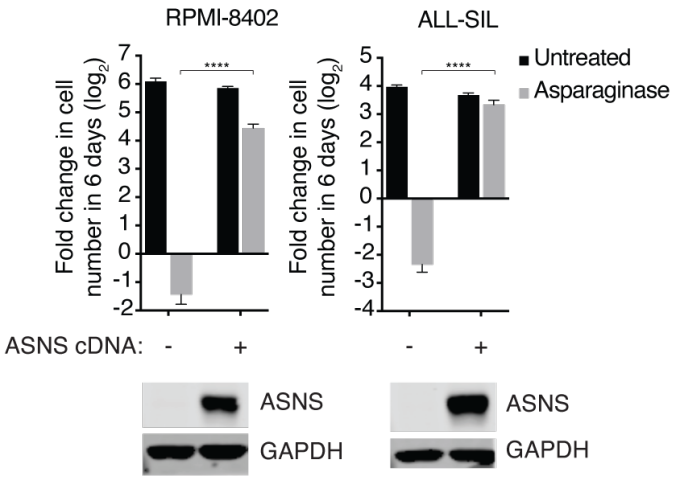

Figure 4.15. ASNS expression is sufficient to rescue the sensitivity of asparagine auxotrophic ALL cell lines

(Top) Fold change in cell number (log_2) of indicated cell lines expressing a control vector or ASNS cDNA after treatment with vehicle (black) or asparaginase (grey) for 6 days (mean ± SD, n=3).

(Bottom) Immunoblot analysis of indicated cells expressing vector or ASNS cDNA, as indicated. GAPDH was used as a loading control.

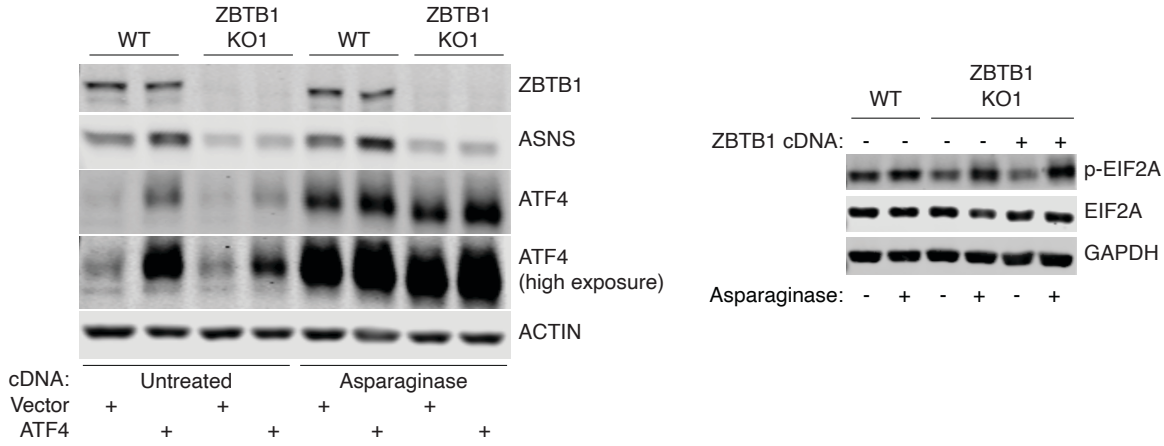

Figure 4.16. ATF4 expression is insufficient to rescue the expression of ASNS in ZBTB1 knockout cells

(Left) Immunoblot analysis of parental and ZBTB1 knockout Jurkat cells grown in HPLM left untreated or treated with L-asparaginase and expressing vector or ATF4 cDNA, as indicated. Actin was used as a loading control.

(Right) Immunoblot analysis of parental, ZBTB1 knockout and ZBTB1 knockout expressing ZBTB1 cDNA Jurkat cells grown in HPLM treated with L-asparaginase, as indicated. GAPDH was used as a loading control.

ZBTB1 binding sites on the ASNS promoter overlap with active chromatin marks histone H3 lysine 27 acetylation (H3K27ac) and H3 lysine 4 trimethylation (H3K27ac and H3K4me3) (Figure 4.5). Furthermore, Assay for Transposase-Accessible Chromatin using sequencing (ATAC-Seq) experiments showed minimal impact on the accessibility of chromatin near the ASNS promoter in ZBTB1 knockout cells, suggesting that ZBTB1 may act downstream of the establishment of transcriptionally permissive chromatin (Figure 4.17).

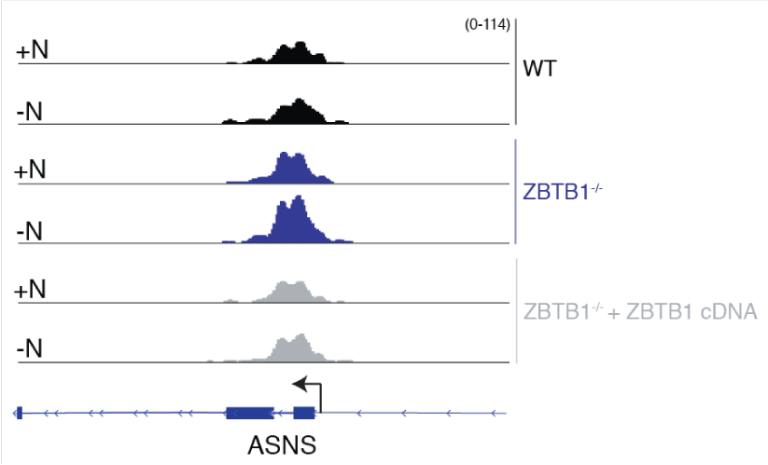

Figure 4.17. ATAC-Seq reveals minimal changes to chromatin accessibility at the ASNS promoter in the absence of ZBTB1
ATAC-Seq tracks near the promoter of ASNS in parental, ZBTB1 knockout, and ZBTB1 knockout expressing ZBTB1 cDNA Jurkat cells in the presence (+N) or absence (-N) of asparagine, as indicated.

CHAPTER 5. ZBTB1 is required for L-asparaginase resistance of T-ALLs *in vivo*

5.1 ZBTB1 knockout sensitizes T and B-ALLs to L-asparaginase *in vitro*

L-asparaginase, which selectively depletes asparagine from serum, is a clinical therapy that inhibits the growth of asparagine-dependent leukemia cells[47,53]. Despite the high survival rate of patients treated with chemotherapeutic agents, about 20% of children and more than 50% of adults with ALL relapse or do not respond to this therapy. Given the role of ZBTB1 in regulating ASNS expression and the response of ZBTB1 knockout cells to asparagine deprivation, we reasoned that loss of ZBTB1 may sensitize asparaginase-resistant cancer cells to L-asparaginase treatment *in vivo*. To address this, we first determined whether the function of ZBTB1 in regulating ASNS is restricted to leukemias or generalizable to other cancer types. Interestingly, loss of ZBTB1 caused L-asparaginase sensitivity in T-ALLs (CUTTL-1, Jurkat, SUPT-1) and, to a lesser extent, B-ALLs (REH, NALM6), but not to other cancer types such as AML (MOLM-13 or SKM-1), breast (MDA-MB-231) or lung (A549) cancer cell lines (Figure 5.1, top). Consistent with this, baseline ASNS expression decreases upon loss of ZBTB1 in T-ALLs, but not in other cell types (Figure 5.1, bottom).

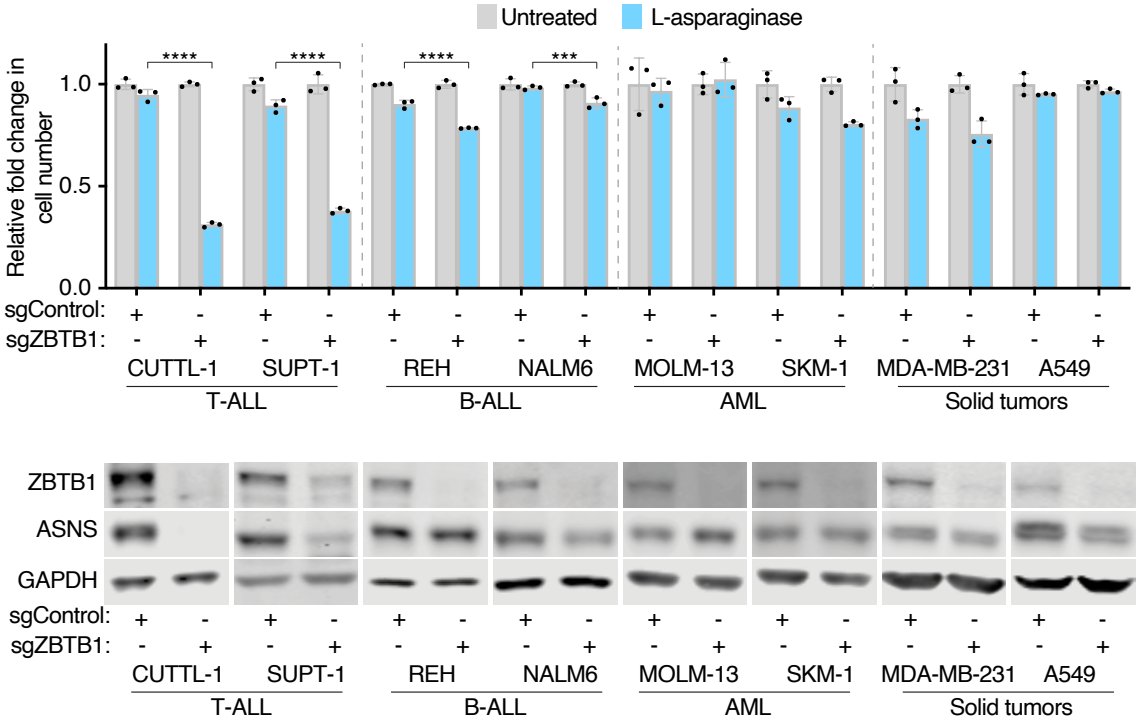

Figure 5.1. Loss of ZBTB1 sensitizes T-ALLs and B-ALLs to L-asparaginase
(Top) Fold change in cell number of sgControl (gray) versus sgZBTB1 (blue) expressing cell lines treated with L-asparaginase (0.03 U/mL) relative to untreated (mean ± SD, n=3).
(Bottom) Immunoblot analysis of indicated cell lines expressing sgControl versus sgZBTB1. GAPDH was used as a loading control.

Given the use of L-asparaginase for the treatment of B-ALL, we further investigated whether an alternative gene might play a similar role as ZBTB1 in T-ALL in the regulation of ASNS. We performed an equivalent CRISPR/Cas-9 epigenetic screen in two B-ALL cell lines, NALM-6 and REH, in order to identify genes required for the proliferation of these cell lines under asparagine deprivation (Figure 5.2). As expected, knock out of ATF4 sensitized both B-ALL cell lines to treatment with L-asparaginase. Similarly, though not to the extent as in T-ALL cell lines, ZBTB1 knockout sensitized NALM-6 and REH cells to treatment with L-asparaginase. Interestingly, another gene, ZMIZ1, was required for the proliferation of both B-ALL cell lines under asparagine deprivation. This gene was not required for the proliferation of T-ALL cells under asparagine deprivation suggesting a B-cell lineage specificity of this gene, however like ZBTB1, it is important to T-cell differentiation. ZMIZ1 has been described as a transcriptional activator involved in activating a subset of NOTCH1 target genes, including c-Myc[142]. Furthermore, ZMIZ1-ABL1 translocations have been observed in ALLs and are transformative in experimental models of ALL[143].

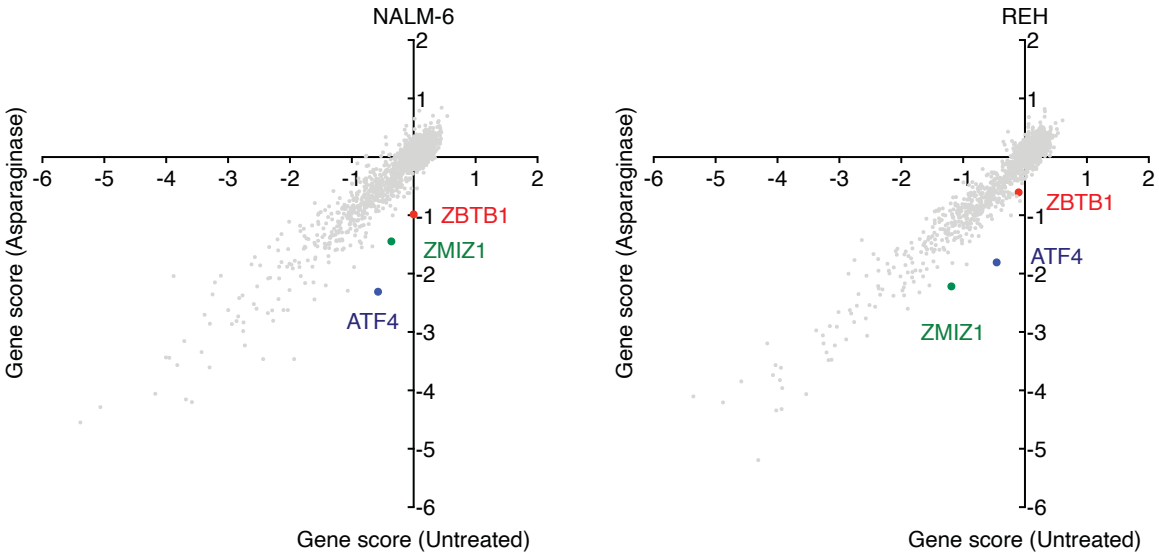

Figure 5.2. CRISPR-based in B-ALL cell lines under L-asparaginase treatment
Gene scores in WT NALM-6 (left) or WT REH (right) cells grown in complete versus asparagine deficient media. Media was depleted of asparagine through the use of L-asparaginase (0.25 U/mL). ZBTB1, ATF4 and ZMIZ1, the top hits of the screens, are highlighted.

5.2 ZBTB1 knockout T-ALLs are sensitized to L-asparaginase *in vivo*

To translate our findings to an *in vivo* model, we engrafted NOD-SCID gamma (NSG) mice with clonal ZBTB1 knockout Jurkat cells or cDNA rescued counterparts and tested the efficacy of L-asparaginase treatment in these mice. Consistent with previous work, L-asparaginase significantly decreased serum asparagine levels, without impacting the levels of abundant amino acids such as glutamine, when measured after 24 hours

(Figure 5.3, right)[144]. The treatment was well-tolerated as indicated by animal weights remaining unchanged during the experiment (Figure 5.3, left)[145,146].

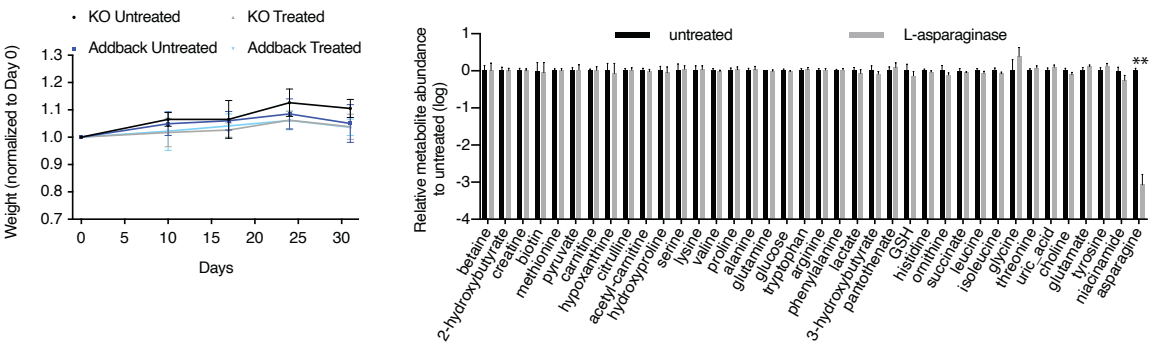

Figure 5.3. L-asparaginase depletes serum asparagine and is well tolerated in NSG mice
(Left) Weight of mice with the indicated engrafted cells and treatment at the indicated day normalized to their initial weight (mean ± SD, n=7).
(Right) Relative abundance of indicated metabolites in the serum of mice treated with L-asparaginase (1000 U/kg, gray) or left untreated (black).

Mice engrafted with ZBTB1 knockout or rescued Jurkat cells had a median survival of 48 days and 49 days, respectively. While L-asparaginase treatment only marginally extended median survival of mice with rescued ZBTB knockout cells (52 days), mice engrafted with ZBTB1 knockout cells had lower tumor burden and had a significant increase in median survival (62 days) (Figure 5.4, right).

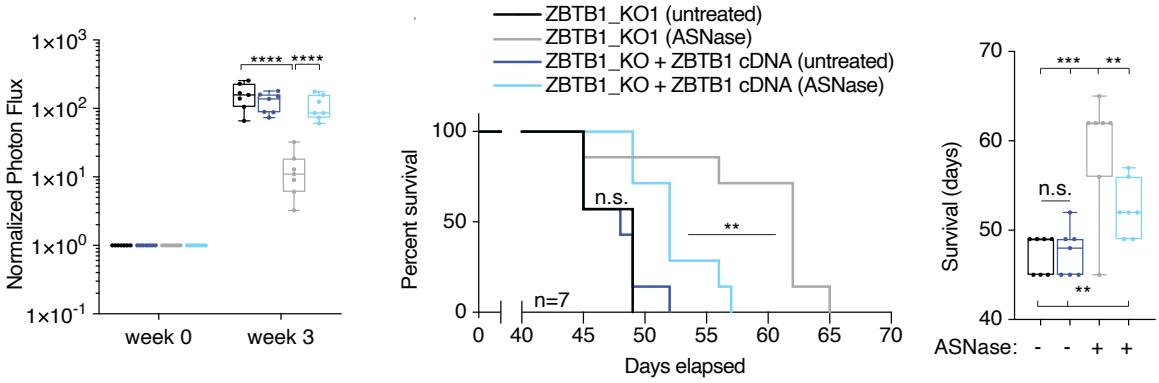

Figure 5.4. Loss of ZBTB1 sensitizes therapy resistant Jurkat cells to L-asparaginase *in vivo*
(Left) Photon flux detected by In Vivo Imaging System for Jurkat cell lines engrafted into NSG mice normalized to initial photon flux.
(Middle) Kaplan-Meier survival curve of NSG mice engrafted with ZBTB1 knockout versus rescued ZBTB1 knockout Jurkat cells and treated with vehicle or asparaginase (1000 U/kg, twice per week).
(Right) Box and whisker plots of survival data.

Similarly, mice engrafted with another L-asparaginase resistant cell line, CUTLL1, that lacked ZBTB1 survived a median of 32 days when treated with L-asparaginase as compared to a median of 27 days when left untreated. Collectively, these findings suggest that loss of ZBTB1 sensitizes T-ALL cell lines to L-asparaginase *in vivo* and that ZBTB1 may be an amenable therapeutic target for the treatment of L-asparaginase non-responsive T-ALLs (Figure 5.5).

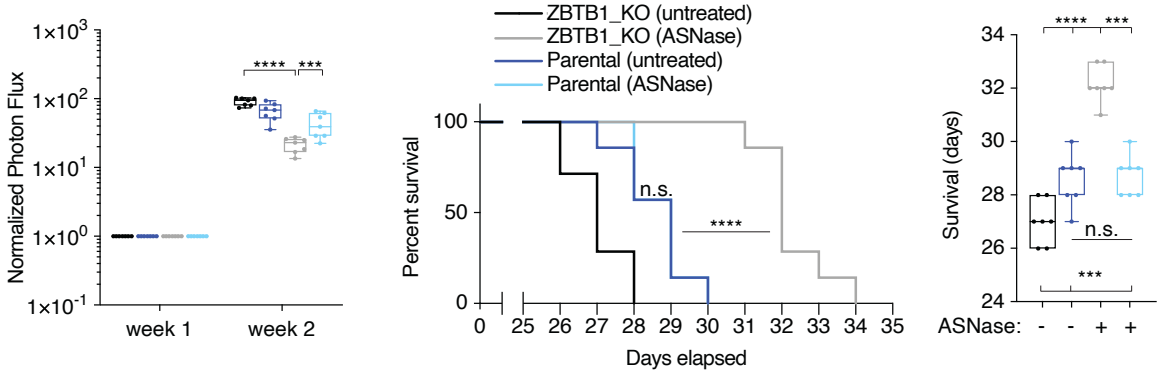

Figure 5.5. Loss of ZBTB1 sensitizes therapy resistant CUTLL1 cells to L-asparaginase *in vivo*

(Left) Photon flux detected by In Vivo Imaging System for CUTLL1 cell lines engrafted into NSG mice normalized to initial photon flux.

(Middle) Kaplan-Meier survival curve of NSG mice engrafted with ZBTB1 knockout versus vector-control CUTLL1 cells and treated with vehicle or asparaginase (1000 U/kg, twice per week).

(Right) Box and whisker plots of survival data.

CHAPTER 6. Toxic incorporation of lipid analogs as a therapeutic strategy in acute leukemia

6.1 CPI-613 is a lipoic acid analog designed to inhibit TCA cycle enzyme complexes

Cancer cells utilize carbon sources, such as glutamine and glucose, to generate biosynthetic intermediates through the TCA cycle for cellular growth and division[147]. The TCA cycle also generates intermediates that act as important signaling and epigenetic regulatory molecules including, in the case of IDH-mutant cancers, oncogenic molecules such as 2-hydroxyglutarate. As such, efforts have been made to design anti-cancer therapies that target the TCA cycle. One such therapy, CPI-613, is a rationally designed lipoic acid analog currently under clinical trial investigation for the treatment of AML and pancreatic cancer[148,149]. Lipoic acid is an essential co-factor for multiple enzyme complexes within mammalian cells, including two within the TCA cycle: pyruvate dehydrogenase (PDH) and α-ketoglutarate/2-oxoglutarate dehydrogenase (OGDH) (Figure 6.1). In PDH, lipoic acid is a cofactor for the oxidative decarboxylation of pyruvate to acetyl-CoA linking glycolysis with the TCA cycle. Similarly, within OGDH, lipoic acid is a cofactor for the oxidative decarboxylation of α-ketoglutarate/2-oxoglutarate to succinyl-CoA.

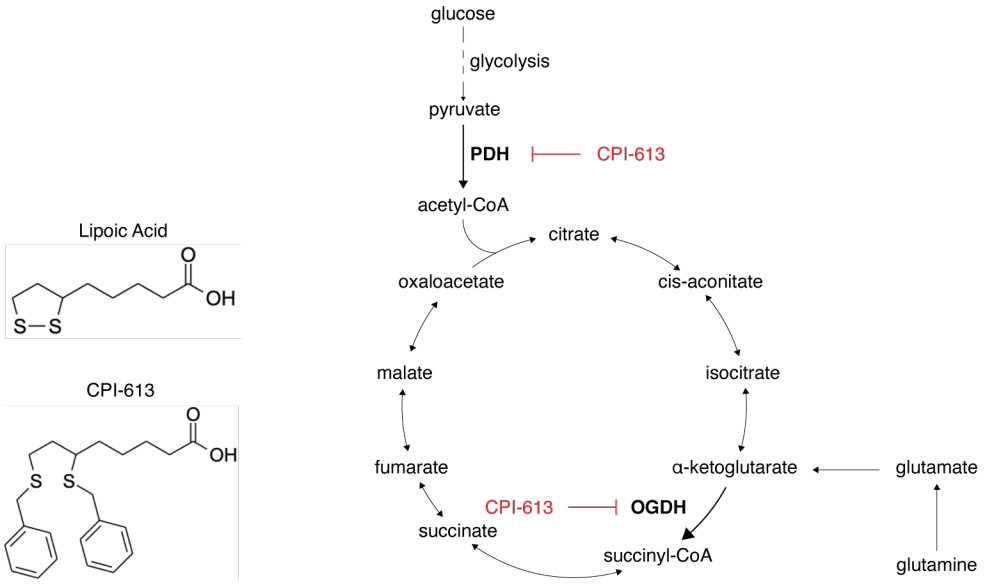

Figure 6.1 CPI-613 is a lipoic acid analog designed to inhibit PDH and OGDH among other enzyme complexes
Schematic depicting the structures of lipoic acid and CPI-613 (left) and its proposed molecular targets (right)

Unlike most cofactors, lipoic acid is covalently attached to enzymes and can act as both an electron hydrogen carrier and as an acyl carrier. Indeed, within both the PDH and OGDH reactions lipoic acid is reduced and subsequently carries an acyl group to assist in the catalysis of each respective reaction[150]. Given the presence of two benzene rings,

CPI-613 is unable to act as an electron hydrogen carrier or an acyl carrier in such reactions. As such, CPI-613 is thought to still covalently attach to enzymes through the conserved carboxylic acid functional group, but it will not participate as a cofactor rendering CPI-613-containing enzymes non-functional.

Given that CPI-613 might inhibit PDH and OGDH, we performed polar metabolite profiling in MOLM-13 AML cells to determine whether the products or substrates of these reactions are reduced or accumulated upon CPI-613 treatment, respectively. Polar profiling revealed a broad and marked increase in a range of metabolites. Of note, pyruvate was increased with CPI-613 treated cells, however, levels of α-ketoglutarate/2-oxoglutarate were not significantly altered by CPI-613 treatment. While acetyl-CoA was not directly detected in this experiment, downstream metabolites, such as isocitrate and cis-aconitate, were decreased upon CPI-613 treatment, though only the decrease in cis-aconitate was statistically significant. Likewise, succinyl-CoA was not directly detected, however, succinate levels were unchanged with CPI-613 treatment. Altogether, these results suggested that CPI-613 might inhibit the production of acetyl-CoA from pyruvate by PDH, but it is unlikely to inhibit the production of succinyl-CoA from α-ketoglutarate/2-oxoglutarate by OGDH in MOLM-13 cells.

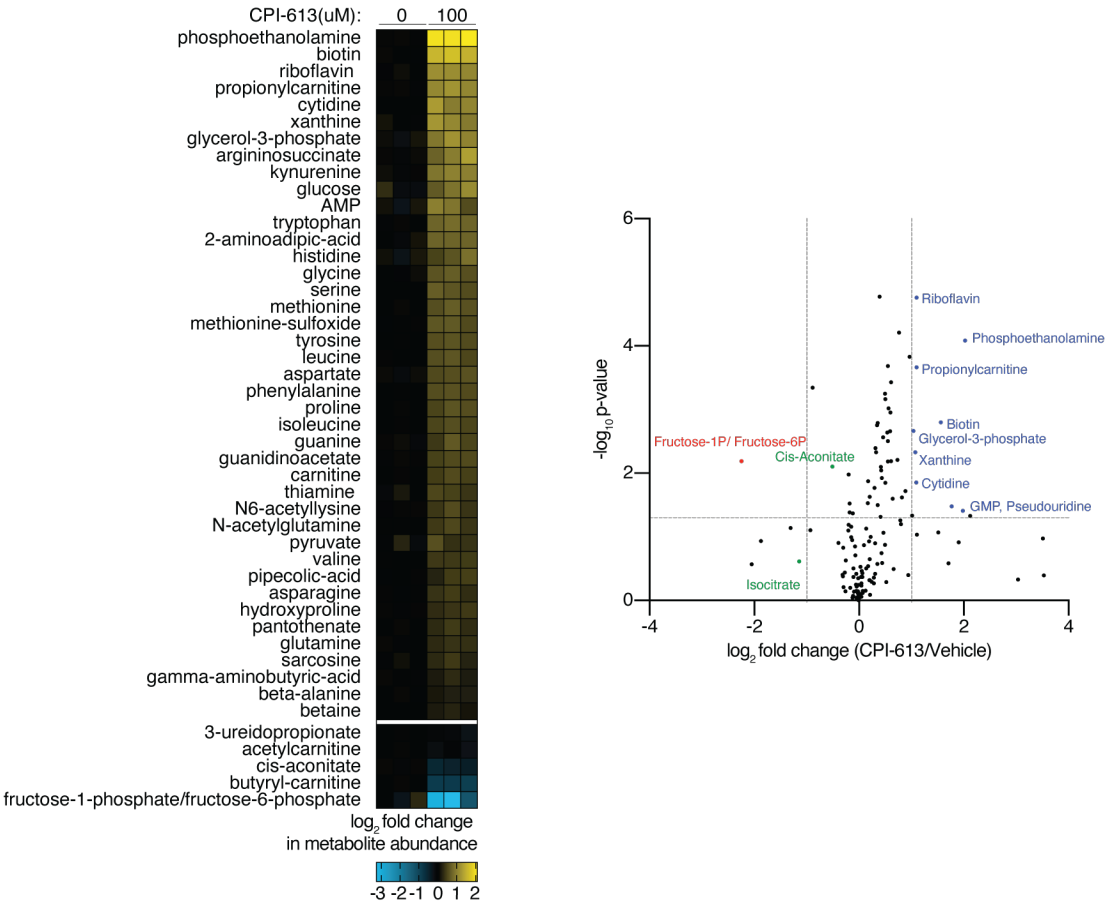

Figure 6.2 Polar metabolite profiling reveals marked changes under CPI-613 treatment

(Left) Fold change in significantly altered metabolites (log_2) in wild-type MOLM-13 cells treated with CPI-613 (100uM) relative to vehicle.

(Right) Volcano plot of statistical significance ($-log_{10}$ p-value) and fold change in metabolites (log_2) in wild-type MOLM-13 cells treated with CPI-613 (100uM) relative to vehicle.

In order to further test the hypothesis that CPI-613 inhibits PDH and does not inhibit OGDH activity, we performed polar metabolite profiling of CPI-613 treated cells grown in the presence of uniformly heavy carbon labelled ([U-13C]) glucose or [U-13C]-L-glutamine. Heavy glucose tracing can quantify the relative amount of acetyl-CoA generated by PDH from glucose-derived pyruvate by its incorporation into citrate or cis-aconitate (Figure 6.3). Similarly, heavy glutamine tracing can quantify the relative amount of succinyl-CoA generated by OGDH from glutamine-derived α-ketoglutarate/2-oxoglutarate (Figure 6.4). This revealed a minimal impact of CPI-613 on the labeling of metabolites downstream of both PDH and OGDH (Figure 6.3 and 6.4) suggesting that CPI-613's primary mechanism of action may not be direct inhibition of these enzymes.

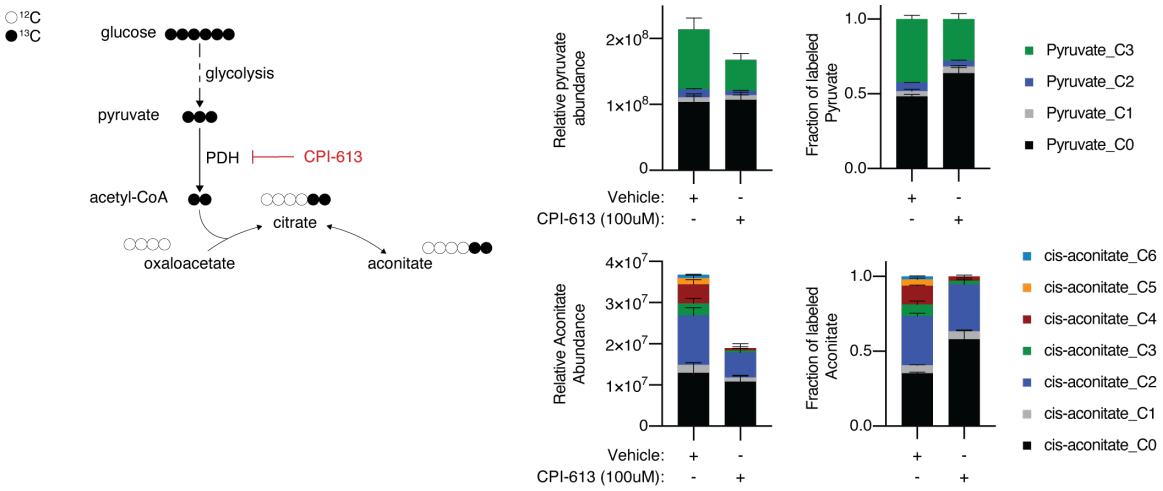

Figure 6.3 Heavy glucose isotope tracing suggests a limited reduction in PDH activity under CPI-613 treatment
(Left) Schematic depicting the labeling of indicated metabolites from [U-13C]-glucose (Right) Relative and fractional abundance of pyruvate and aconitate isotopes in CPI-613 (100uM) or vehicle treated MOLM-13 cells.

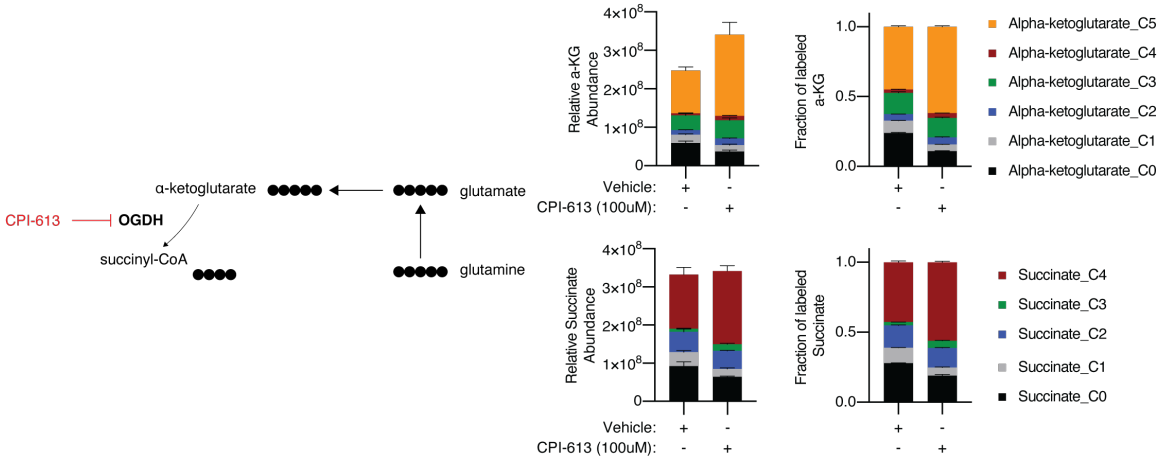

Figure 6.4 Heavy glutamine isotope tracing suggests no reduction in OGDH activity under CPI-613 treatment
(Left) Schematic depicting the labeling of indicated metabolites from [U-13C]-glutamine (Right) Relative and fractional abundance of α-ketoglutarate/2-oxoglutarate and succinate isotopes in CPI-613 (100uM) or vehicle treated MOLM-13 cells.

Altogether, metabolite profiling in CPI-613 treated cells did not suggest robust inhibition of PDH or OGDH in MOLM-13 cells. As such, the precise mechanism of action of CPI-613 remained unclear and as its simple structure suggested that it may have more than a few protein targets[151].

6.2 CRISPR-based screen identifies metabolic genes required for proliferation under CPI-613 treatment

In order to explore alternative mechanisms of CPI-613-induced toxicity in MOLM-13 cells, we performed a negative selection CRISPR/Cas9-based genetic screen to identify metabolic genes whose loss would sensitize cells to treatment with CPI-613 (Figure 6.5).

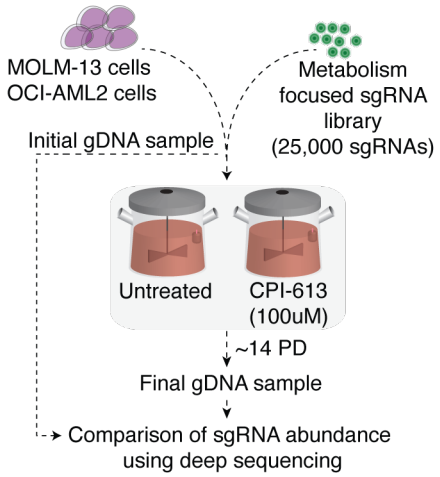

Figure 6.5 CRISPR-based screen in AML cells treated with CPI-613
Schematic depicting a metabolism-focused CRISPR screen to identify genes required for AML cell proliferation under CPI-613 treatment

Interestingly, knockout of PDHA, PDHB and OGDH, the proposed direct targets of CPI-613, were essential for the proliferation of MOLM-13 cells under CPI-613 treatment (Figure 6.6). Additionally, a number of genes encoding subunits of various complexes of the electron transport chain were also required for proliferation in CPI-613 treated cells. The essentiality of these genes under CPI-613 treatment are consistent with the TCA cycle being the primary target of the drug.

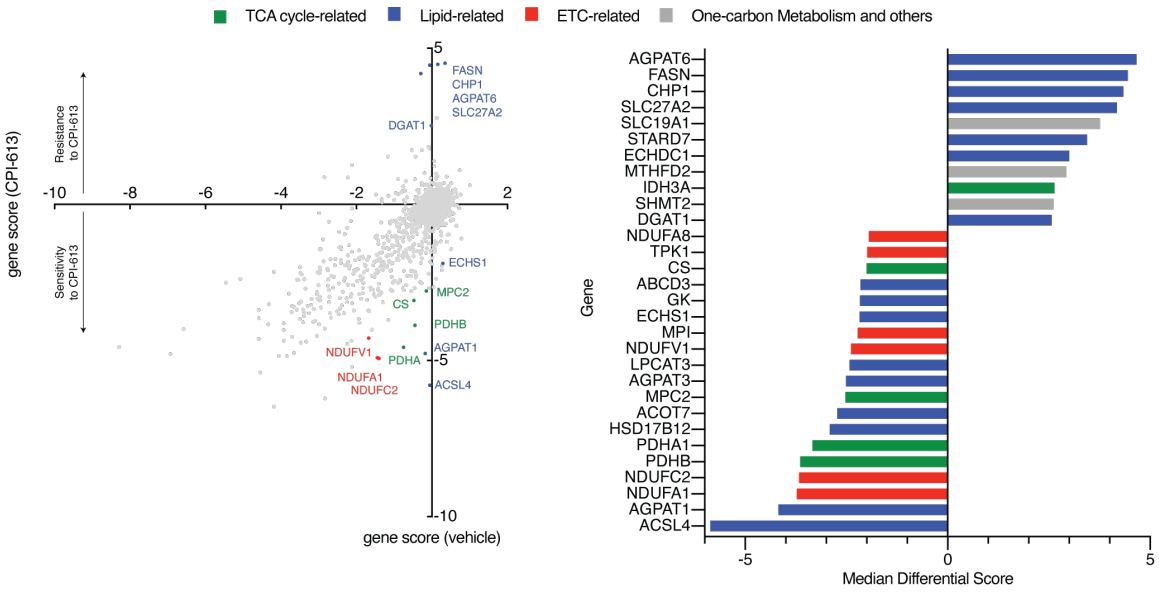

Figure 6.6 CRISPR-based screen in AML cells identifies genes essential for survival under CPI-613 treatment in MOLM-13 cells
(Left) Gene scores for vehicle versus CPI-613 treated MOLM-13 cells. Most genes scored similarly under untreated or treated conditions.
(Right) Median differential score for top 11 or 19 genes in the positive or negative direction, respectively.
Genes are highlighted as belonging to the TCA cycle (green), lipid metabolism (blue), electron transport chain (red), and one-carbon metabolism (gray).

Unexpectedly, however, the strongest hits in the genetic screen are involved in lipid metabolism (Figure 6.6). Knockout of Acyl-CoA Synthetase Long Chain Family Member 4 (ACSL4) or 1-Acylglycerol-3-Phosphate O-Acyltransferase 1 (AGPAT1), genes involved in the activation and incorporation of free fatty acids into glycerolipid species, sensitized MOLM-13 cells to treatment with CPI-613. On the other hand, knockout of 1-Acylglycerol-3-Phosphate O-Acyltransferase 6 (AGPAT6), Calcineurin Like EF-Hand Protein 1 (CHP1), genes involved in the incorporation of the first fatty acid onto glycerol-3-phosphate, reduced the sensitivity of MOLM-13 cells to CPI-613. In addition to these most significant hits, the enzyme responsible for long-chain saturated fatty acid synthesis, Fatty Acid Synthase (FASN), was detrimental to cells under CPI-613 treatment as knockout of FASN reduced the sensitivity of cells to the drug. Conversely, knockout of the second step of mitochondrial fatty acid beta oxidation, Enoyl-CoA Hydratase Short Chain 1 (ECHS1), sensitized cells to CPI-613. Altogether these hits revealed a critical reliance on lipid metabolism in cells treated with CPI-613, and suggested that cells require beta oxidation, rather than synthesis of fatty acids under drug treatment.

In order to investigate the role of these lipid metabolism genes under CPI-613 treatment, we generated two clonal CHP1 knockout MOLM-13 cells in which CHP1

protein was undetectable by immunoblotting (Figure 6.7). Consistent with the genetic screen, CHP1 knockout cells were resistant to doses of CPI-613 that resulted in cell death in wild-type cells. Importantly, overexpression of CHP1 within these CHP1 knockout cells restored their sensitivity to CPI-613. These data confirmed the findings of our genetic screen and implicate glycerolipid synthesis as an important mediator of sensitivity to CPI-613.

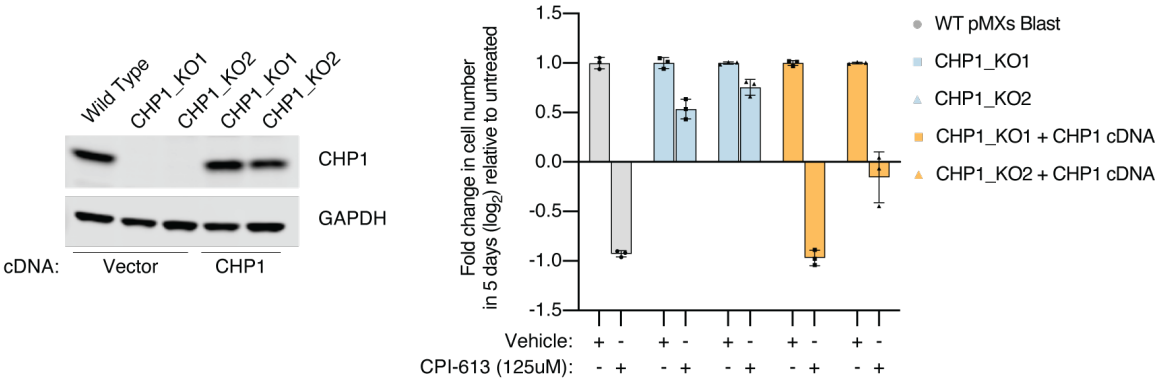

Figure 6.7 Loss of CHP1 renders cells resistant to CPI-613 treatment
(Left) Immunoblot analysis of parental, CHP1 knockout, or CHP1 cDNA expressing CHP1 knockout MOLM13 cells. GAPDH was used as a loading control.
(Right) Fold change in cell number relative to vehicle control (log_2) of parental, CHP1 knockout, or CHP1 cDNA-expressing CHP1 knockout MOLM13 cells after treatment with indicated concentration of CPI-613 for 5 days (mean ± SD, n=3).

Previous work in our laboratory identified CHP1 as an important regulator of glycerolipid synthesis within the endoplasmic reticulum[110]. This work revealed that CHP1 promotes the incorporation of fatty acids through a direct interaction with AGPAT6/GPAT4, which catalyzes the initial step of glycerolipid synthesis. To begin to understand how loss of CHP1 confers resistance to CPI-613, we examined the effects of CPI-613 on lipid metabolism (Figure 6.8). In wild-type cells, CPI-613 caused significant changes in a broad range of lipid species classes. Interestingly, CHP1 KO cells appear to have less dramatic changes in most lipid species classes with the exception of triglycerides, the synthesis of which has previously shown to be diminished in CHP1 KO cells.

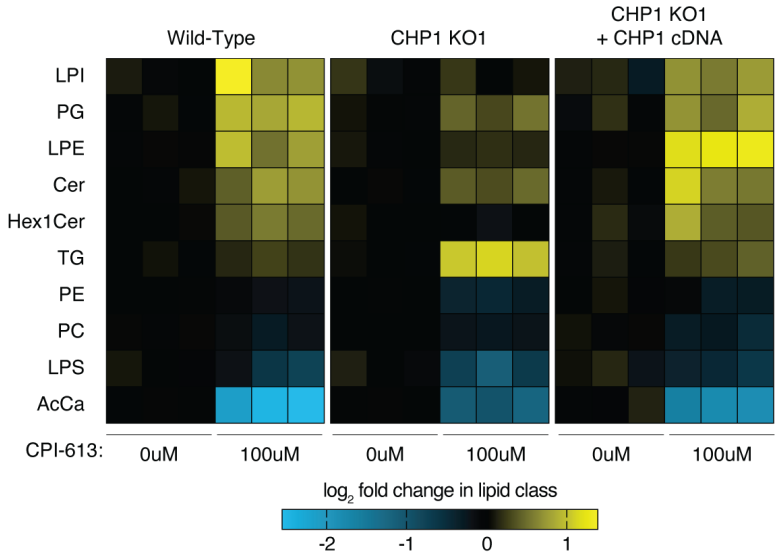

Figure 6.8 CPI-613 induces a variety of changes in lipid species
Fold change relative to respective untreated controls (log_2) of indicated lipid classes significantly altered between parental (left), CHP1 knockout (middle), or CHP1 cDNA-expressing CHP1 knockout (right) MOLM13 cells grown in 100uM of CPI-613. Lipid classes are ranked by the fold change of treated versus untreated parental cells. LPI = lysophosphatidylinositol; PG = phosphatidylglycerol; LPE = lysophosphatidylethanolamine ; Cer = Ceramides; Hex1Cer = Simple Glc series; TG = triglyceride; PE = phosphatidylethanolamine; PC = phosphatidylcholine; LPS = lysophosphatidylserine; AcCa = Acyl Carnitine

Notably, CPI-613 induced a dramatic reduction in acyl carnitine species. This effect was not as dramatic in CHP1 KO cells, whereas certain acyl carnitine species were unchanged in the presence of CPI-613 (Figure 6.9). Decreased acyl carnitines is typically a sign of reduced beta oxidation, and is often seen in CPT-I deficiency or with etomoxir treatment[103,152]. This finding is in agreement with the requirement for ECHS1 under CPI-613 treatment in our genetic screen. Interestingly, CPI-613 itself has been shown to be beta-oxidized to CPI-2850, a compound containing six rather than eight carbons ahead of the carboxylic acid group on CPI-613.

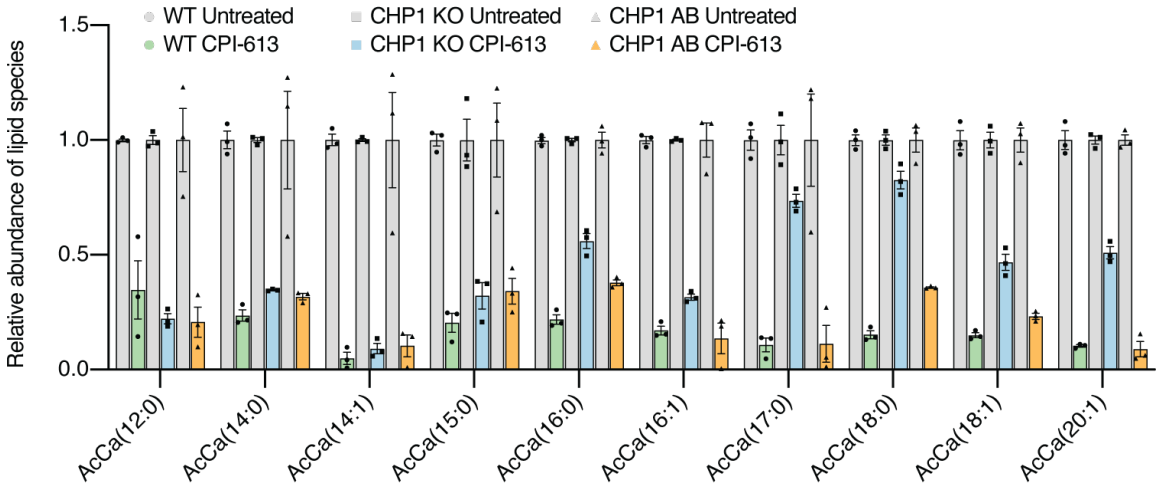

Figure 6.9 Acyl carnitines are dramatically reduced in cells treated with CPI-613
Fold change relative to respective untreated controls (log_2) of indicated lipid classes significantly altered between parental (left), CHP1 knockout (middle), or CHP1 cDNA-expressing CHP1 knockout (right) MOLM13 cells grown in 100uM of CPI-613. Lipid classes are ranked by the fold change of treated versus untreated parental cells.

6.3 CPI-613 is incorporated into glycerolipid species

Given the role of CHP1 and AGPAT6 in the incorporation of fatty acids into lipid species, we hypothesized that CPI-613 itself might be activated for incorporation into lipid species given the presence of a carboxylic acid in its structure. Lipid profiling in wild-type MOLM-13 cells revealed a striking abundance of lipid species containing CPI-613 as an acyl-chain (Figure 6.10 and Figure 6.11). Amongst these lipid species were 19 phospholipids and 88 triglyceride species containing CPI-613 including seven triglyceride species in which two molecules of CPI-613 were incorporated as acyl chains.

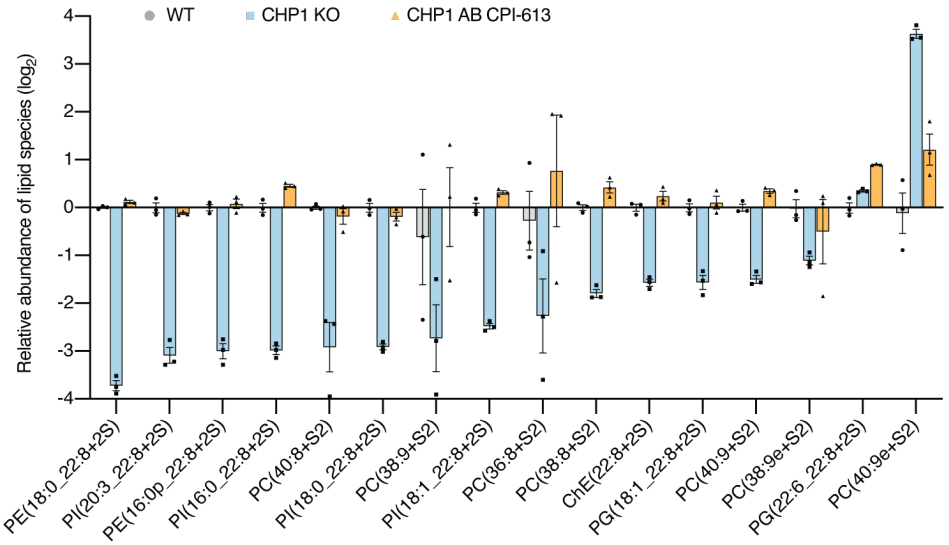

Figure 6.10 CPI-613 is incorporated into phospholipid species
Abundance of indicated lipid species relative to wild-type (log_2) in wild-type, CHP1 KO and CHP1 expressing CHP1 KO MOLM-13 cells. CPI-613 is defined as "22:8+2S" within each lipid species. PI = phosphatidylinositol; PG = phosphatidylglycerol ; PE = phosphatidylethanolamine ; PC = phosphatidylcholine; ChE = cholesterol ester.

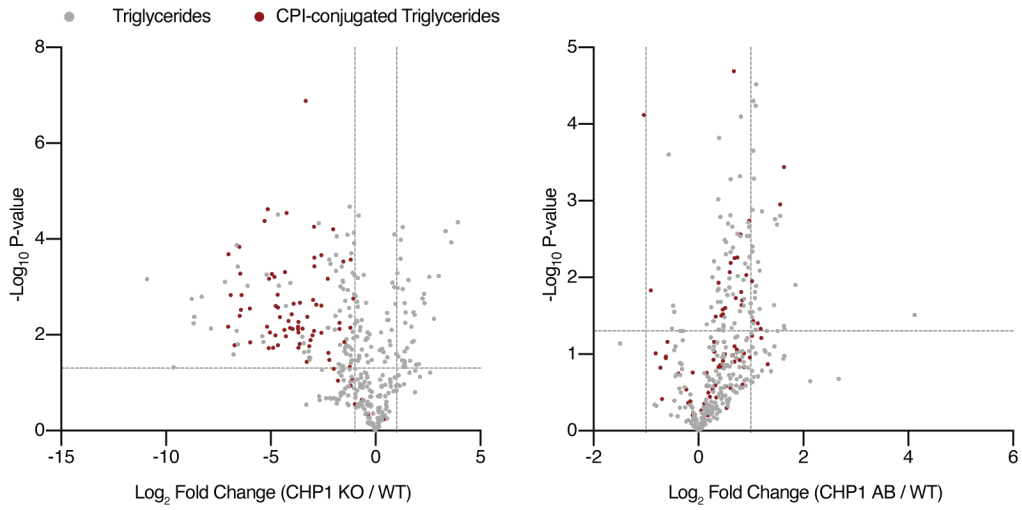

Figure 6.11 CPI-613 is incorporated into triglyceride species
Volcano plot of fold change (log_2) versus statistical significance ($-log_{10}$ p-value) of triglycerides present in CHP1 KO cells relative to WT cells (left) or CHP1 expressing CHP1 KO cells (right). Triglycerides containing CPI-613 are colored red, whereas normal triglyceride species are colored gray.

Importantly, incorporation of CPI-613 into lipid species was dependent on the presence of CHP1 as CHP1 knockout cells showed a striking reduction in CPI-613 lipid incorporation. This finding correlates with the insensitivity of CHP1 knockout cells to

CPI-613 treatment. Whether the incorporation of CPI-613 into phospholipids or triglycerides is directly related to the toxicity of the drug, however, remained unclear. Further evidence that incorporation of CPI-613 into triglycerides is toxic to cells comes from the observation that loss of DGAT1, the enzyme responsible for the final step of triglyceride synthesis, was protective for MOLM-13 cells treated with CPI-613 in the genetic screen. Altogether this suggests that the CPI-613-containing triglycerides may represent the toxic species within cells as prevention of CPI-613-triglyceride formation is equally protective as prevention of CPI-613-phospholipid formation.

6.4 CRISPR-based genetic screens reveal electron transport chain and beta oxidation activities are required under CPI-613 treatment across cell types

Genetic screening data from the cancer dependency map (DepMap) reveals that MOLM-13 is within a subset of AML cell lines that show enhanced proliferation upon loss of CHP1 and AGPAT6 (Figure 6.12). Indeed, a recent study classified this subset of cell lines as a “lipid sensitive” subtype of AML. Given the unique lipid metabolism of MOLM-13, we sought to determine whether genetic screening with CPI-613 would yield similar results in an AML cell line, OCI-AML2, as well as, a pancreatic cell line, MiA-PaCa-2. Notably, these cell lines do not appear to benefit from loss of CHP1 in the DepMap.

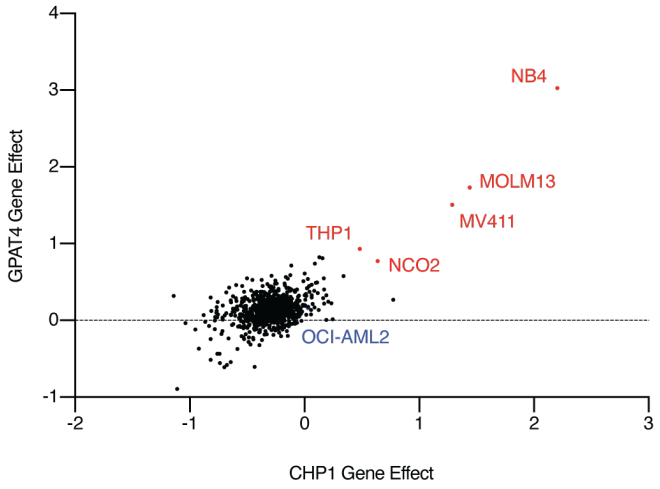

Figure 6.12 A subset of AML cell lines thrive in the absence of CHP1 or GPAT4
Gene effect scores from the DepMap for AGPAT6/GPAT4 and CHP1 across cell lines. AML “lipid sensitive” cell lines are highlighted in red, and an insensitive cell line, OCI-AML2, is highlighted in blue.

Across all three cell lines, knockout of electron transport chain complex subunits, ECHS1, or citrate synthase (CS) were among the top hits that sensitized cells to treatment with CPI-613 suggesting these genes may be required for cellular proliferation under CPI-613 regardless of cell type (Table 6.1). Interestingly, knockout of PDHA and PDHB were only sensitizing hits within AML cell lines. Within MiA-PaCa-2 cells,

monocarboxylate transporter 1 (MCT1) was important for resistance to CPI-613, a gene that was not important for resistance within either AML cell line. Altogether, these results suggest that electron transport chain activity and the activity of citrate synthase are generalized requirements under CPI-613, however, many genes are differentially essential depending on cell type.

Table 6.1 Genes essential for survival under CPI-613 treatment in MOLM-13, OCI-AML2 and MiA-PaCa-2 cells

Overlap of the top 100 genes required for proliferation under CPI-613 treatment in each cell line.

Genes essential for proliferation under CPI-613 treatment
NDUFA6
NDUFA3
NDUFA10
ECHS1
ACAD9
ALG8
NDUFA1
CS
NDUFA2
NDUFV1
TSC1
MECR
NDUFA11
NDUFC1

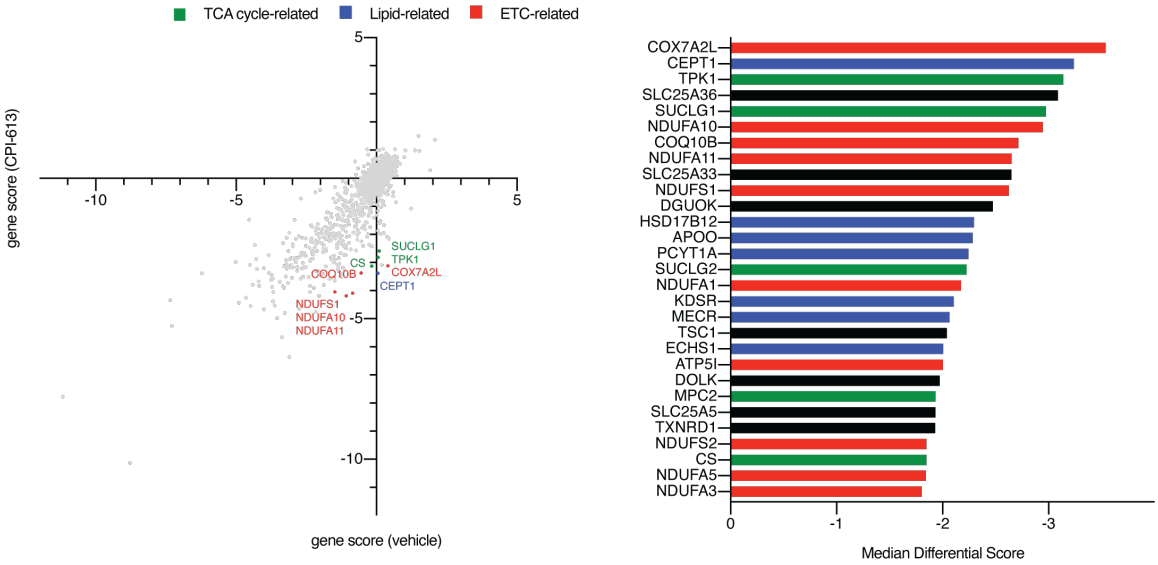

Figure 6.13 CRISPR-based screen in AML cells identifies genes essential for survival under CPI-613 treatment in OCI-AML2 cells
(Left) Gene scores for vehicle versus CPI-613 treated OCI-AML2 cells. Most genes scored similarly under untreated or treated conditions.
(Right) Median differential score for top 29 genes negative selected in the screen. Genes are highlighted as belonging to the TCA cycle (green), lipid metabolism (blue), and the electron transport chain (red).

Interestingly, loss of CHP1 was also protective for MiA-PaCa-2 cells under CPI-613 treatment, and, instead of AGPAT6, loss of a closely related gene, AGPAT9, was also protective suggesting a similar mechanism of action may exist within MiA-PaCa-2 cells as in MOLM-13 cells (Figure 6.14). OCI-AML2, however, displayed a limited number of lipid genes that sensitized cells to CPI-613 suggesting incorporation of the drug into lipid species may not be the predominant mechanism of action within this cell line (Figure 6.13).

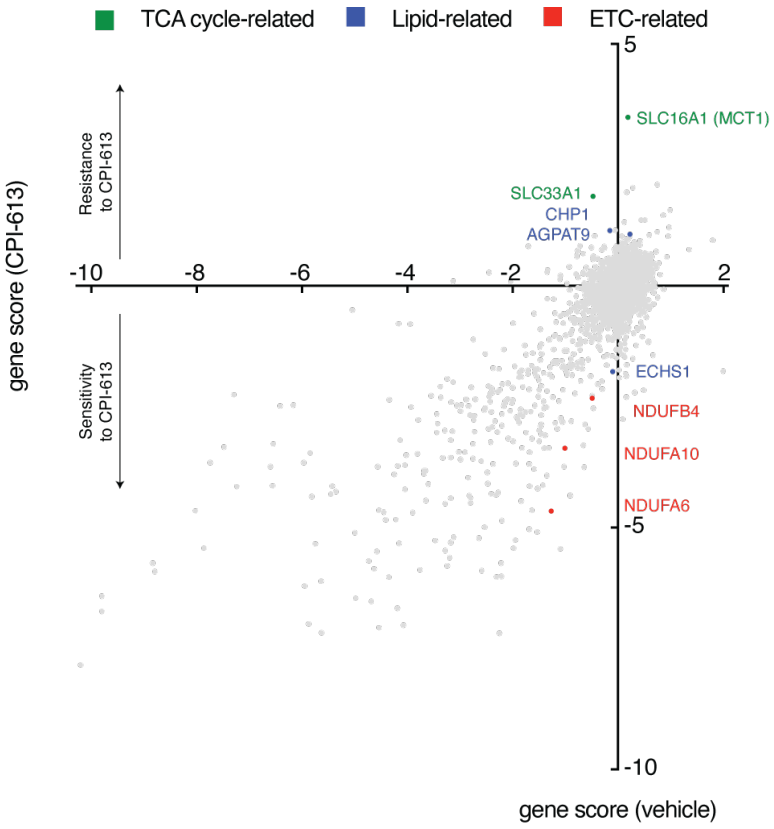

Figure 6.14 CRISPR-based screen in AML cells identifies genes essential for survival under CPI-613 treatment in MiA-PaCa-2 cells
(Left) Gene scores for vehicle versus CPI-613 treated MiA-PaCa-2 cells. Most genes scored similarly under untreated or treated conditions.
Genes are highlighted as belonging to the TCA cycle (green), lipid metabolism (blue), and the electron transport chain (red).

To determine whether the incorporation of CPI-613 into glycerolipid species was a generalizable finding, we performed lipid profiling on the OCI-AML2 given the general lack of lipid genes in our genetic screen of this cell line. Surprisingly, OCI-AML2 cells displayed a similar degree of incorporation of CPI-613 into lipid species (Figure 6.15).

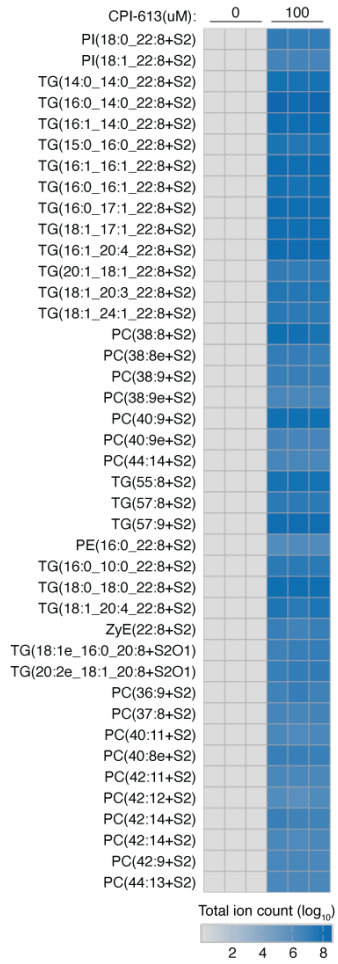

Figure 6.15 Lipidomics in OCI-AML2 cells reveals incorporation of CPI-613 into glycerolipids
Total ion count (log_{10}) of indicated CPI-613-containing lipid species in wild-type OCI-AML2 cells grown in 100uM of CPI-613.

Altogether, these findings suggested two possibilities: first, certain cell lines are more dependent on specific glycerolipid synthesis genes where others exhibit redundancy, or second, that CPI-613-containing lipid species are differentially toxic to cell lines. Further work will be required to define the precise mechanism by which CPI-613-containing triglycerides are toxic to cells.

CHAPTER 7. Discussion

Cancer cells are under constant stress due to the requirements of constant proliferation. Within the tumor microenvironment they are often faced with oxidative stress, hypoxia and a poor supply of nutrients. Furthermore, their rapid and continuous cell growth and division make protein, nucleotide and lipid synthesis a constant requirement. To address these demands, cancer cells rely upon cellular stress pathways. The mTOR/AMPK pathway, for example, responds to the nutrient and energy status of the cell to control metabolic pathways. Likewise, nuclear erythroid 2-related factor 2 (NRF2) and Kelch-like ECH-associated protein 1 (KEAP1) monitor levels of oxidative stress within the cell to produce an antioxidant transcriptional program in response to increased reactive oxygen species. Finally, hypoxia-inducible factor 1 (HIF1α) coordinates the transcription of genes in response to hypoxia. Importantly, each of these pathways have been implicated in oncogenesis and enhancement of their activities has been shown to promote tumor survival.

Analogous, to these stress response pathways, the integrated stress response (ISR) mediates a transcriptional program under certain cellular stresses. Canonically, the ISR is activated upon ER stress, amino acid starvation, viral infection and heme deprivation, however, hypoxia, glucose deprivation, and oxidative stress have also been shown to activate the ISR. Thus, the ISR acts alongside mTOR/AMPK, HIF1α, NRF2 pathways to promote cellular homeostasis and also plays an important role in tumor survival.

The ISR ultimately leads to the upregulation of activating transcription factor 4 (ATF4), a transcription factor that promotes a cytoprotective and homeostatic gene expression program. ATF4, like NRF2 and HIF1α, addresses cellular stresses through the direct transcriptional regulation of target genes. These target genes include metabolic enzymes and transporters for the restoration of nutrient homeostasis, or genes involved in the unfolded protein response to address unfolded protein stress within the endoplasmic reticulum. Interestingly, while NRF2 and HIF1α are activated by a specific cellular stress and promote gene expression, ATF4 is activated by a wide range of cellular stresses and coordinates transcriptional programs to address each uniquely. The ability to address such diverse stresses implies either complex activities of ATF4 or the contribution of additional transcriptional factors to each unique cellular stress.

Cancer cells are particularly prone to nutrient stress as their growth requires a constant supply of glucose, nucleotides, amino acids and lipids. Indeed, altered cellular metabolism was one of the earliest findings in tumor tissues with the observation and description of the Warburg effect. Recently it has been appreciated that numerous oncogenic mutations co-opt cellular stress pathways to drive the anabolic metabolism required for cell growth and proliferation. The transcriptional regulation of such metabolic pathways has been explored with a number of important oncogenes shown to directly influence metabolic gene regulation. There is, perhaps, no better example of the transcriptional regulation of metabolic pathways than that of Myc. Oncogenic expression of Myc drives nucleotide synthesis, glycolysis, glutaminolysis, mitochondrial replication,

and lipid accumulation[153–157]. Myc responds to the metabolic state of the cell through feedback received from mTORC1 and HIF1A signaling and alters its genetic regulation in a context-dependent manner.

Direct oncogenic mutations to ATF4 have not been observed, however, the central role of ATF4 in promoting nutrient acquisition is relied upon by numerous transformative oncogenes[158–160]. Myc and BRAF, for example, have been shown to co-opt ATF4 gene regulation to provide anabolic support for continued cellular proliferation[14,161]. Furthermore, KRAS controls asparagine synthesis and amino acid abundance through ATF4 activity[162]. While much has been described about the regulation of metabolic genes by ATF4, transcriptional regulators that cooperate with ATF4 under specific nutrient deprivation or metabolic stress conditions have not been thoroughly defined.

Here, we provide a proof-of-concept approach to identify transcriptional factors that are required for cellular proliferation under various metabolic stresses. Using CRISPR/Cas9 forward genetic screens, we hypothesized that we could discover transcriptional regulators that are important for cellular stress response pathways analogous to ATF4, NRF2, and HIF1α. We validated this approach by identifying SREBF1 as essential for cellular proliferation under saturated fatty acid stress and lipotoxicity. The sterol regulatory element binding proteins (SREBPs) play a broad role in the regulation of lipid metabolism through the direct regulation of enzymes that catalyze lipid and cholesterol synthesis[163]. Under lipotoxicity, SREBF1 bind to sterol regulatory elements within the promoters of genes to coordinate a transcriptional program to restore lipid homeostasis[113]. This approach also identified KANSL1, a member of the MOF acetyl transferase complex, as essential for proliferation under electron transport chain inhibition. The MOF complex has previously been implicated in the regulation of mitochondrial transcription and respiration[121]. Finally, screening cells under amino acid deprivation revealed a universal role of ATF4 under these conditions. These findings suggested that our forward genetic screening approach was capable of identifying genes known to play a role in the transcriptional response to certain metabolic stresses.

In addition to identifying transcriptional regulators know to play a role in stress response pathways, we also identified novel factors essential under amino acid deprivation conditions. Under deprivation of conditionally essential amino acids, for example, we found that MARCH5, a mitochondrial E3 ubiquitin ligase, was required for proliferation. This gene has been described to play a role in mitochondrial fission and quality control, however, its role in cell survival under essential amino acid deprivation remains unclear[123]. Altogether, our approach provides a methodology to identify transcriptional regulators that regulate the cellular response to specific nutrient or metabolic stresses.

Unexpectedly, we identified ZBTB1, in addition to ATF4, as an essential transcription factor for cellular proliferation under asparagine deprivation in ALL cell lines. Our work revealed that ZBTB1 is required for the induction of ASNS upon asparagine depletion[162]. Our work suggests that ATF4 requires ZBTB1 for the induction of ASNS

expression upon asparagine deprivation as ZBTB1 knockout cells express ATF4 under asparagine depletion but do not upregulate ASNS (Figure 7.1). While we have confirmed that ZBTB1 binds directly to a sequence within the promoter of ASNS, the precise mechanism by which ZBTB1 promotes the transcription of ASNS is still not clear. Loss of ZBTB1 did not alter the accessibility of chromatin, nor did it reduce histone marks associated with active gene expression at the ASNS promotor. Given the partial rescue of ZBTB1 knockout cells by ATF4 overexpression, we believe that these transcription factors act in parallel to regulate ASNS. While dimerization partners of ATF4 have been described, our work did not identify a direct interaction between ATF4 and ZBTB1[164]. Future biochemical studies will be necessary to determine the precise mechanisms by which ATF4 and ZBTB1 promote ASNS transcription.

ZBTB1 was previously independently described by two groups to play a role in the differentiation of T, B and NK cells[132–134]. Siggs et al. identified a mouse with an absence of CD3+ T cells, and a general deficiency in the differentiation of the lymphoid lineage[133]. Similarly, Punwani et al. found a transgenic mouse with absent T cells and defective B and NK cells. Both groups mapped observed phenotypes to the ZBTB1 genomic locus, and targeted knockout of ZBTB1 recapitulated their findings. Interestingly, our work suggests that ZBTB1 is required for ASNS expression in T-ALLs, but it is not required for ASNS expression in other cell types. This finding may relate to the importance of ZBTB1 in the differentiation of T cells specifically. Further work to define the transcription targets of ZBTB1 critical for hematopoiesis may yield more insight into its role in hematopoiesis and may reveal a link between asparagine abundance and T cell differentiation.

Early functional studies suggested that ZBTB1 is involved in the suppression of cAMP response elements (CREs) through its zinc finger and BTB domains[165]. ZBTB1 has more recently been described to play a role in translesion DNA synthesis through a ubiquitin-binding UBZ4 domain[137]. Through an association with KAP-1, ZBTB1 mediates the relaxation of chromatin after DNA damage thereby promoting recruitment of RAD18 prior to translesion repair. While ZBTB1 had previously been demonstrated to suppress gene expression, our work suggests it may also promote gene expression, depending on the target. The precise mechanisms by which it promotes or suppresses gene expression are unclear.

The transcriptional regulation of ASNS by ATF4 and ZBTB1 under asparagine deprivation is particularly relevant to a metabolic therapy used to treat ALL. L-asparaginase, a bacterial enzyme that degrades asparagine, exploits the dependency on asparagine for proliferation that has been observed in ALL. While the precise cause for the asparagine dependencies of leukemias is not been fully understood, it is thought to primarily involve reduced or complete loss of ASNS expression in ALL. Protein levels of ASNS have been shown to strongly correlate with the response to L-asparaginase, and there is a strong positive correlation between ASNS enzyme activity and L-asparaginase resistance[166]. Likewise, a study of 60 human cancer cell lines from the

National Cancer Institute revealed that ASNS cDNA levels negatively correlate with sensitivity to L-asparaginase – a correlation that was even stronger among leukemic cell lines[167]. Finally, a competitive growth assay with 554 barcoded cell lines revealed that cell lines with high ASNS expression outcompete those with low expression under asparagine depletion[62]. Indeed, in our work, overexpression of ASNS in cell lines that do not express ASNS is sufficient to rescue their proliferation under asparagine deprivation or L-asparaginase treatment. Taken together, these findings suggest that ASNS is the primary cell autonomous determinant of L-asparaginase sensitivity in leukemia, though alternative means of acquiring asparagine have been described[168].

Importantly, we have shown that T-ALL cell lines that are resistant to L-asparaginase can be sensitized to this therapy and asparagine depletion through loss of ZBTB1. This finding held true *in vivo* where loss of ZBTB1 improved the survival of mice treated with L-asparaginase when engrafted with T-ALL cell line xenografts. The establishment of ZBTB1 as an important factor in the response of T-ALLs to L-asparaginase is an important contribution to our understanding of resistance to this therapy. Furthermore, the role of ZBTB1 in directly regulating ASNS further argues that this gene is the predominant determinant of resistance to L-asparaginase.

The transcriptional regulation of ASNS by ATF4 has been well described, and the resistance to L-asparaginase must depend upon the expression and activity of ATF4[169]. Our work suggests this resistance must also depend upon the presence and positive regulation of ASNS by ZBTB1 in T-ALLs. Conversely, the asparagine auxotrophy observed in ALLs suggests that ASNS expression is absent in ALLs or within the hematopoietic progenitors from which they arise. The reasons for absent or reduced expression of ASNS in ALLs have not yet been defined. Alternatively, loss of ASNS expression may be beneficial in order to maintain higher levels of aspartate, a growth limiting metabolite for some tumors from which asparagine is synthesized[170–172]. The ASNS promoter has been shown to be regulated by methylation of specific histone marks that associated with active or inactive transcription, however the factors required to place such methylation marks have not been described. Similarly, ALL cell lines with low baseline ASNS expression exhibit hypermethylation of CpG islands within the ASNS promoter [173,174]. A recent study found that T-ALLs exhibit lower levels of ASNS due to hypermethylation of the ASNS promoter, a finding that is associated with better outcomes with asparaginase therapy[175]. Factors responsible for DNA methylation of the ASNS promoter are also unclear. Further work is required to define the totality of transcriptional regulators and mechanisms by which ASNS expression is controlled across different ALLs and through therapy (Figure 7.2).

Indeed, the discovery of ZBTB1's role in activating ASNS expression, even in T-cell lineage alone, suggests our understanding of ASNS transcriptional regulation is incomplete. More broadly, the role of ZBTB1 in parallel with ATF4 mediated regulation of ASNS argues for the presence of similar transcriptional regulators in other ATF4 target genes. While serine deprivation genetic screening did not reveal any clear

regulators of the serine deprivation other than ATF4, it remains possible that factors analogous to ZBTB1 regulate the expression of serine synthesis genes. Future work employing the approach detailed herein may elucidate transcriptional regulators that assist ATF4 in the transcriptional regulation of stress response genes.

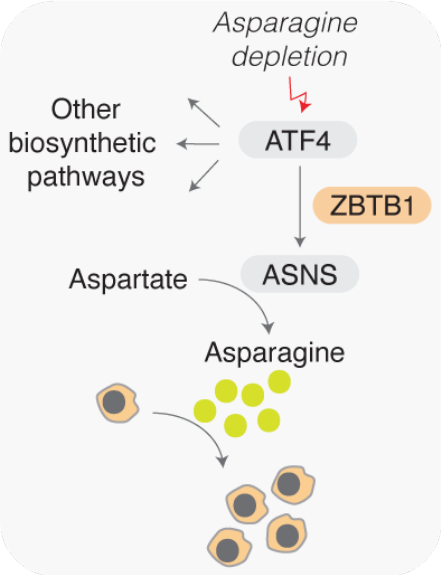

Figure 7.1. ZBTB1 controls the expression of ASNS under asparagine deprivation

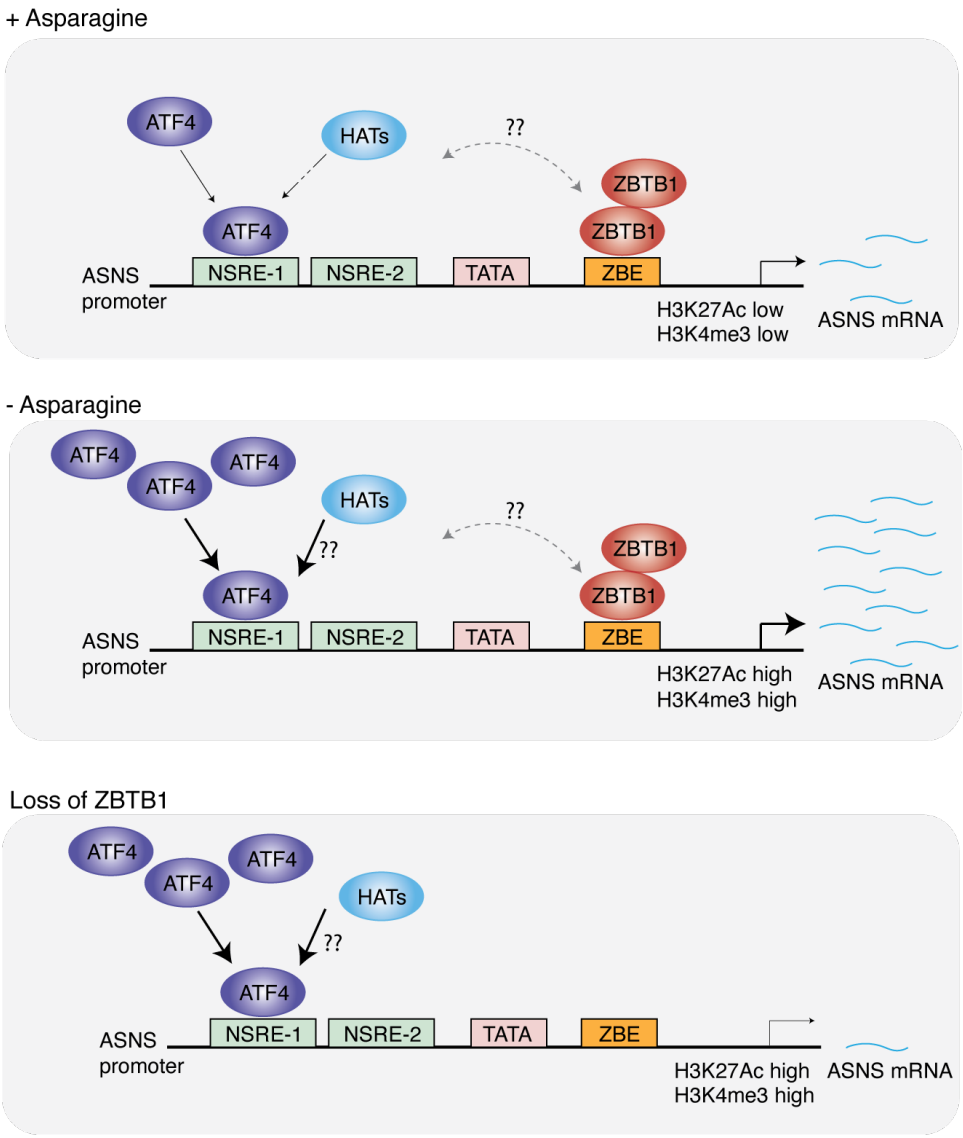

Figure 7.2 Transcriptional regulation of the ASNS promoter
Schematic depicting the transcriptional regulators of the ASNS promoter. NSRE = nutrient sensing response element, TATA = TATA box, ZBE = ZBTB1 binding element

Finally, our work provides rationale for a therapeutic approach targeting the increased lipid uptake and synthesis observed in various cancers. Here, we have identified the unexpected incorporation of CPI-613, a first-in-class lipoic acid analog, into glycerolipid species, a finding that correlates with toxicity of the drug. This observation led to the hypothesis that compounds structurally similar to CPI-613 could be designed for uptake and incorporation into lipid species to induce cellular toxicity through numerous mechanisms such as ER stress, lipotoxicity or inhibition of lipid metabolism pathways such as FAO or lipid synthesis. While a number of compounds have been rationally designed to target enzymatic processes, such as etomoxir for the inhibition of FAO, we hypothesize that compounds containing carboxylic acids for lipid incorporation may be

designed to deliver toxic payloads upon lipid incorporation. Such compounds could influence membrane fluidity by disrupting the balance of saturated and unsaturated lipids or sensitize cells to oxidative stress and ferroptosis through the propagation of peroxides.

While CPI-613 is thought to directly inhibit the TCA cycle enzyme complexes PDH and OGDH, here we have identified its primary incorporation into glycerolipid species. Our work did not reveal a significant accumulation of the substrates of PDH or OGDH nor a depletion of their metabolic products. Instead, a genetic screen in an AML cell line revealed a striking role of lipid metabolism genes in the sensitivity or resistance of cells to CPI-613. Further work to delineate the role of lipid metabolism in CPI-613 treatment revealed that the drug is incorporated into glycerolipid species, including phospholipids and triglyceride species, across multiple different cell lines and cell types. Importantly, this phenomenon appears to be the primary mechanism by which CPI-613 induces cellular toxicity as genetic knockout of genes required for this process are protective against the drug *in vitro*.

While we have yet to define the precise mechanism of toxicity associated with the incorporation of CPI-613 into lipids, these findings suggested a therapeutic strategy to exploit the lipogenic phenotype of certain cancers. Analogous to the incorporation of CPI-613 into lipid species, a class of drugs known as fibrates are integrated into lipid species. Previous work attempting to repurpose existing drugs for the treatment of AML even identified a combination of bezafibrate and medroxyprogesterone acetate (MPA) as a potent anti-AML treatment *in vitro*, suggesting this may be a viable therapeutic approach[90].

Among other targets within lipid metabolism pathways, compounds that have previously been shown to be activated by CoA and incorporate into lipid species inhibit FAO[101,102,176,177]. Etomoxir, for example, is activated by CoA to etomoxiryl-CoA, which irreversibly inhibits CPT1 to inhibit beta-oxidation. A similar compound, C75, has been shown to reversibly inhibit CPT1 in additional to its primary mechanism of inhibiting FASN. Indeed, our work revealed a striking depletion of acyl-carnitine species within CPI-613 treated cells, a finding observed upon treatment with other beta oxidation inhibitors. Furthermore, CPI-613 is known to be beta oxidized to CPI-2850, a compound with two less carbons after one cycle of beta oxidation. While we were able to detect CPI-2850, we were unable to detect further beta oxidations possibly suggesting that CPI-2850 is not further beta oxidized and may inhibit that process. Whether CPI-613's toxicity is associated with direct inhibition of lipid enzyme targets or through an undefined lipotoxic mechanism remains to be determine. The therapeutic strategy proposed here, however, may facilitate the development of compounds that alter lipid metabolism to selectively target the lipogenic phenotype observed in cancer. In AML, for example, such compounds may prevent the metabolic switch to FAO observed with chemotherapeutic resistance and relapse[178]. Notably, compounds targeting FA metabolism have not seen much success in clinical trials due to significant toxicities[70].

Whether our findings related to CPI-613's involvement in lipid metabolism are relevant *in vivo* remains to be determined, however, early phase clinical trials with the compound suggest it is safe and efficacious – a distinction from other lipid-targeting drugs previously tested in cancer.

CHAPTER 8. Future directions and perspectives

8.1 Alternative mechanisms of asparagine acquisition in ALL

While ASNS seems to be the primary cell autonomous mechanism of asparagine production, whether ASNS expression is the sole determinant of L-asparaginase resistance is debated. Conflicting results have been concluded when correlating ASNS expression to L-asparaginase sensitivity in ALLs[179–182]. For example, a study of clinical ALL samples found no correlation between baseline ASNS expression and response to L-asparaginase in vitro[183]. This discrepancy may be explained by alternative cellular sources of asparagine from catabolic protein degradation. Indeed, a proteasomal degradation and recycling pathway may provide sufficient asparagine to leukemias cells under asparaginase treatment. Inhibition of WNT leads to proteasomal degradation of proteins providing asparagine to leukemia cells. Activation of Wnt, then, sensitizes leukemic cells to L-asparaginase[168].

Other cell types in the bone marrow environment may also provide asparagine to leukemia cells under asparaginase treatment. For example, bone marrow-derived mesenchymal cells express high levels of ASNS and its expression has been shown to correlate with both the synthesis and secretion of asparagine by these cells[184,185]. Furthermore, ALL cells secrete insulin-like growth factor (IGF)-binding protein 7 (IGFBP7) when co-cultured with bone marrow stromal cells to stimulate ASNS expression and asparagine secretion[186]. Adipocytes may also provide anaplerotic substrates to leukemic cells and counteract the effects of L-asparaginase[187]. Furthermore, in AML, monocytes and macrophages have been shown to prevent the activity of L-asparaginase through the production of a lysosomal cysteine protease, cathepsin B[188]. Altogether these studies implicate potential resistance mechanisms for L-asparaginase therapy that extend beyond cell-autonomous synthesis of asparagine through ASNS activity. Indeed, in our work absence of ASNS expression secondary to loss of ZBTB1 slowed tumor growth under asparaginase treatment but was not sufficient to eliminate tumor burden. While a combination of ASNS inhibition and L-asparaginase treatment has been proposed to improve the efficacy of asparaginase, further work is needed to delineate mechanisms by which ASNS depleted ALLs survive asparaginase therapy to optimize such combinational therapies[145].

8.2 Tumor and tissue-specific transcriptional regulators of the amino acid stress response

Interestingly, the metabolic role of ZBTB1 in regulating ASNS appears to be restricted to T-cell leukemias, suggesting that there may be tumor or tissue-specific transcriptional programs involved in the regulation of the amino acid stress response pathway. Given that ZBTB1 is required for the transcription of ASNS in T cells, perhaps other transcription factors are required for this same role in different tissue types. Given the prospect of using L-asparaginase for the treatment of melanoma and pancreatic cancer, discovery of an analogous transcription factor that is essential for the transcription of ASNS in these cell types may be an important finding[64].

The essential role of ZBTB1 in the ATF4-driven transcription of ASNS suggests that there may be similar factors required for the regulation of other ATF4 target genes. Given recent interest in the use of serine deprivation for the treatment of various cancers, studies to identify transcription factors required for the ATF4-driven transcription of serine synthesis enzymes are warranted[189]. While our work did not identify any serine synthesis transcriptional regulators, our work provides a framework identify transcription factors and study the transcriptional regulation of other metabolic genes that are activated by ATF4.

Finally, targeting ZBTB1 with small molecules may provide an opportunity to specifically inhibit the transcriptional response to L-asparaginase treatment in therapy resistant leukemic cells. Due to the tissue specific function of ZBTB1, such an approach may mitigate toxicities associated with concomitant targeting of amino acid response pathway and L-asparaginase[145,190]. Likewise, targeting of other factors required for the ATF4-mediated transcriptional response to various cellular stresses may be a viable therapeutic strategy.

8.3 Asparagine availability may play a role in normal lymphoid hematopoiesis

Investigations into the role of ZBTB1 in hematopoiesis and lymphocyte development have suggested that ZBTB1-deficient lymphoid-primed progenitors develop into myeloid rather than lymphoid cell types[134]. ZBTB1 expression is upregulated in lymphoid progenitors but downregulated during myeloid differentiation suggesting that ZBTB1 suppresses a myeloid gene expression program. Related to its role in DNA repair, ZBTB1 knockout progenitors exhibit increased sensitivity to DNA replication stress due to an inadequate S-phase checkpoint and, as a result, show increased p53-induced apoptosis[191]. Interestingly, Bcl2 overexpression or p53 knockout restored development of ZBTB1 deficient lymphoid cells, though T cell differentiation eventually stalled at a later stage. Altogether these findings suggest that ZBTB1's role in lymphoid development may relate to its ability to prevent DNA damage in early lymphoid progenitors.

ChIP-sequencing results from our work may yield further insight into the direct transcriptional targets of ZBTB1 that influence normal hematopoiesis, particularly the later stages of T-cell development. For example, ZBTB1 enriches in the promoter of poly [ADP-ribose] polymerase 1 (PARP1), an enzyme responsible for the detection and response to DNA damage[192]. Furthermore, ZBTB1 enriches near the promoter of TRIM28, also known as KAP-1, which it has previously been shown to interact with in promoting chromatin relaxation in the DNA repair response. While it remains unclear whether ZBTB1 positively or negatively regulates PARP1 and KAP-1, changes in the transcription of these genes likely relates to ZBTB1's role in the DNA damage response.

Other than genes associated with DNA repair, a number of genes known to be involved in normal hematopoiesis showed enrichment of ZBTB1 within their promoters suggesting that ZBTB1's role in lymphoid development may extend beyond its role in the DNA damage response. ZBTB1 enriches within the enhancer region of RUNX1, and within the promoter regions of LMO1, LMO2, TAL1, and IKZF2 among a number of other poorly described transcription factors. Each of these transcription factors are critical for normal hematopoiesis[193]. TAL1 associates with LMO1, LMO2, and LDB1 to specify hematopoiesis during development[194]. RUNX1 is required for activation and repression of hematopoietic gene programs and it is often dysregulated in acute myeloid leukemia[195,196]. The identical DNA binding motifs of RUNX1 and ZBTB1 further supports the hypothesis that these genes may overlap in the regulation of genes involved in hematopoiesis. Finally, IKZF2, a member of the *Ikaros* transcription factor family, is involved in the development of lymphocytes[197]. Further work into the role of ZBTB1 in regulating these genes, and potentially other genes, in facilitating the normal differentiation of lymphocytes will be needed.

Given the direct regulation of ASNS by ZBTB1, we hypothesize that ZBTB1 might maintain asparagine abundance as a requirement for proper lymphoid development. Perhaps asparagine plays a major role in the differentiation of lymphoid progenitors, and in the absence of ZBTB1 these progenitors lack sufficient asparagine for differentiation. There is precedent for the involvement of a single amino acid in regulating normal differentiation wherein a serine auxotrophy was identified within epidermal stem cells, and serine supplementation was sufficient to prevent malignant transformation of these stem cells[198]. Future studies to explore whether restoration of lymphoid development in ZBTB1 knockout cells or mice is possible through the supplementation of asparagine may yield insight into the role of asparagine and ASNS regulation by ZBTB1 in lymphoid development.

Finally, it will be important to determine whether any signaling pathway directs ZBTB1 to mediate the transcription of ASNS. In our study, ChIP-sequencing suggested that ZBTB1 was present at the ASNS promoter regardless of asparagine presence, however, these studies were performed in cells overexpressing ZBTB1 protein. Perhaps, ZBTB1 enriches in the promoter of ASNS in a nutrient-dependent manner. Similarly, our studies exploring interaction partners with ZBTB1 did not yield any high affinity interacting proteins other than ZBTB1 itself. These experiments could be repeated under protein cross-linking conditions to identify transient or low-affinity interaction partners, if any exist. Information about upstream activation or direct interaction partners of ZBTB1 may yield important insights into the biology of ZBTB1 and its role both in asparagine metabolism and lymphoid hematopoiesis.

8.4 Toxic lipid species as a novel anti-cancer therapeutic approach

Finally, our work highlights the potential for carboxylic acid-containing small molecules to be incorporated into lipid species to cause toxicity to cancer cells. Such a therapeutic

approach remains, to our knowledge, untested, though compounds have been demonstrated to incorporate into lipid species following CoA activation. Cancer cells rely upon uptake and direct synthesis of fatty acids[73]. This increased reliance upon fatty acid metabolism may be exploitable to target rapidly growing cancer cells through the delivery of toxic lipid species. CPI-613, a lipoic acid analog, represents one such small molecule incorporated into lipids through a carboxylic acid functional group. The precise mechanism underlying the toxicity of CPI-613-containing lipid species remains unclear, however, prevention of CPI-613 incorporation into lipid species by genetic means prevents drug toxicity. Future work to decipher the precise mechanism of toxicity associated with CPI-613-laden triglycerides will be critical. While CPI-613's clinical success remains to be determined, future work to rationally design carboxylic acids capable of lipid incorporation and cellular toxicity may yield therapeutic small molecules.

In addition to their primary role in the structure of biological membranes, lipids act as signaling molecules that can alter cellular migration and immune regulation among other cellular processes. Future work will be necessary to define the role of CPI-613 in cellular signaling, and whether the drugs incorporation into lipids influences interactions between cancer cells and the immune system. Given the foreign nature of CPI-613, it is possible that CPI-613 produces a novel antigen or foreign membrane structure detectable by the immune system.

CHAPTER 9. Materials and Methods

9.1 Experimental Design

This study was designed to investigate transcriptional regulators of the amino acid response pathway in leukemia. To address this we (i) performed forward genetic screens to identify transcription-related genes that are required for cellular proliferation under various amino acid deprivation conditions, (ii) validated the universal role of ATF4 in enabling cellular proliferation under amino acid deprivation conditions and the role of ZBTB1 in permitting proliferation specifically under asparagine deprivation, (iii) identified genomic regions to which ZBTB1 enriches by ChIP-sequencing and elucidated ZBTB1's direct regulation of asparagine synthetase (ASNS), and (iv) determined that loss of ZBTB1 sensitizes therapy-resistant T-cell acute lymphoblastic leukemia cell lines to L-asparaginase *in vivo*.

9.2 Compounds, Cell lines and Constructs

Antibodies to ZBTB1 (26287-1-AP) and ASNS (14681-1-AP) were from Proteintech, to ATF4 (11815S), eIF2α (5324S), p-eIF2α (3597S) were from Cell Signaling Technology, to GAPDH (GTX627408) and Actin (GTX109639) were from Genetex, to H3K27ac (39133) and H3K4me3 (39159) were from Active Motif, to FLAG (F1804) was from Sigma, and anti-mouse Alexa Fluor 568 secondary antibody (A10037) was from Thermo Fisher Scientific. Secondary antibodies, IR-Dye680LT-conjugated Donkey anti-mouse IgG and IR-Dye800CW-conjugated Donkey anti-rabbit IgG, were from LI-COR Biosciences.

Polybrene, Puromycin, Asparagine, PhosSTOP, BL21 Rosetta Cells and Fetal Bovine Serum were from Sigma. Dialyzed Fetal Bovine Serum, RPMI-1640, Trypsin, Penicillin-Streptomycin, L-Glutamine were from Gibco. Blasticidin was from Invivogen. HPLC Grade Water, HPLC Grade Methanol and Pierce BCA Protein Assay Kit were from Thermo Fisher. [U-^{13}C5]-glutamine and heavy labeled amino acid internal standards were from Cambridge Isotopes. Phusion High Fidelity PCR Master Mix with HF Buffer, BsmBI, T4 DNA Ligase, BamHI and NotI were from New England Biolabs. X-tremeGENE 9 DNA Transfection Reagent and Protease Inhibitor was frome Roche. Fibronectin was from Corning. Asparaginase was from Biovendor. SYBR Green PCR Master Mix was from Applied Biosystems. Normal Donkey Serum was from Jackson ImmunoResearch. Serine was from Acros Organics. Cystine was from Alfa Aesar. Luciferin was from Biovision. RPMI without Amino Acids was from US Biologicals. IPTG was from Research Products International. Cell Titer Glo Luimenscent Cell Viability Assay was from Promega. DNeasy Blood & Tissue Kit, QIAprep Spin Miniprep Kit and RNeasy Mini Kit were from Qiagen. NEBNext Ultra RNA Library Prep Kit was from Illumina. Superscript III RT Kit and Prolong Gold antifade mounting media were from Invitrogen.

Cell lines (Jurkat, HeLa, HEK293T, CUTLL1, SUPT1, REH, NALM6, MOLM-13, SKM-1, MDA-MB-231, A549, RPMI-8402, and ALL-SIL) were purchased from ATCC. Cell lines were verified to be free of mycoplasma contamination and the identities of all were authenticated by STR profiling.

9.3 Cell Culture Conditions

All cell lines were cultured in RPMI medium containing 2 mM glutamine (Gibco), 10% fetal bovine serum (Sigma), penicillin and streptomycin (Gibco), unless noted otherwise. For experiments performed in human plasma-like medium (HPLM), cells were cultured in HPLM containing penicillin and streptomycin[199]. For proliferation assays under asparagine depletion and for tracing experiments, RPMI without amino acids (US Biologicals- R9010-01) was supplemented with individual amino acids at RPMI concentrations. For tracing experiments, [U-13C]-Glutamine (CIL, CLM-1822-H) was used. All cells were maintained at 37C and 5% CO2.

9.4 Cell Proliferation assays

Cell lines were cultured in 96-well plates at 1,000 cells per well in triplicate in a final volume of 0.2 ml RPMI-1640 media (Corning) under the conditions described in each experiment. A separate group of 3 wells was also plated for each cell line as an initial time point of untreated cells for normalization. After 5 days of growth, 40 μl of Cell Titer Glo reagent (Promega) was added to each well, mixed briefly, and luminescence was read using a SpectraMax M3 plate reader (Molecular Devices). For each well, the fold change in luminescence was calculated as the final luminescence of cells relative to the initial luminescence and reported on a $\log_2$ scale and reported as the number of population doublings. In certain figures, fold change in luminescence is calculated relative to untreated cells. Cell culture images were taken using a Primovert microscope (Zeiss).

9.5 Generation of Knockout or cDNA Overexpression Cell Lines

sgRNAs (indicated below) were ligated into BsmBI-linearized lentiCRISPR-v2 with T4 ligase (NEB). Lentiviral vectors expressing sgRNAs were transfected into HEK293T cells with lentiviral packaging vectors CMV VSV-G and Delta-VPR using XtremeGene 9 transfection reagent (Roche). Similarly, for overexpression, gBlocks (IDT) containing the cDNA of interest were cloned into pMXS linearized with BamHI and NotI by Gibson Assembly (NEB). cDNA retroviral vectors with indicated cDNAs were transfected into HEK293T cells with retroviral packaging plasmids Gag-pol and CMV VSV-G. After 24 hours, media was aspirated and replaced by fresh media. The virus-containing supernatant was collected 48 hours after transfection and filtered using a 0.45 mm filter to eliminate cells. Cells to be transduced were plated in 6-well tissue culture plates and infected in media containing virus and 8 mg/ml of polybrene. Cells were spin infected by centrifugation at 1,100g for 1.5 hr. After transduction, media was changed and cells

were selected with puromycin (for sgRNA lentiviral vector) or blasticidin (for overexpression retroviral vectors). Clonal knockout cells were generated from a single cell isolated by serial dilution of selected cells into a 96-well plate. Single cell clones were grown for two weeks, and the resultant knockout clones were expanded. Clones were validated for loss of the relevant protein by immunoblotting.

sgZBTB1_6F	5'-caccGCTGAAGGACATAGCTGCTG-3'	sgRNA cloning
sgZBTB1_6F	5'-aaacCAGCAGCTATGTCCTTCAGC-3'	sgRNA cloning
sgATF4_2F	caccgTCTCTTAGATGATTACCTGG	sgRNA cloning
sgATF4_2R	aaacCCAGGTAATCATCTAAGAGAc	sgRNA cloning

9.6 Immunoblotting

Cells were collected by centrifugation at 600 g for 5 min. Cell pellets were washed twice with ice-cold PBS prior to lysis in cold RIPA lysis buffer (20 mM Tris-Cl pH 7.5, 150 mM NaCl, 1 mM EDTA, 1% Triton X-100, 0.1% SDS, 0.5% sodium deoxycholate) supplemented with protease inhibitors and phosphatase inhibitors (Roche). After sonication of each cell lysate and centrifugation at 20,000 g for 15 min at 4C, supernatants were collected and protein concentration was determined using the Pierce BCA Protein Assay Kit (Thermo Scientific) with bovine serum albumin as a protein standard. Samples were then resolved on 8% or 12% SDS-PAGE gels and analyzed by immunoblotting. Blots were developed using the Li-Cor Odyssey CLx infrared imaging system.

9.7 Mouse Studies

All animal studies and procedures were conducted according to a protocol approved by the Institutional Animal Care and Use Committee (IACUC) at the Rockefeller University. Animals were housed in ventilated caging in a specific pathogen free animal facility. Animals were maintained on a standard light-dark cycle with food and water ad libitum. Xenograft tumors were initiated into NOD/SCID male littermates approximately 6-8 weeks in age by injecting 1 million GFP+, luciferase+ cells in 100 uL of PBS through the tail vein[200]. Tumor burden was measured weekly with an In Vivo Imaging System (IVIS) by injecting 50 uL of d-luciferin (30 mg/mL, BioVision) retro-orbitally. Mice were weighed weekly, and sacrificed after 20% weight loss, or if showing signs of significant distress or loss of limb or motor function. Mice were treated with L-asparaginase (1000 U/kg) twice weekly. Whole blood (100uL) was collected by submandibular vein bleed, and centrifuged at 500g for 5 min at 4C to yield a serum supernatant. Serum was analyzed by LC-MS, as described.

9.8 Immunofluorescence

For immunofluorescence assays, 300,000 cells were seeded onto coverslips previously coated with fibronectin. After 12 hours, cells were fixed for 15 minutes at room

temperature with 4% paraformaldehyde in PBS. After three PBS washes, cells were permeabilized with cold methanol for 10 minutes at -20C. Cells were washed an additional three times, blocked with 5% normal donkey serum, and incubated with the indicated primary antibody diluted 1:500 in blocking solution for one hour. Cells were washed three times with PBS and incubated with a donkey anti-mouse secondary Alexa Fluor 568 antibody for one hour. Cells were washed three times with PBS, and incubated with a 200 nM solution of DAPI in the dark. Cells were washed three final times, and the coverslip was mounted onto slides with Prolong Gold antifade mounting media (Invitrogen). Images were taken on a Revolve fluorescent microscope (Echo Laboratories).

9.9 Metabolite Profiling and Isotope Tracing

Each indicated cell line was cultured in triplicate in 6-well plates and grown for 8 hours in media with or without asparagine. For glutamine tracing experiment, cells were grown in media lacking glutamine supplemented with [U-13C]-glutamine at 2000 uM. Cells were washed three times with 1 mL of cold 0.9% NaCl, and polar metabolites were extracted in 1 mL of cold 80% methanol containing internal standards (MSK-A2-1.2, Cambridge Isotope Laboratories, Inc.). After 10 min extraction by vortexing, samples were centrifuged for 10 min at 10,000 ×g at 4^0C and samples were nitrogen-dried before storage at -80C until analysis by LCMS. Analysis was conducted on a QExactive benchtop orbitrap mass spectrometer equipped with an Ion Max source and a HESI II probe, which was coupled to a Dionex UltiMate 3000 UPLC system (Thermo Fisher Scientific, San Jose, CA). External mass calibration was performed using the standard calibration mixture every 7 days.

Dried polar samples were resuspended in 100 μL water and 2 μL were injected into a ZIC-pHILIC 150 x 2.1 mm (5 μm particle size) column (EMD Millipore). Chromatographic separation was achieved using the following conditions: Buffer A was 20 mM ammonium carbonate, 0.1% ammonium hydroxide; buffer B was acetonitrile. The column oven and autosampler tray were held at 25°C and 4°C, respectively. The chromatographic gradient was run at a flow rate of 0.150 mL/min as follows: 0–20 min.: linear gradient from 80% to 20% B; 20–20.5 min.: linear gradient from 20% to 80% B; 20.5–28 min.: hold at 80% B. The mass spectrometer was operated in full-scan, polarity switching mode with the spray voltage set to 3.0 kV, the heated capillary held at 275°C, and the HESI probe held at 350°C. The sheath gas flow was set to 40 units, the auxiliary gas flow was set to 15 units, and the sweep gas flow was set to 1 unit. The MS data acquisition was performed in a range of 70–1000 m/z, with the resolution set at 70,000, the AGC target at 10e6, and the maximum injection time at 20 msec. Relative quantitation of polar metabolites was performed with XCalibur QuanBrowser 2.2 (Thermo Fisher Scientific) using a 5 ppm mass tolerance and referencing an in-house library of chemical standards. Metabolite levels were normalized by cell counting for each condition.

9.10 Lipid Metabolite Profiling

Each indicated cell line was cultured in triplicate in 6-well plates and grown for the indicated amount of time in RPMI media containing the indicated concentration of drug or vehicle control. Cells were washed two times with 1 mL of cold 0.9% NaCl, and non-polar metabolites were extracted by the addition of 240 μL of cold 100% methanol, followed by 800 μL of cold methyl tert-butyl ether. After 10 minute extraction by vortexing, an additional 200 μL of cold water was added to each sample. After an additional minute of vortexing, samples were centrifuged for 10 minutes at 16,000 xg at 4^{0}C. The lipid-containing phase (top) and the polar phase (bottom) were collected separately, and samples were nitrogen-dried before storage at -80C until analysis by LCMS.

9.11 RNA Extraction, Reverse Transcription, Real-time PCR and RNA-Sequencing

RNA was extracted from Jurkat cells using the Qiagen RNeasy mini kit according to the manufacturer's instructions. 1 ug of RNA was reverse transcribed using the Superscript III Reverse Transcriptase kit (Invitrogen) according to the manufacturer's instructions. Quantitative real-time PCR (qPCR) was performed using SYBR green master mix and GAPDH was used as a control. The primer sequences were:

GAPDH forward	5'-TTGGTATCGTGGAAGGACTC-3'	qPCR
GAPDH reverse	5'-ACAGTCTTCTGGGTGGCAGT-3'	qPCR
ATF4 forward	5'-GGGACAGATTGGATGTTGGAGA-3'	qPCR
ATF4 reverse	5'-ACCCAACAGGGCATCCAAGT-3'	qPCR
PHGDH forward	5'-CTGCGGAAAGTGCTCATCAGT-3'	qPCR
PHGDH reverse	5'-TGGCAGAGCGAACAATAAGGC-3'	qPCR
PSAT1 forward	5'-TGCCGCACTCAGTGTTGTTAG-3'	qPCR
PSAT1 reverse	5'-GCAATTCCCGCACAAGATTCT-3'	qPCR
SLC1A5 forward	5'-GAGCTGCTTATCCGCTTCTTC-3'	qPCR
SLC1A5 reverse	5'-GGGGCGTACCACATGATCC-3'	qPCR
DDIT3 forward	5'-GGAAACAGAGTGGTCATTCCC-3'	qPCR
DDIT3 reverse	5'-CTGCTTGAGCCGTTCATTCTC-3'	qPCR

RNA library preparations and sequencing reactions were conducted at GENEWIZ, LLC. (South Plainfield, NJ, USA). RNA samples received were quantified using Qubit 2.0 Fluorometer (Life Technologies, Carlsbad, CA, USA) and RNA integrity was checked using Agilent TapeStation 4200 (Agilent Technologies, Palo Alto, CA, USA).

RNA sequencing libraries were prepared using the NEBNext Ultra RNA Library Prep Kit for Illumina using manufacturer's instructions (NEB, Ipswich, MA, USA). The sequencing libraries were clustered on a single lane of a flowcell. After clustering, the flowcell was loaded on the Illumina HiSeq instrument (4000 or equivalent) according to

manufacturer's instructions. The samples were sequenced using a 2x150bp Paired End (PE) configuration. Raw sequence data (.bcl files) generated from Illumina HiSeq was converted into fastq files and de-multiplexed using Illumina's bcl2fastq 2.17 software.

9.12 CRISPR-Cas9 Genetic Screen

The epigenetic-focused sgRNA library was designed and the screen performed as previously described (Wang, 2014). Oligonucleotides containing sgRNA sequences were synthesized by Agilent and amplified by PCR and cloned into lentiCRISPR-v2. Briefly, amplicons were inserted into lentiCRISPR-v2, linearized by BsmBI digestion, by Gibson Assembly (NEB). Gibson Assembly products were then transformed into E. coli 10G SUPREME electrocompetent cells (Lucigen). This plasmid pool was used to generate lentivirus-containing supernatants. The titer of lentiviral supernatants was determined by infecting targets cells at several amounts of virus in the presence of polybrene (4 ug/ml), counting the number of drug resistant infected cells after 3 days of selection. 40 million target cells were infected at an MOI of ~0.5 and selected with puromycin (4 ug/ml) 72 hours after infection. An initial pool of 30 million cells was harvested for genomic DNA extraction. The remaining cells were cultured for 14 doublings under specified amino acid deprivation conditions, after which cells were harvested for genomic DNA extraction. sgRNA inserts were PCR amplified, purified and sequenced on a HiSeq 2500 (Illumina) (primer sequences provided below). Sequencing reads were mapped and the abundance of each sgRNA was tallied. Gene score is defined as the median log2 fold change in the abundance between the initial and final population of all sgRNAs targeting that gene. Full result of the screen can be found in the supplementary data. The differential gene score is the difference between the untreated and amino acid deprivation condition gene scores.

9.13 Chromatin Immunoprecipitation Sequencing

ChIP analysis was performed as described previously. Briefly, cells were cross-linked with 1% paraformaldehyde for 10 minutes at 37C. Cross-linking was quenched with 125 mM glycine. Cells were pelleted and flash-frozen in liquid nitrogen. Nuclei were isolated and sonicated using a Covaris sonicator. Protein A/G beads were added to 2-4 ug of appropriate antibodies and bound at room temperature for 1.5 hours. Samples were immunoprecipitated with appropriate protein A/G-antibody complexes overnight at 4C. Immunoprecipitates were collected and washed twice each with low salt, high salt, and lithium chloride wash buffers. DNA was eluted, reverse-crosslinked and treated with RNAse and proteinase K before being isolated with a PCR purification kit (Zymogen). DNA was analyzed by quantitative real-time PCR on a QuantStudio 6 Flex Real Time PCR system using SYBR green PCR Master Mix (Applied Biosystems).

ChIP-sequencing samples were sequenced using the Illumina NextSeq 500. ChIP-seq reads are aligned using Rsubread's align method and predicted fragment lengths calculated by the ChIPQC package [201,202]. Normalised, fragment extended signal

bigWigs are created using the rtracklayer package. Peak calls are made in HOMER software [203] and their peak summits used in MEME-ChIP software for known and denovo motif discovery. Read counts in peaks are calculated using the featureCounts method in the Rsubread library [202]. Differential ChIP-seq signal is identified using the binomTest from the edgeR package [204]. High confidence ZBTB1 binding events were derived from the intersection of differential ChIP-seq of ZBTB flag samples over their condition matched GFP flag samples (padj < 0.05). Consensus ATF4 peaks are defined as peaks occurring in at least one condition of ATF4 ChIP-seq. Annotation of genomic regions to genes, biological functions and pathways is performed using the ChIPseeker package [205]. Meta-peak plot are produced using the soGGi package and ChIP-seq signal heatmaps using the Deeptools and profileplyr software [206,207].

9.14 Assay for Transposase-Accessible Chromatin using sequencing

ATAC-seq was performed as previously described[208]. Wild-type, ZBTB1 KO or ZBTB1 KO expressing ZBTB1 cDNA cells were treated in the presence or absence of asparagine for 24 hours. Nuclear extracts were prepared from 100,000 cells for each cell line and condition, and incubated with 2.5 µl of transposase (Illumina) in a 50 µl reaction for 30 min at 37 °C. Transposase-fragmented DNA was purified, and the library was amplified by PCR. The library was subjected to high-throughput sequencing using the HiSeq 2000 platform (Illumina). ATAC-seq reads were normalized and displayed as read counts per million mapped reads.

9.15 Protein Expression and Purification

The zinc-finger domains of ZBTB1 were N-terminally tagged with a 6X-histidine tag and cloned into a pET vector (Novagen). BL21 Rosetta cells were transformed with the ZBTB1-pET vector and a colony was grown overnight in ampicillin and chloramphenicol at 37C. The overnight culture was scaled to 1L and grown to an A_{600} of 0.6 before the addition of 0.5mM IPTG and transfer to 16C for growth for 16 hours. Cells were harvested by centrifugation and pellets were lysed with lysis buffer (50 mM Tris-HCl pH 8.0, 300 mM NaCl, 10 mM Imidazole, 1 mM b-mercaptoethanol) containing protease inhibitor. Cells were sonicated and insoluble material was removed by centrifugation. Lysate was loaded onto Ni-NTA resin (Qiagen) and washed twice with wash buffer (50mM Tris-HCl pH 8.0, 300 mM NaCl, 20 mM Imidazole). Protein was eluted with wash buffer containing 250 mM Imidazole, and purity was analyzed by SDS-PAGE.

9.16 Electrophoretic Mobility Shift Assay

IRDye 700 and competitor oligonucleotides were purchased from Integrated DNA Technologies (IDT). Oligonucleotide sequences are provided in below. EMSA assays were performed according to Odyssey instructions. Briefly, oligonucleotides were diluted in TE to a final concentration of 20 pmol/uL, and 100 pmol of F and R primers were annealed by heating to 100C and left to slowly cool back to room temperature.

Annealed oligos were diluted 1:200 for a working stock solution. Binding reactions contained 10X binding buffer, poly dI-dC, 25 mM DTT, 2.5% Tween 20, relevant oligonucleotides and purified ZBTB1 zinc-finger domain protein. Reactions were performed at room temperature for 30 minutes prior to electrophoresis through a 6% TBE gel (Novex). Gels were imaged using the Odyssey CLx.

ASNS-IRDye700-F 5'-
GGGTGGAGGATGCGGTCTTCAGCCTGGCACCCGGCAGACGCGGTTCGCGGGCG
CCTGCTGATGCTGCGGCTCCTGCGGTAGGGAGGGCG-3'
ASNS-IRDye700-R 5'-
CGCCCTCCCTACCGCAGGAGCCGCAGCATCAGCAGGCGCCCGCGAACCGCGTCT
GCCGGGTGCCAGGCTGAAGACCGCATCCTCCACCC-3'
ASNS-Competitor-F 5'-
GGGTGGAGGATGCGGTCTTCAGCCTGGCACCCGGCAGACGCGGTTCGCGGGCG
CCTGCTGATGCTGCGGCTCCTGCGGTAGGGAGGGCG-3'
ASNS-Competitor-R 5'-
CGCCCTCCCTACCGCAGGAGCCGCAGCATCAGCAGGCGCCCGCGAACCGCGTCT
GCCGGGTGCCAGGCTGAAGACCGCATCCTCCACCC-3'
ASNS-Mutant-Competitor-F 5'-
GGGTGGAGGATTCCCTCTTCAGCCTGGCACCCGGCAGACTCCCTTCGCGGGCGC
CTGCTGATGCTTCCCCTCCTTCCCTAGGGAGGGCG-3'
ASNS-Mutant-Competitor-R 5'-
CGCCCTCCCTAGGGAAGGAGGGGAAGCATCAGCAGGCGCCCGCGAAGGGAGTCT
GCCGGGTGCCAGGCTGAAGAGGGAATCCTCCACCC-3' EMSA

9.17 Statistical Analysis

Statistical analyses were performed on GraphPad Prism 8 or with appropriate computational tools. Error bars represent standard deviation from independent samples or experiments. Sample means, *P* values, and sample sizes are indicated in text or figure legends. $P \leq 0.05$ was the threshold for statistical significance, and the specific statistical test used is indicated in each figure legend.

PUBLICATIONS

Parts of this thesis were published in:

R. T. Williams, R. Guarecuco, L. A. Gates, D. Barrows, M. C. Passarelli, B. Carey, L. Baudrier, S. Jeewajee, K. La, B. Prizer, S. Malik, J. Garcia-Bermudez, X. G. Zhu, J. Cantor, H. Molina, T. Carroll, R. G. Roeder, O. Abdel-Wahab, C. D. Allis, K. Birsoy, ZBTB1 Regulates Asparagine Synthesis and Leukemia Cell Response to L-Asparaginase. Cell Metab 31, 852-861 e856 (2020).

J. Garcia-Bermudez, **R. T. Williams**, R. Guarecuco, K. Birsoy, Targeting extracellular nutrient dependencies of cancer cells. Mol Metab 33, 67-82 (2020).

REFERENCES

1. Costa-Mattioli M, Walter P. The integrated stress response: From mechanism to disease. *Science (80-)*. 2020;368(6489):eaat5314. doi:10.1126/science.aat5314
2. Hinnebusch AG. Translational regulation of GCN4 and the general amino acid control of yeast. *Annu Rev Microbiol*. 2005;59:407-450. doi:10.1146/annurev.micro.59.031805.133833
3. Vattem KM, Wek RC. Reinitiation involving upstream ORFs regulates ATF4 mRNA translation in mammalian cells. *Proc Natl Acad Sci U S A*. 2004;101(31):11269-11274. doi:10.1073/pnas.0400541101
4. Harding HP, Novoa I, Zhang Y, et al. Regulated translation initiation controls stress-induced gene expression in mammalian cells. *Mol Cell*. 2000;6(5):1099-1108. http://www.ncbi.nlm.nih.gov/pubmed/11106749.
5. Palam LR, Baird TD, Wek RC. Phosphorylation of eIF2 facilitates ribosomal bypass of an inhibitory upstream ORF to enhance CHOP translation. *J Biol Chem*. 2011;286(13):10939-10949. doi:10.1074/jbc.M110.216093
6. Harding HP, Novoa I, Zhang Y, et al. Regulated translation initiation controls stress-induced gene expression in mammalian cells. *Mol Cell*. 2000;6(5):1099-1108. doi:10.1016/S1097-2765(00)00108-8
7. Harding HP, Zhang Y, Zeng H, et al. An integrated stress response regulates amino acid metabolism and resistance to oxidative stress. *Mol Cell*. 2003;11(3):619-633. doi:10.1016/S1097-2765(03)00105-9
8. Vallejo M, Ron D, Miller CP, Habener JF. C/ATF, a member of the activating transcription factor family of DNA-binding proteins, dimerizes with CAAT/enhancer-binding proteins and directs their binding to cAMP response elements. *Proc Natl Acad Sci U S A*. 1993;90(10):4679-4683. doi:10.1073/pnas.90.10.4679
9. Ohoka N, Yoshii S, Hattori T, Onozaki K, Hayashi H. TRB3, a novel ER stress-inducible gene, is induced via ATF4-CHOP pathway and is involved in cell death. *EMBO J*. 2005;24(6):1243-1255. doi:10.1038/sj.emboj.7600596
10. Wang Q, Mora-Jensen H, Weniger MA, et al. ERAD inhibitors integrate ER stress with an epigenetic mechanism to activate BH3-only protein NOXA in cancer cells. *Proc Natl Acad Sci U S A*. 2009;106(7):2200-2205. doi:10.1073/pnas.0807611106
11. Novoa I, Zeng H, Harding HP, Ron D. Feedback inhibition of the unfolded protein response by GADD34-mediated dephosphorylation of eIF2alpha. *J Cell Biol*. 2001;153(5):1011-1022. doi:10.1083/jcb.153.5.1011
12. Jousse C, Deval C, Maurin A-C, et al. TRB3 Inhibits the Transcriptional Activation of Stress-regulated Genes by a Negative Feedback on the ATF4 Pathway. *J Biol Chem*. 2007;282(21):15851-15861. doi:10.1074/jbc.M611723200
13. Hart LS, Cunningham JT, Datta T, et al. ER stress-mediated autophagy promotes Myc-dependent transformation and tumor growth. *J Clin Invest*. 2012;122(12):4621-4634. doi:10.1172/JCI62973
14. Tameire F, Verginadis II, Leli NM, et al. ATF4 couples MYC-dependent translational activity to bioenergetic demands during tumour progression. *Nat Cell*

Biol. 2019;21(7):889-899. doi:10.1038/s41556-019-0347-9
15. Lageix S, Zhang J, Rothenburg S, Hinnebusch AG. Interaction between the tRNA-binding and C-terminal domains of Yeast Gcn2 regulates kinase activity in vivo. *PLoS Genet*. 2015;11(2):e1004991. doi:10.1371/journal.pgen.1004991
16. Wek SA, Zhu S, Wek RC. The histidyl-tRNA synthetase-related sequence in the eIF-2 alpha protein kinase GCN2 interacts with tRNA and is required for activation in response to starvation for different amino acids. *Mol Cell Biol*. 1995;15(8):4497-4506. doi:10.1128/mcb.15.8.4497
17. Siu F, Bain PJ, Leblanc-Chaffin R, Chen H, Kilberg MS. ATF4 is a mediator of the nutrient-sensing response pathway that activates the human asparagine synthetase gene. *J Biol Chem*. 2002;277(27):24120-24127. doi:10.1074/jbc.M201959200
18. Pike LRG, Singleton DC, Buffa F, et al. Transcriptional up-regulation of ULK1 by ATF4 contributes to cancer cell survival. *Biochem J*. 2013;449(2):389-400. doi:10.1042/BJ20120972
19. Harding HP, Zhang Y, Zeng H, et al. An integrated stress response regulates amino acid metabolism and resistance to oxidative stress. *Mol Cell*. 2003;11(3):619-633. http://www.ncbi.nlm.nih.gov/pubmed/12667446.
20. Warburg O. Injuring of Respiration the Origin of Cancer Cells. *Science (80-)*. 1956;123(3191):309-314. doi:10.1126/science.123.3191.309
21. Vander Heiden MG, Cantley LC, Thompson CB. Understanding the Warburg Effect: The Metabolic Requirements of Cell Proliferation. *Science (80-)*. 2009;324(5930):1029-1033. doi:10.1126/science.1160809
22. Hanahan D, Weinberg RA. The hallmarks of cancer. *Cell*. 2000;100(1):57-70. doi:10.1016/s0092-8674(00)81683-9
23. Hanahan D, Weinberg RA. Hallmarks of cancer: the next generation. *Cell*. 2011;144(5):646-674. doi:10.1016/j.cell.2011.02.013
24. Dang C V, Semenza GL. Oncogenic alterations of metabolism. *Trends Biochem Sci*. 1999;24(2):68-72. doi:10.1016/S0968-0004(98)01344-9
25. Erikson J, Finger L, Sun L, et al. Deregulation of c-myc by translocation of the alpha-locus of the T-cell receptor in T-cell leukemias. *Science (80-)*. 1986;232(4752):884-886. doi:10.1126/science.3486470
26. Palomero T, Lim WK, Odom DT, et al. NOTCH1 directly regulates c-MYC and activates a feed-forward-loop transcriptional network promoting leukemic cell growth. *Proc Natl Acad Sci U S A*. 2006;103(48):18261-18266. doi:10.1073/pnas.0606108103
27. Herranz D, Ambesi-Impiombato A, Palomero T, et al. A NOTCH1-driven MYC enhancer promotes T cell development, transformation and acute lymphoblastic leukemia. *Nat Med*. 2014;20(10):1130-1137. doi:10.1038/nm.3665
28. Palomero T, Sulis ML, Cortina M, et al. Mutational loss of PTEN induces resistance to NOTCH1 inhibition in T-cell leukemia. *Nat Med*. 2007;13(10):1203-1210. doi:10.1038/nm1636
29. Belver L, Ferrando A. The genetics and mechanisms of T cell acute lymphoblastic leukaemia. *Nat Rev Cancer*. 2016;16(8):494-507. doi:10.1038/nrc.2016.63

30. Škrtić M, Sriskanthadevan S, Jhas B, et al. Inhibition of Mitochondrial Translation as a Therapeutic Strategy for Human Acute Myeloid Leukemia. *Cancer Cell*. 2011;20(5):674-688. doi:10.1016/j.ccr.2011.10.015
31. Herst PM, Howman RA, Neeson PJ, Berridge M V., Ritchie DS. The level of glycolytic metabolism in acute myeloid leukemia blasts at diagnosis is prognostic for clinical outcome. *J Leukoc Biol*. 2011;89(1):51-55. doi:10.1189/jlb.0710417
32. Willems L, Jacque N, Jacquel A, et al. Inhibiting glutamine uptake represents an attractive new strategy for treating acute myeloid leukemia. *Blood*. 2013;122(20):3521-3532. doi:10.1182/blood-2013-03-493163
33. Mardis ER, Ding L, Dooling DJ, et al. Recurring Mutations Found by Sequencing an Acute Myeloid Leukemia Genome. *N Engl J Med*. 2009;361(11):1058-1066. doi:10.1056/NEJMoa0903840
34. Dang L, White DW, Gross S, et al. Cancer-associated IDH1 mutations produce 2-hydroxyglutarate. *Nature*. 2009;462(7274):739-744. doi:10.1038/nature08617
35. Figueroa ME, Abdel-Wahab O, Lu C, et al. Leukemic IDH1 and IDH2 Mutations Result in a Hypermethylation Phenotype, Disrupt TET2 Function, and Impair Hematopoietic Differentiation. *Cancer Cell*. 2010;18(6):553-567. doi:10.1016/j.ccr.2010.11.015
36. Boutzen H, Saland E, Larrue C, et al. Isocitrate dehydrogenase 1 mutations prime the all-trans retinoic acid myeloid differentiation pathway in acute myeloid leukemia. *J Exp Med*. 2016;213(4):483-497. doi:10.1084/jem.20150736
37. Losman JA, Looper RE, Koivunen P, et al. (R)-2-hydroxyglutarate is sufficient to promote leukemogenesis and its effects are reversible. *Science (80-)*. 2013;340(6127):1621-1625. doi:10.1126/science.1231677
38. Liu X, Gong Y. Isocitrate dehydrogenase inhibitors in acute myeloid leukemia. *Biomark Res*. 2019;7:22. doi:10.1186/s40364-019-0173-z
39. Wang F, Travins J, DeLaBarre B, et al. Targeted Inhibition of Mutant IDH2 in Leukemia Cells Induces Cellular Differentiation. *Science (80-)*. 2013;340(6132):622-626. doi:10.1126/science.1234769
40. Garcia-Bermudez J, Williams RT, Guarecuco R, Birsoy K. Targeting extracellular nutrient dependencies of cancer cells. *Mol Metab*. 2020;33:67-82. doi:10.1016/j.molmet.2019.11.011
41. Sykes DB, Kfoury YS, Mercier FE, et al. Inhibition of Dihydroorotate Dehydrogenase Overcomes Differentiation Blockade in Acute Myeloid Leukemia. *Cell*. 2016;167(1):171-186.e15. doi:10.1016/j.cell.2016.08.057
42. Cole A, Wang Z, Coyaud E, et al. Inhibition of the Mitochondrial Protease ClpP as a Therapeutic Strategy for Human Acute Myeloid Leukemia. *Cancer Cell*. 2015;27(6):864-876. doi:10.1016/j.ccell.2015.05.004
43. Molina JR, Sun Y, Protopopova M, et al. An inhibitor of oxidative phosphorylation exploits cancer vulnerability. *Nat Med*. 2018;24(7):1036-1046. doi:10.1038/s41591-018-0052-4
44. Miraki-Moud F, Ghazaly E, Ariza-McNaughton L, et al. Arginine deprivation using pegylated arginine deiminase has activity against primary acute myeloid leukemia cells in vivo. *Blood*. 2015;125(26):4060-4068. doi:10.1182/blood-2014-10-608133

45. Tsai H-J, Jiang SS, Hung W-C, et al. A Phase II Study of Arginine Deiminase (ADI-PEG20) in Relapsed/Refractory or Poor-Risk Acute Myeloid Leukemia Patients. *Sci Rep*. 2017;7(1):11253. doi:10.1038/s41598-017-10542-4
46. Wang Y-H, Israelsen WJ, Lee D, et al. Cell-state-specific metabolic dependency in hematopoiesis and leukemogenesis. *Cell*. 2014;158(6):1309-1323. doi:10.1016/j.cell.2014.07.048
47. John G. Kidd MD. Regression of Transplanted Lymphomas Induced in Vivo by Means of Normal Guinea Pig Serum. *J Exp Med*. 1953;98(6):565-582.
48. Broome JD. Evidence that the L-asparaginase of guinea pig serum is responsible for its antilymphoma effects. I. Properties of the L-asparaginase of guinea pig serum in relation to those of the antilymphoma substance. *J Exp Med*. 1963;118:99-120. http://www.ncbi.nlm.nih.gov/pubmed/14015821.
49. NEUMAN RE, MCCOY TA. Dual Requirement of Walker Carcinosarcoma 256 in vitro for Asparagine and Glutamine. *Science (80-)*. 1956;124(3212):124-125. doi:10.1126/science.124.3212.124
50. Dolowy WC, Henson D, Cornet J, Sellin H. Toxic and antineoplastic effects of l-asparaginase: Study of mice with lymphoma and normal monkeys and report on a child with leukemia. *Cancer*. 1966;19(12):1813-1819. doi:10.1002/1097-0142(196612)19:12<1813::AID-CNCR2820191208>3.0.CO;2-E
51. Mashburn L, Wriston J. TUMOR INHIBITORY EFFECT OF L-ASPARAGINASE FROM ESCHERICHIA COLI. *Arch Biochem Biophys*. 1964;105(2):450-452. doi:10.1016/0003-9861(64)90032-3
52. Jaffe N, Traggis D, Das L, et al. L-asparaginase in the treatment of neoplastic diseases in children. *Cancer Res*. 1971;31(7):942-949. http://www.ncbi.nlm.nih.gov/pubmed/4327086.
53. Haskell CM, Canellos GP, Leventhal BG, et al. L-asparaginase: therapeutic and toxic effects in patients with neoplastic disease. *N Engl J Med*. 1969;281(19):1028-1034. doi:10.1056/NEJM196911062811902
54. Tallal L, Tan C, Oettgen H, et al. E. coli L-asparaginase in the treatment of leukemia and solid tumors in 131 children. *Cancer*. 1970;25(2):306-320. http://www.ncbi.nlm.nih.gov/pubmed/4905155.
55. Lomelino CL, Andring JT, McKenna R, Kilberg MS. Asparagine synthetase: Function, structure, and role in disease. *J Biol Chem*. 2017;292(49):19952-19958. doi:10.1074/jbc.R117.819060
56. Loayza-Puch F, Rooijers K, Buil LCM, et al. Tumour-specific proline vulnerability uncovered by differential ribosome codon reading. *Nature*. 2016;530(7591):490-494. doi:10.1038/nature16982
57. Ubuka T, Meister A. Studies on the utilization of asparagine by mouse leukemia cells. *J Natl Cancer Inst*. 1971;46(2):291-298. http://www.ncbi.nlm.nih.gov/pubmed/5115904.
58. Pavlova NN, Hui S, Ghergurovich JM, et al. As Extracellular Glutamine Levels Decline, Asparagine Becomes an Essential Amino Acid. *Cell Metab*. 2018;27(2):428-438.e5. doi:10.1016/j.cmet.2017.12.006
59. Métayer LE, Brown RD, Carlebur S, Burke GAA, Brown GC. Mechanisms of cell

death induced by arginase and asparaginase in precursor B-cell lymphoblasts. *Apoptosis*. 2019;24(1-2):145-156. doi:10.1007/s10495-018-1506-3
60. Zhang J, Fan J, Venneti S, et al. Asparagine plays a critical role in regulating cellular adaptation to glutamine depletion. *Mol Cell*. 2014;56(2):205-218. doi:10.1016/j.molcel.2014.08.018
61. Krall AS, Xu S, Graeber TG, Braas D, Christofk HR. Asparagine promotes cancer cell proliferation through use as an amino acid exchange factor. *Nat Commun*. 2016;7:11457. doi:10.1038/ncomms11457
62. Li H, Ning S, Ghandi M, et al. The landscape of cancer cell line metabolism. *Nat Med*. 2019;25(5):850-860. doi:10.1038/s41591-019-0404-8
63. Zhang B, Dong L-W, Tan Y-X, et al. Asparagine synthetase is an independent predictor of surgical survival and a potential therapeutic target in hepatocellular carcinoma. *Br J Cancer*. 2013;109(1):14-23. doi:10.1038/bjc.2013.293
64. Dufour E, Gay F, Aguera K, et al. Pancreatic tumor sensitivity to plasma L-asparagine starvation. *Pancreas*. 2012;41(6):940-948. doi:10.1097/MPA.0b013e318247d903
65. Knott SRV, Wagenblast E, Khan S, et al. Asparagine bioavailability governs metastasis in a model of breast cancer. *Nature*. 2018;554(7692):378-381. doi:10.1038/nature25465
66. Miller HK, Salser JS, Balis ME. Amino acid levels following L-asparagine amidohydrolase (EC.3.5.1.1) therapy. *Cancer Res*. 1969;29(1):183-187. http://www.ncbi.nlm.nih.gov/pubmed/5763976.
67. Tardito S, Chiu M, Uggeri J, et al. L-Asparaginase and inhibitors of glutamine synthetase disclose glutamine addiction of β-catenin-mutated human hepatocellular carcinoma cells. *Curr Cancer Drug Targets*. 2011;11(8):929-943. http://www.ncbi.nlm.nih.gov/pubmed/21834755.
68. Chan WK, Lorenzi PL, Anishkin A, et al. The glutaminase activity of L-asparaginase is not required for anticancer activity against ASNS-negative cells. *Blood*. 2014;123(23):3596-3606. doi:10.1182/blood-2013-10-535112
69. Nguyen HA, Su Y, Zhang JY, et al. A Novel l-Asparaginase with low l-Glutaminase Coactivity Is Highly Efficacious against Both T- and B-cell Acute Lymphoblastic Leukemias In Vivo. *Cancer Res*. 2018;78(6):1549-1560. doi:10.1158/0008-5472.CAN-17-2106
70. Snaebjornsson MT, Janaki-Raman S, Schulze A. Greasing the Wheels of the Cancer Machine: The Role of Lipid Metabolism in Cancer. *Cell Metab*. 2020;31(1):62-76. doi:10.1016/j.cmet.2019.11.010
71. Pietrocola F, Galluzzi L, Bravo-San Pedro JM, Madeo F, Kroemer G. Acetyl Coenzyme A: A Central Metabolite and Second Messenger. *Cell Metab*. 2015;21(6):805-821. doi:10.1016/j.cmet.2015.05.014
72. Weiss L, Hoffmann GE, Schreiber R, et al. Fatty-acid biosynthesis in man, a pathway of minor importance. Purification, optimal assay conditions, and organ distribution of fatty-acid synthase. *Biol Chem Hoppe Seyler*. 1986;367(9):905-912. doi:10.1515/bchm3.1986.367.2.905
73. Röhrig F, Schulze A. The multifaceted roles of fatty acid synthesis in cancer. *Nat*

Rev Cancer. 2016;16(11):732-749. doi:10.1038/nrc.2016.89
74. Menendez JA, Lupu R. Fatty acid synthase and the lipogenic phenotype in cancer pathogenesis. *Nat Rev Cancer*. 2007;7(10):763-777. doi:10.1038/nrc2222
75. MEDES G, THOMAS A, WEINHOUSE S. Metabolism of neoplastic tissue. IV. A study of lipid synthesis in neoplastic tissue slices in vitro. *Cancer Res*. 1953;13(1):27-29. http://www.ncbi.nlm.nih.gov/pubmed/13032945.
76. Rysman E, Brusselmans K, Scheys K, et al. De novo Lipogenesis Protects Cancer Cells from Free Radicals and Chemotherapeutics by Promoting Membrane Lipid Saturation. *Cancer Res*. 2010;70(20):8117-8126. doi:10.1158/0008-5472.CAN-09-3871
77. Talebi A, Dehairs J, Rambow F, et al. Sustained SREBP-1-dependent lipogenesis as a key mediator of resistance to BRAF-targeted therapy. *Nat Commun*. 2018;9(1):2500. doi:10.1038/s41467-018-04664-0
78. Pascual G, Avgustinova A, Mejetta S, et al. Targeting metastasis-initiating cells through the fatty acid receptor CD36. *Nature*. 2017;541(7635):41-45. doi:10.1038/nature20791
79. Watt MJ, Clark AK, Selth LA, et al. Suppressing fatty acid uptake has therapeutic effects in preclinical models of prostate cancer. *Sci Transl Med*. 2019;11(478):eaau5758. doi:10.1126/scitranslmed.aau5758
80. Tabe Y, Konopleva M, Andreeff M. Fatty Acid Metabolism, Bone Marrow Adipocytes, and AML. *Front Oncol*. 2020;10:155. doi:10.3389/fonc.2020.00155
81. Shafat MS, Oellerich T, Mohr S, et al. Leukemic blasts program bone marrow adipocytes to generate a protumoral microenvironment. *Blood*. 2017;129(10):1320-1332. doi:10.1182/blood-2016-08-734798
82. Boroughs LK, DeBerardinis RJ. Metabolic pathways promoting cancer cell survival and growth. *Nat Cell Biol*. 2015;17(4):351-359. doi:10.1038/ncb3124
83. Behan JW, Yun JP, Proektor MP, et al. Adipocytes impair leukemia treatment in mice. *Cancer Res*. 2009;69(19):7867-7874. doi:10.1158/0008-5472.CAN-09-0800
84. Hermetet F, Mshaik R, Simonet J, Callier P, Delva L, Quéré R. High-fat diet intensifies MLL-AF9-induced acute myeloid leukemia through activation of the FLT3 signaling in mouse primitive hematopoietic cells. *Sci Rep*. 2020;10(1):16187. doi:10.1038/s41598-020-73020-4
85. De Schrijver E, Brusselmans K, Heyns W, Verhoeven G, Swinnen J V. RNA interference-mediated silencing of the fatty acid synthase gene attenuates growth and induces morphological changes and apoptosis of LNCaP prostate cancer cells. *Cancer Res*. 2003;63(13):3799-3804. doi:12839976
86. Menendez JA, Vellon L, Colomer R, Lupu R. Pharmacological and small interference RNA-mediated inhibition of breast cancer-associated fatty acid synthase (oncogenic antigen-519) synergistically enhances Taxol (paclitaxel)-induced cytotoxicity. *Int J cancer*. 2005;115(1):19-35. doi:10.1002/ijc.20754
87. Tabe Y, Saitoh K, Yang H, et al. Inhibition of FAO in AML co-cultured with BM adipocytes: mechanisms of survival and chemosensitization to cytarabine. *Sci Rep*. 2018;8(1):16837. doi:10.1038/s41598-018-35198-6
88. Ricciardi MR, Mirabilii S, Allegretti M, et al. Targeting the leukemia cell

metabolism by the CPT1a inhibition: functional preclinical effects in leukemias. *Blood*. 2015;126(16):1925-1929. doi:10.1182/blood-2014-12-617498
89. Estañ MC, Calviño E, Calvo S, et al. Apoptotic efficacy of etomoxir in human acute myeloid leukemia cells. Cooperation with arsenic trioxide and glycolytic inhibitors, and regulation by oxidative stress and protein kinase activities. *PLoS One*. 2014;9(12):e115250. doi:10.1371/journal.pone.0115250
90. Southam AD, Khanim FL, Hayden RE, et al. Drug Redeployment to Kill Leukemia and Lymphoma Cells by Disrupting SCD1-Mediated Synthesis of Monounsaturated Fatty Acids. *Cancer Res*. 2015;75(12):2530-2540. doi:10.1158/0008-5472.CAN-15-0202
91. Pizer ES, Wood FD, Pasternack GR, Kuhajda FP. Fatty acid synthase (FAS): a target for cytotoxic antimetabolites in HL60 promyelocytic leukemia cells. *Cancer Res*. 1996;56(4):745-751. http://www.ncbi.nlm.nih.gov/pubmed/8631008.
92. Clutterbuck RD, Millar BC, Powles RL, et al. Inhibitory effect of simvastatin on the proliferation of human myeloid leukaemia cells in severe combined immunodeficient (SCID) mice. *Br J Haematol*. 1998;102(2):522-527. doi:10.1046/j.1365-2141.1998.00783.x
93. Cunnane SC. The conditional nature of the dietary need for polyunsaturates: a proposal to reclassify “essential fatty acids” as “conditionally-indispensable” or “conditionally-dispensable” fatty acids. *Br J Nutr*. 2000;84(6):803-812. http://www.ncbi.nlm.nih.gov/pubmed/11177196.
94. Vickery S, Dodds PF. Incorporation of xenobiotic carboxylic acids into lipids by cultured 3T3-L1 adipocytes. *Xenobiotica*. 34(11-12):1025-1042. doi:10.1080/02772240400015248
95. Darnell M, Weidolf L. Metabolism of xenobiotic carboxylic acids: focus on coenzyme A conjugation, reactivity, and interference with lipid metabolism. *Chem Res Toxicol*. 2013;26(8):1139-1155. doi:10.1021/tx400183y
96. Moorhouse KG, Dodds PF, Hutson DH. Xenobiotic triacylglycerol formation in isolated hepatocytes. *Biochem Pharmacol*. 1991;41(8):1179-1185. doi:10.1016/0006-2952(91)90656-p
97. Mayer JM, Roy-De Vos M, Audergon C, Testa B, Etter JC. Interactions of anti-inflammatory 2-arylpropionates (profens) with the metabolism of fatty acids: in vitro studies. *Int J Tissue React*. 1994;16(2):59-72. http://www.ncbi.nlm.nih.gov/pubmed/7960502.
98. Staels B, Dallongeville J, Auwerx J, Schoonjans K, Leitersdorf E, Fruchart JC. Mechanism of action of fibrates on lipid and lipoprotein metabolism. *Circulation*. 1998;98(19):2088-2093. doi:10.1161/01.cir.98.19.2088
99. Schoonjans K, Staels B, Grimaldi P, Auwerx J. Acyl-CoA synthetase mRNA expression is controlled by fibric-acid derivatives, feeding and liver proliferation. *Eur J Biochem*. 1993;216(2):615-622. doi:10.1111/j.1432-1033.1993.tb18181.x
100. Alegret M, Ferrando R, Vázquez M, Adzet T, Merlos M, Laguna JC. Relationship between plasma lipids and palmitoyl-CoA hydrolase and synthetase activities with peroxisomal proliferation in rats treated with fibrates. *Br J Pharmacol*. 1994;112(2):551-556. doi:10.1111/j.1476-5381.1994.tb13109.x

101. Divakaruni AS, Hsieh WY, Minarrieta L, et al. Etomoxir Inhibits Macrophage Polarization by Disrupting CoA Homeostasis. *Cell Metab*. 2018;28(3):490-503.e7. doi:10.1016/j.cmet.2018.06.001
102. Bentebibel A, Sebastián D, Herrero L, et al. Novel Effect of C75 on Carnitine Palmitoyltransferase I Activity and Palmitate Oxidation †. *Biochemistry*. 2006;45(14):4339-4350. doi:10.1021/bi052186q
103. Yao C-H, Liu G-Y, Wang R, Moon SH, Gross RW, Patti GJ. Identifying off-target effects of etomoxir reveals that carnitine palmitoyltransferase I is essential for cancer cell proliferation independent of β-oxidation. *PLoS Biol*. 2018;16(3):e2003782. doi:10.1371/journal.pbio.2003782
104. Grillo MP, Tadano Lohr M, Wait JCM. Metabolic activation of mefenamic acid leading to mefenamyl-S-acyl-glutathione adduct formation in vitro and in vivo in rat. *Drug Metab Dispos*. 2012;40(8):1515-1526. doi:10.1124/dmd.112.046102
105. Olsen J, Li C, Skonberg C, et al. Studies on the metabolism of tolmetin to the chemically reactive acyl-coenzyme A thioester intermediate in rats. *Drug Metab Dispos*. 2007;35(5):758-764. doi:10.1124/dmd.106.013334
106. Sallustio BC, Nunthasomboon S, Drogemuller CJ, Knights KM. In vitro covalent binding of nafenopin-CoA to human liver proteins. *Toxicol Appl Pharmacol*. 2000;163(2):176-182. doi:10.1006/taap.1999.8868
107. Leite S, Martins NM, Dorta DJ, Curti C, Uyemura SA, dos Santos AC. Mitochondrial uncoupling by the sulindac metabolite, sulindac sulfide. *Basic Clin Pharmacol Toxicol*. 2006;99(4):294-299. doi:10.1111/j.1742-7843.2006.pto_490.x
108. Krause MM, Brand MD, Krauss S, et al. Nonsteroidal antiinflammatory drugs and a selective cyclooxygenase 2 inhibitor uncouple mitochondria in intact cells. *Arthritis Rheum*. 2003;48(5):1438-1444. doi:10.1002/art.10969
109. Fromenty B, Pessayre D. Inhibition of mitochondrial beta-oxidation as a mechanism of hepatotoxicity. *Pharmacol Ther*. 1995;67(1):101-154. doi:10.1016/0163-7258(95)00012-6
110. Zhu XG, Nicholson Puthenveedu S, Shen Y, et al. CHP1 Regulates Compartmentalized Glycerolipid Synthesis by Activating GPAT4. *Mol Cell*. 2019;74(1):45-58.e7. doi:10.1016/j.molcel.2019.01.037
111. Inoguchi T, Li P, Umeda F, et al. High glucose level and free fatty acid stimulate reactive oxygen species production through protein kinase C--dependent activation of NAD(P)H oxidase in cultured vascular cells. *Diabetes*. 2000;49(11):1939-1945. doi:10.2337/diabetes.49.11.1939
112. van de Weijer T, Schrauwen-Hinderling VB, Schrauwen P. Lipotoxicity in type 2 diabetic cardiomyopathy. *Cardiovasc Res*. 2011;92(1):10-18. doi:10.1093/cvr/cvr212
113. Piccolis M, Bond LM, Kampmann M, et al. Probing the Global Cellular Responses to Lipotoxicity Caused by Saturated Fatty Acids. *Mol Cell*. 2019;74(1):32-44.e8. doi:10.1016/j.molcel.2019.01.036
114. Griffiths B, Lewis CA, Bensaad K, et al. Sterol regulatory element binding protein-dependent regulation of lipid synthesis supports cell survival and tumor growth. *Cancer Metab*. 2013;1(1):3. doi:10.1186/2049-3002-1-3

115. Shao W, Espenshade PJ. Expanding roles for SREBP in metabolism. *Cell Metab*. 2012;16(4):414-419. doi:10.1016/j.cmet.2012.09.002
116. Wang X, Sato R, Brown MS, Hua X, Goldstein JL. SREBP-1, a membrane-bound transcription factor released by sterol-regulated proteolysis. *Cell*. 1994;77(1):53-62. doi:10.1016/0092-8674(94)90234-8
117. Williams KJ, Argus JP, Zhu Y, et al. An Essential Requirement for the SCAP/SREBP Signaling Axis to Protect Cancer Cells from Lipotoxicity. *Cancer Res*. 2013;73(9):2850-2862. doi:10.1158/0008-5472.CAN-13-0382-T
118. Quirós PM, Prado MA, Zamboni N, et al. Multi-omics analysis identifies ATF4 as a key regulator of the mitochondrial stress response in mammals. *J Cell Biol*. 2017;216(7):2027-2045. doi:10.1083/jcb.201702058
119. Guo X, Aviles G, Liu Y, et al. Mitochondrial stress is relayed to the cytosol by an OMA1–DELE1–HRI pathway. *Nature*. 2020;579(7799):427-432. doi:10.1038/s41586-020-2078-2
120. Fessler E, Eckl E-M, Schmitt S, et al. A pathway coordinated by DELE1 relays mitochondrial stress to the cytosol. *Nature*. 2020;579(7799):433-437. doi:10.1038/s41586-020-2076-4
121. Chatterjee A, Seyfferth J, Lucci J, et al. MOF Acetyl Transferase Regulates Transcription and Respiration in Mitochondria. *Cell*. 2016;167(3):722-738.e23. doi:10.1016/j.cell.2016.09.052
122. Morris CR, Hamilton-Reeves J, Martindale RG, Sarav M, Ochoa Gautier JB. Acquired Amino Acid Deficiencies: A Focus on Arginine and Glutamine. *Nutr Clin Pract*. 2017;32(1_suppl):30S-47S. doi:10.1177/0884533617691250
123. Escobar-Henriques M, Joaquim M. Mitofusins: Disease Gatekeepers and Hubs in Mitochondrial Quality Control by E3 Ligases. *Front Physiol*. 2019;10:517. doi:10.3389/fphys.2019.00517
124. Ding W-X, Yin X-M. Mitophagy: mechanisms, pathophysiological roles, and analysis. *Biol Chem*. 2012;393(7):547-564. doi:10.1515/hsz-2012-0119
125. Cheng PN-M, Lam T-L, Lam W-M, et al. Pegylated recombinant human arginase (rhArg-peg5,000mw) inhibits the in vitro and in vivo proliferation of human hepatocellular carcinoma through arginine depletion. *Cancer Res*. 2007;67(1):309-317. doi:10.1158/0008-5472.CAN-06-1945
126. Mussai F, Egan S, Higginbotham-Jones J, et al. Arginine dependence of acute myeloid leukemia blast proliferation: a novel therapeutic target. *Blood*. 2015;125(15):2386-2396. doi:10.1182/blood-2014-09-600643
127. Zhao E, Ding J, Xia Y, et al. KDM4C and ATF4 Cooperate in Transcriptional Control of Amino Acid Metabolism. *Cell Rep*. 2016;14(3):506-519. doi:10.1016/j.celrep.2015.12.053
128. Yang X, Xia R, Yue C, et al. ATF4 Regulates CD4+T Cell Immune Responses through Metabolic Reprogramming. *Cell Rep*. 2018;23(6):1754-1766. doi:10.1016/j.celrep.2018.04.032
129. Ding J, Li T, Wang X, et al. The histone H3 methyltransferase G9A epigenetically activates the serine-glycine synthesis pathway to sustain cancer cell survival and proliferation. *Cell Metab*. 2013;18(6):896-907. doi:10.1016/j.cmet.2013.11.004

130. Darman RB, Seiler M, Agrawal AA, et al. Cancer-Associated SF3B1 Hotspot Mutations Induce Cryptic 3' Splice Site Selection through Use of a Different Branch Point. *Cell Rep*. 2015;13(5):1033-1045. doi:10.1016/j.celrep.2015.09.053
131. Brian Dalton W, Helmenstine E, Walsh N, et al. Hotspot SF3B1 mutations induce metabolic reprogramming and vulnerability to serine deprivation. *J Clin Invest*. 2019;129(11):4708-4723. doi:10.1172/JCI125022
132. Punwani D, Simon K, Choi Y, et al. Transcription factor zinc finger and BTB domain 1 is essential for lymphocyte development. *J Immunol*. 2012;189(3):1253-1264. doi:10.4049/jimmunol.1200623
133. Siggs OM, Li X, Xia Y, Beutler B. ZBTB1 is a determinant of lymphoid development. *J Exp Med*. 2012;209(1):19-27. doi:10.1084/jem.20112084
134. Zhang X, Lu Y, Cao X, Zhen T, Kovalovsky D. Zbtb1 prevents default myeloid differentiation of lymphoid-primed multipotent progenitors. *Oncotarget*. 2014;7(37). doi:10.18632/oncotarget.11356
135. Ben-Sahra I, Howell JJ, Asara JM, Manning BD. Stimulation of de novo pyrimidine synthesis by growth signaling through mTOR and S6K1. *Science*. 2013;339(6125):1323-1328. doi:10.1126/science.1228792
136. Han J, Back SH, Hur J, et al. ER-stress-induced transcriptional regulation increases protein synthesis leading to cell death. *Nat Cell Biol*. 2013;15(5):481-490. doi:10.1038/ncb2738
137. Kim H, Dejsuphong D, Adelmant G, et al. Transcriptional Repressor ZBTB1 Promotes Chromatin Remodeling and Translesion DNA Synthesis. *Mol Cell*. 2014;54(1):107-118. doi:10.1016/j.molcel.2014.02.017
138. Matic I, Schimmel J, Hendriks IA, et al. Site-Specific Identification of SUMO-2 Targets in Cells Reveals an Inverted SUMOylation Motif and a Hydrophobic Cluster SUMOylation Motif. *Mol Cell*. 2010;39(4):641-652. doi:10.1016/j.molcel.2010.07.026
139. Zollman S, Godt D, Prive GG, Couderc JL, Laski FA. The BTB domain, found primarily in zinc finger proteins, defines an evolutionarily conserved family that includes several developmentally regulated genes in Drosophila. *Proc Natl Acad Sci*. 1994;91(22):10717-10721. doi:10.1073/pnas.91.22.10717
140. Bowers SR, Calero-Nieto FJ, Valeaux S, Fernandez-Fuentes N, Cockerill PN. Runx1 binds as a dimeric complex to overlapping Runx1 sites within a palindromic element in the human GM-CSF enhancer. *Nucleic Acids Res*. 2010;38(18):6124-6134. doi:10.1093/nar/gkq356
141. Aslanian AM, Fletcher BS, Kilberg MS. Asparagine synthetase expression alone is sufficient to induce l-asparaginase resistance in MOLT-4 human leukaemia cells. *Biochem J*. 2001;357(Pt 1):321-328. doi:10.1042/0264-6021:3570321
142. Pinnell N, Yan R, Cho HJ, et al. The PIAS-like Coactivator Zmiz1 Is a Direct and Selective Cofactor of Notch1 in T Cell Development and Leukemia. *Immunity*. 2015;43(5):870-883. doi:10.1016/j.immuni.2015.10.007
143. De Braekeleer E, Douet-Guilbert N, Rowe D, et al. ABL1 fusion genes in hematological malignancies: a review. *Eur J Haematol*. 2011;86(5):361-371. doi:10.1111/j.1600-0609.2011.01586.x

144. LeBoeuf SE, Wu WL, Karakousi TR, et al. Activation of Oxidative Stress Response in Cancer Generates a Druggable Dependency on Exogenous Non-essential Amino Acids. *Cell Metab*. November 2019:1-12. doi:10.1016/j.cmet.2019.11.012
145. Nakamura A, Nambu T, Ebara S, et al. Inhibition of GCN2 sensitizes ASNS-low cancer cells to asparaginase by disrupting the amino acid response. *Proc Natl Acad Sci*. 2018:201805523. doi:10.1073/pnas.1805523115
146. Chan WK, Horvath TD, Tan L, et al. Glutaminase activity of L-asparaginase contributes to durable preclinical activity against acute lymphoblastic leukemia. *Mol Cancer Ther*. 2019;18(9):1587-1592. doi:10.1158/1535-7163.MCT-18-1329
147. Pavlova NN, Thompson CB. The Emerging Hallmarks of Cancer Metabolism. *Cell Metab*. 2016;23(1):27-47. doi:10.1016/j.cmet.2015.12.006
148. Philip PA, Buyse ME, Alistar AT, et al. A Phase III open-label trial to evaluate efficacy and safety of CPI-613 plus modified FOLFIRINOX (mFFX) versus FOLFIRINOX (FFX) in patients with metastatic adenocarcinoma of the pancreas. *Future Oncol*. 2019;15(28):3189-3196. doi:10.2217/fon-2019-0209
149. Pardee TS, Luther S, Buyse M, Powell BL, Cortes J. Devimistat in combination with high dose cytarabine and mitoxantrone compared with high dose cytarabine and mitoxantrone in older patients with relapsed/refractory acute myeloid leukemia: ARMADA 2000 Phase III study. *Future Oncol*. 2019;15(28):3197-3208. doi:10.2217/fon-2019-0201
150. Boyle J. Lehninger principles of biochemistry (4th ed.): Nelson, D., and Cox, M. *Biochem Mol Biol Educ*. 2005;33(1):74-75. doi:10.1002/bmb.2005.494033010419
151. Gao L, Xu Z, Huang Z, et al. CPI-613 rewires lipid metabolism to enhance pancreatic cancer apoptosis via the AMPK-ACC signaling. *J Exp Clin Cancer Res*. 2020;39(1):73. doi:10.1186/s13046-020-01579-x
152. Saiki S, Hatano T, Fujimaki M, et al. Decreased long-chain acylcarnitines from insufficient β-oxidation as potential early diagnostic markers for Parkinson's disease. *Sci Rep*. 2017;7(1):7328. doi:10.1038/s41598-017-06767-y
153. Li F, Wang Y, Zeller KI, et al. Myc stimulates nuclearly encoded mitochondrial genes and mitochondrial biogenesis. *Mol Cell Biol*. 2005;25(14):6225-6234. doi:10.1128/MCB.25.14.6225-6234.2005
154. Wise DR, DeBerardinis RJ, Mancuso A, et al. Myc regulates a transcriptional program that stimulates mitochondrial glutaminolysis and leads to glutamine addiction. *Proc Natl Acad Sci*. 2008;105(48):18782-18787. doi:10.1073/pnas.0810199105
155. Liu Y-C, Li F, Handler J, et al. Global regulation of nucleotide biosynthetic genes by c-Myc. *PLoS One*. 2008;3(7):e2722. doi:10.1371/journal.pone.0002722
156. Gao P, Tchernyshyov I, Chang TC, et al. C-Myc suppression of miR-23a/b enhances mitochondrial glutaminase expression and glutamine metabolism. *Nature*. 2009;458(7239):762-765. doi:10.1038/nature07823
157. Morrish F, Noonan J, Perez-Olsen C, et al. Myc-dependent mitochondrial generation of acetyl-CoA contributes to fatty acid biosynthesis and histone acetylation during cell cycle entry. *J Biol Chem*. 2010;285(47):36267-36274.

doi:10.1074/jbc.M110.141606
158. Horiguchi M, Koyanagi S, Okamoto A, Suzuki SO, Matsunaga N, Ohdo S. Stress-regulated transcription factor ATF4 promotes neoplastic transformation by suppressing expression of the INK4a/ARF cell senescence factors. *Cancer Res*. 2012;72(2):395-401. doi:10.1158/0008-5472.CAN-11-1891
159. Heydt Q, Larrue C, Saland E, et al. Oncogenic FLT3-ITD supports autophagy via ATF4 in acute myeloid leukemia. *Oncogene*. 2018;37(6):787-797. doi:10.1038/onc.2017.376
160. Nagasawa I, Koido M, Tani Y, Tsukahara S, Kunimasa K, Tomida A. Disrupting ATF4 Expression Mechanisms Provides an Effective Strategy for BRAF-Targeted Melanoma Therapy. *iScience*. 2020;23(4):101028. doi:10.1016/j.isci.2020.101028
161. Pathria G, Lee JS, Hasnis E, et al. Translational reprogramming marks adaptation to asparagine restriction in cancer. *Nat Cell Biol*. 2019;21(12):1590-1603. doi:10.1038/s41556-019-0415-1
162. Gwinn DM, Lee AG, Briones-Martin-del-Campo M, et al. Oncogenic KRAS Regulates Amino Acid Homeostasis and Asparagine Biosynthesis via ATF4 and Alters Sensitivity to L-Asparaginase. *Cancer Cell*. 2018;33(1):91-107.e6. doi:10.1016/j.ccell.2017.12.003
163. Brown MS, Goldstein JL. The SREBP pathway: regulation of cholesterol metabolism by proteolysis of a membrane-bound transcription factor. *Cell*. 1997;89(3):331-340. doi:10.1016/s0092-8674(00)80213-5
164. Wortel IMN, van der Meer LT, Kilberg MS, van Leeuwen FN. Surviving Stress: Modulation of ATF4-Mediated Stress Responses in Normal and Malignant Cells. *Trends Endocrinol Metab*. 2017;28(11):794-806. doi:10.1016/j.tem.2017.07.003
165. Liu Q, Yao F, Wang M, et al. Novel human BTB/POZ domain-containing zinc finger protein ZBTB1 inhibits transcriptional activities of CRE. *Mol Cell Biochem*. 2011;357(1-2):405-414. doi:10.1007/s11010-011-0911-5
166. Haskell CM, Canellos GP. l-asparaginase resistance in human leukemia--asparagine synthetase. *Biochem Pharmacol*. 1969;18(10):2578-2580. http://www.ncbi.nlm.nih.gov/pubmed/4935103.
167. Scherf U, Ross DT, Waltham M, et al. A gene expression database for the molecular pharmacology of cancer. *Nat Genet*. 2000;24(3):236-244. doi:10.1038/73439
168. Hinze L, Pfirrmann M, Karim S, et al. Synthetic Lethality of Wnt Pathway Activation and Asparaginase in Drug-Resistant Acute Leukemias. *Cancer Cell*. 2019;35(4):664-676.e7. doi:10.1016/j.ccell.2019.03.004
169. Balasubramanian MN, Butterworth EA, Kilberg MS. Asparagine synthetase: regulation by cell stress and involvement in tumor biology. *AJP Endocrinol Metab*. 2013;304(8):E789-E799. doi:10.1152/ajpendo.00015.2013
170. Sullivan LB, Gui DY, Hosios AM, Bush LN, Freinkman E, Vander Heiden MG. Supporting Aspartate Biosynthesis Is an Essential Function of Respiration in Proliferating Cells. *Cell*. 2015;162(3):552-563. doi:10.1016/j.cell.2015.07.017
171. Rabinovich S, Adler L, Yizhak K, et al. Diversion of aspartate in ASS1-deficient tumours fosters de novo pyrimidine synthesis. *Nature*. 2015;527(7578):379-383.

doi:10.1038/nature15529
172. Garcia-Bermudez J, Baudrier L, La K, et al. Aspartate is a limiting metabolite for cancer cell proliferation under hypoxia and in tumours. *Nat Cell Biol*. 2018;20(7):775-781. doi:10.1038/s41556-018-0118-z
173. Ren Y, Roy S, Ding Y, Iqbal J, Broome JD. Methylation of the asparagine synthetase promoter in human leukemic cell lines is associated with a specific methyl binding protein. *Oncogene*. 2004;23(22):3953-3961. doi:10.1038/sj.onc.1207498
174. Peng H, Shen N, Qian L, et al. Hypermethylation of CpG islands in the mouse asparagine synthetase gene: Relationship to asparaginase sensitivity in lymphoma cells. Partial methylation in normal cells. *Br J Cancer*. 2001;85(6):930-935. doi:10.1054/bjoc.2001.2000
175. Touzart A, Lengliné E, Latiri M, et al. Epigenetic Silencing Affects l-Asparaginase Sensitivity and Predicts Outcome in T-ALL. *Clin Cancer Res*. 2019;25(8):2483-2493. doi:10.1158/1078-0432.CCR-18-1844
176. Kuhajda FP, Pizer ES, Li JN, Mani NS, Frehywot GL, Townsend CA. Synthesis and antitumor activity of an inhibitor of fatty acid synthase. *Proc Natl Acad Sci U S A*. 2000;97(7):3450-3454. doi:10.1073/pnas.050582897
177. Kiorpes TC, Hoerr D, Ho W, Weaner LE, Inman MG, Tutwiler GF. Identification of 2-tetradecylglycidyl coenzyme A as the active form of methyl 2-tetradecylglycidate (methyl palmoxirate) and its characterization as an irreversible, active site-directed inhibitor of carnitine palmitoyltransferase A in isolated rat liver. *J Biol Chem*. 1984;259(15):9750-9755. http://www.ncbi.nlm.nih.gov/pubmed/6547720.
178. Jones CL, Stevens BM, D'Alessandro A, et al. Inhibition of Amino Acid Metabolism Selectively Targets Human Leukemia Stem Cells. *Cancer Cell*. 2018;34(5):724-740.e4. doi:10.1016/j.ccell.2018.10.005
179. Appel IM, Boer ML Den, Meijerink JPP, Veerman AJP, Reniers NCM, Pieters R. Up-regulation of asparagine synthetase expression is not linked to the clinical response to. *Pharmacia*. 2006;107(11):4244-4249. doi:10.1182/blood-2005-06-2597.Reprints
180. Chen SH. Asparaginase Therapy in Pediatric Acute Lymphoblastic Leukemia: A Focus on the Mode of Drug Resistance. *Pediatr Neonatol*. 2015;56(5):287-293. doi:10.1016/j.pedneo.2014.10.006
181. Stams WAG, den Boer ML, Beverloo HB, et al. Sensitivity to L-asparaginase is not associated with expression levels of asparagine synthetase in t(12;21)+ pediatric ALL. *Blood*. 2003;101(7):2743-2747. doi:10.1182/blood-2002-08-2446
182. Krejci O, Starkova J, Otava B, et al. Upregulation of asparagine synthetase fails to avert cell cycle arrest induced by L-asparaginase in TEL/AML1-positive leukemic cells. *Leukemia*. 2004;18(3):434-441. doi:10.1038/sj.leu.2403259
183. Fine BM, Kaspers GJL, Ho M, Loonen AH, Boxer LM. A genome-wide view of the in vitro response to l-asparaginase in acute lymphoblastic leukemia. *Cancer Res*. 2005;65(1):291-299. http://www.ncbi.nlm.nih.gov/pubmed/15665306.
184. Iwamoto S, Mihara K. Mesenchymal cells regulate the response of acute lymphoblastic leukemia cells to asparaginase. *J Clin …*. 2007;117(4):1049-1057.

doi:10.1172/JCI30235.Stams
185. Dimitriou H, Choulaki C, Perdikogianni C, Stiakaki E, Kalmanti M. Expression levels of ASNS in mesenchymal stromal cells in childhood acute lymphoblastic leukemia. *Int J Hematol*. 2014;99(3):305-310. doi:10.1007/s12185-014-1509-y
186. Laranjeira ABA, de Vasconcellos JF, Sodek L, et al. IGFBP7 participates in the reciprocal interaction between acute lymphoblastic leukemia and BM stromal cells and in leukemia resistance to asparaginase. *Leukemia*. 2012;26(5):1001-1011. doi:10.1038/leu.2011.289
187. Ehsanipour EA, Sheng X, Behan JW, et al. Adipocytes cause leukemia cell resistance to l-asparaginase via release of glutamine. *Cancer Res*. 2013;73(10):2998-3006. doi:10.1158/0008-5472.CAN-12-4402
188. Michelozzi IM, Granata V, De Ponti G, et al. Acute myeloid leukaemia niche regulates response to L-asparaginase. *Br J Haematol*. May 2019:bjh.15920. doi:10.1111/bjh.15920
189. Maddocks ODK, Athineos D, Cheung EC, et al. Modulating the therapeutic response of tumours to dietary serine and glycine starvation. *Nature*. 2017;544(7650):372-376. doi:10.1038/nature22056
190. Gutierrez JA, Pan Y-X, Koroniak L, Hiratake J, Kilberg MS, Richards NGJ. An inhibitor of human asparagine synthetase suppresses proliferation of an L-asparaginase-resistant leukemia cell line. *Chem Biol*. 2006;13(12):1339-1347. doi:10.1016/j.chembiol.2006.10.010
191. Cao X, Lu Y, Zhang X, Kovalovsky D. Zbtb1 Safeguards Genome Integrity and Prevents p53-Mediated Apoptosis in Proliferating Lymphoid Progenitors. *J Immunol*. 2016;197(4):1199-1211. doi:10.4049/jimmunol.1600013
192. Ray Chaudhuri A, Nussenzweig A. The multifaceted roles of PARP1 in DNA repair and chromatin remodelling. *Nat Rev Mol Cell Biol*. 2017;18(10):610-621. doi:10.1038/nrm.2017.53
193. Bodine DM. Introduction to the review series on transcription factors in hematopoiesis and hematologic disease. *Blood*. 2017;129(15):2039. doi:10.1182/blood-2017-02-766840
194. Porcher C, Chagraoui H, Kristiansen MS. SCL/TAL1: a multifaceted regulator from blood development to disease. *Blood*. 2017;129(15):2051-2060. doi:10.1182/blood-2016-12-754051
195. de Bruijn M, Dzierzak E. Runx transcription factors in the development and function of the definitive hematopoietic system. *Blood*. 2017;129(15):2061-2069. doi:10.1182/blood-2016-12-689109
196. Sood R, Kamikubo Y, Liu P. Role of RUNX1 in hematological malignancies. *Blood*. 2017;129(15):2070-2082. doi:10.1182/blood-2016-10-687830
197. Kim H-J, Barnitz RA, Kreslavsky T, et al. Stable inhibitory activity of regulatory T cells requires the transcription factor Helios. *Science*. 2015;350(6258):334-339. doi:10.1126/science.aad0616
198. Baksh SC, Todorova PK, Gur-Cohen S, et al. Extracellular serine controls epidermal stem cell fate and tumour initiation. *Nat Cell Biol*. May 2020. doi:10.1038/s41556-020-0525-9

199. Cantor JR, Abu-Remaileh M, Kanarek N, et al. Physiologic Medium Rewires Cellular Metabolism and Reveals Uric Acid as an Endogenous Inhibitor of UMP Synthase. *Cell*. 2017;169(2):258-272.e17. doi:10.1016/j.cell.2017.03.023
200. Ponomarev V, Doubrovin M, Serganova I, et al. A novel triple-modality reporter gene for whole-body fluorescent, bioluminescent, and nuclear noninvasive imaging. *Eur J Nucl Med Mol Imaging*. 2004;31(5):740-751. doi:10.1007/s00259-003-1441-5
201. Carroll TS, Liang Z, Salama R, Stark R, de Santiago I. Impact of artifact removal on ChIP quality metrics in ChIP-seq and ChIP-exo data. *Front Genet*. 2014;5:75. doi:10.3389/fgene.2014.00075
202. Liao Y, Smyth GK, Shi W. The R package Rsubread is easier, faster, cheaper and better for alignment and quantification of RNA sequencing reads. *Nucleic Acids Res*. 2019;47(8):e47. doi:10.1093/nar/gkz114
203. Heinz S, Benner C, Spann N, et al. Simple combinations of lineage-determining transcription factors prime cis-regulatory elements required for macrophage and B cell identities. *Mol Cell*. 2010;38(4):576-589. doi:10.1016/j.molcel.2010.05.004
204. Nikolayeva O, Robinson MD. edgeR for differential RNA-seq and ChIP-seq analysis: an application to stem cell biology. *Methods Mol Biol*. 2014;1150:45-79. doi:10.1007/978-1-4939-0512-6_3
205. Yu G, Wang L-G, He Q-Y. ChIPseeker: an R/Bioconductor package for ChIP peak annotation, comparison and visualization. *Bioinformatics*. 2015;31(14):2382-2383. doi:10.1093/bioinformatics/btv145
206. Ramírez F, Dündar F, Diehl S, Grüning BA, Manke T. deepTools: a flexible platform for exploring deep-sequencing data. *Nucleic Acids Res*. 2014;42(Web Server issue):W187-91. doi:10.1093/nar/gku365
207. Carroll T, Barrows D. profileplyr: Visualization and annotation of read signal over genomic ranges with profileplyr. *R Packag version 101*. 2019.
208. Buenrostro JD, Giresi PG, Zaba LC, Chang HY, Greenleaf WJ. Transposition of native chromatin for fast and sensitive epigenomic profiling of open chromatin, DNA-binding proteins and nucleosome position. *Nat Methods*. 2013;10(12):1213-1218. doi:10.1038/nmeth.2688